MINERALI, ENI, M.S. Asymmetric Synthesis of Enantioenriched Spirocycles via a Chiral Brønsted Acid Catalyzed Desymmetrization. (2019)
Directed by Dr. Kimberly S. Petersen 80 pp.

Asymmetric methodologies are very important as they allow chemists to produce significant quantities of complex chiral molecules as enantiopure or enantioenriched compounds. The Petersen group has previously developed chiral Brønsted acid catalyzed desymmetrization reactions for the asymmetric synthesis of lactones. The work described in this thesis provides an application for this methodology to the synthesis of enantioenriched spirocycles, motifs present in many biologically active molecules. This synthesis is performed in the presence of TRIP, a chiral BINOL-derived phosphoric acid catalyst, which guides the cyclization of symmetric prochiral intermediates. The research in this thesis describes the synthesis of two enantioenriched spirocycles, one of which posed many synthetic challenges. Even though the results were nonconclusive, more synthetic work towards the understanding of the mechanistic pathway is also introduced. Therefore, the work described herein not only contributes to the substrate scope of the reaction that was developed, but also provides discussion to the challenges faced during the synthesis of these compounds.

ASYMMETRIC SYNTHESIS OF ENANTIOENRICHED SPIROCYCLES VIA A CHIRAL BRØNSTED ACID CATALYZED DESYMMETRIZATION

by

Eni Minerali

A Thesis Submitted to
the Faculty of The Graduate School at
The University of North Carolina at Greensboro
in Partial Fulfillment
of the Requirement for the Degree
Master of Science

Greensboro
2019

Approved by

_____
Committee Chair

To my sister and family for their continuous support throughout this journey, to all the friends I have made in this department, and to every faculty member who helped me cultivate my love for chemistry and grow as an individual.

APPROVAL PAGE

This thesis written by Eni Minerali has been approved by the following committee of the Faculty of The Graduate School at the University of North Carolina at Greensboro.

Committee Chair _____

Committee Members _____

_____

_____
Date of Acceptance by Committee

_____
Date of Final Oral Examination

ACKNOWLEDGEMENTS

Dr. Mitchell Croatt and Dr. Jason Reddick, for your time and support as my committee members. Dr. Daniel Todd, for your help in using the HPLC instruments and developing methods. Dr. Jennifer Wilent and Dr. Ghassan Qabaja, for training me and helping me become a better organic chemist. All the members of my research group, past and present, for the countless jokes and for challenging my thinking process. Members of other research groups and faculty members, for always taking the time to discuss challenging problems or explain difficult concepts. And most importantly, Dr. Kimberly Petersen, for the continuous advice, support, thought-provoking discussions, training, and for being a great role model.

TABLE OF CONTENTS

Page

LIST OF FIGURES

Page

CHAPTER I

INTRODUCTION

1.1 Definition of Chirality and Types of Chiral Molecules

The spatial orientation of atoms can sometimes create molecules that are mirror images of each other but cannot be superimposed (Figure 1). These types of compounds are chiral and are called enantiomers or optical isomers. Optical isomerism is attributed to the enantiomers' ability to rotate plane-polarized light in opposite directions thanks to their three-dimensional shape. Unlike other types of isomers, these seemingly identical molecules cannot be obtained by simple bond rotations. The unique 3D structure resulting from this type of isomerism is usually due to the presence of a chiral center, or stereocenter (noted as X in Figure 1). A stereocenter can be a sp^3-hybridized atom bound to four different atoms that give the molecule its stereospecificity.

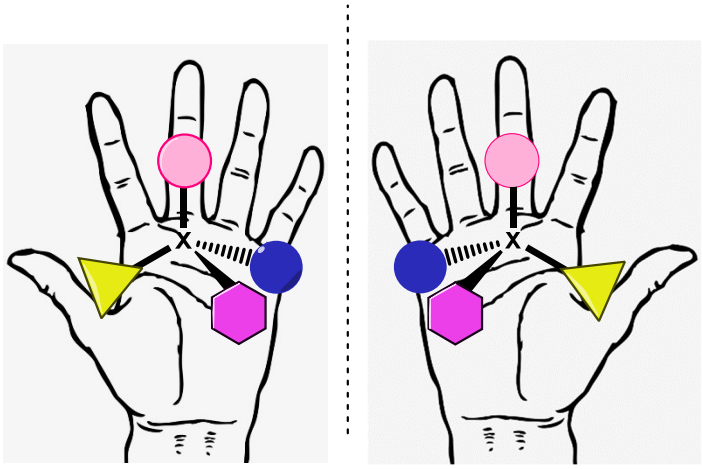

Figure 1. Enantiomers as Non-superimposable Mirror Images

Chirality, however, can also be observed in molecules that don't have a stereocenter but are trapped in a certain conformation. Most of these molecules exhibit an axis of chirality and rotation around that axis is not viable. Examples of such chiral molecules include allenes ***1*** where rotation is not possible because it requires the destruction of π bonds or binapthyls (***2***, ***3***) where the rotation is restricted because of steric hindrance (Figure 2).

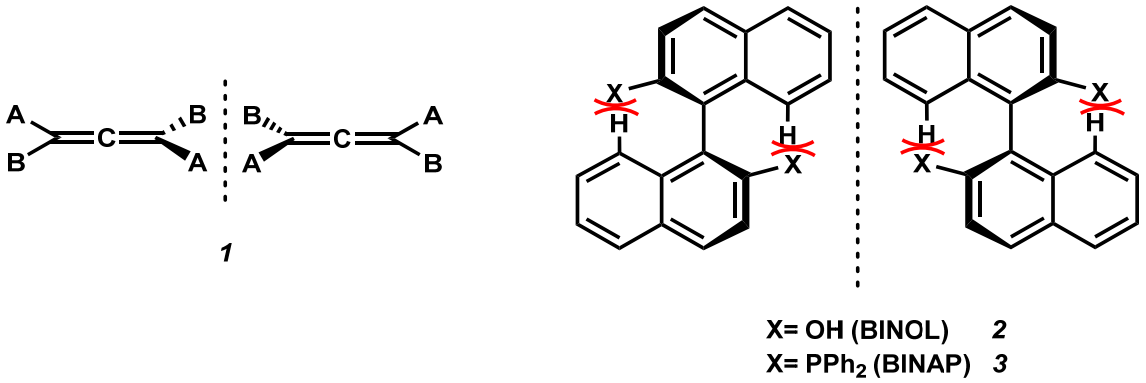

1

Figure 2. Examples of Molecules with Axial Chirality

1.2 Absolute Configuration and Chiral Environments

To distinguish enantiomers from each other, chemists have been using the Cahn−Ingold−Prelog Sequence Rules since 1956 when they were first introduced.[1] These rules are used to assign a name to the absolute configuration of the molecules and help differentiate one enantiomer from the other by naming one as (*R*) and the other as (*S*). When the absolute configuration (absolute spatial orientation of the atoms) is determined experimentally, the CIP rules can be used to assign a name to that specific enantiomer. X-Ray crystallography is one of the most commonly used techniques to determine the absolute configuration of compounds. Other techniques that can provide insight on the spatial orientation of atoms include the Mosher ester analysis,[2] chiral

liquid crystallography,[3] circular dichroism (CD), optical rotatory dispersion (ORD), vibrational circular di-chroism (VCD),[3] or Raman optical activity (ROA).[4]

This intrinsic three-dimensional shape is a crucial component of chiral compounds as it dictates how they interact with other chiral molecules or chiral environments. Proteins provide an important chiral environment and examples of these interactions include protein-protein, receptor-ligand, or enzyme-substrate interactions.[5] These macromolecules have an essential quaternary structure that is created during protein folding and is aided by intramolecular and intermolecular bonds. The quaternary protein structure can interact with the chiral molecules that surround them in a very specific way (usually understood through a lock and key model- Figure 3).

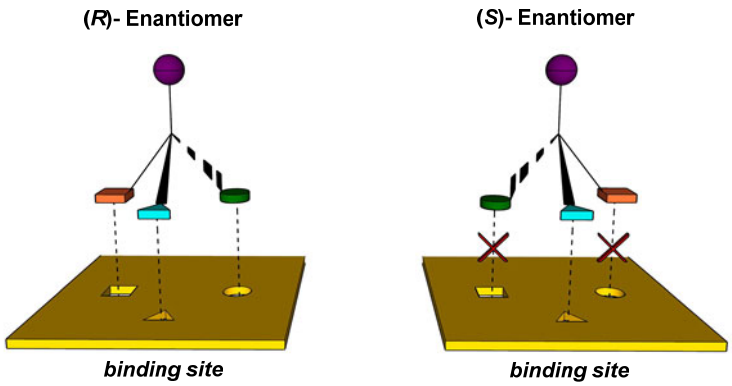

Figure 3. Enantiomers and Their Binding Specificity

1.3 Importance of Chirality and the Need for Enantiopure APIs

The molecules that bind to the quaternary structure of the proteins can often affect the macromolecule by changing its conformation and eventually, through a series of chain reactions, cause desired or undesired effects in living organisms. Many of the molecules or drugs that are intentionally prescribed to patients to achieve a certain

outcome are chiral or have chiral active ingredients. More than half of all marketed drugs are chiral and almost 9 out of the top 10 drugs have chiral active ingredients.[6] Since 1992 the United States Food and Drug Administration has implemented rules that shift the focus towards single enantiomers and the establishment of the absolute stereochemistry early in drug development.[5] After the change in regulations, the worldwide sales of single enantiomer drugs in 2000 were reported as growing at 13% annually and totally $133 billion.[5] This shift of focus towards enantiopure or single enantiomeric drugs is closely related to the undesired effects that have been observed over the years when prescribing racemic mixtures (50:50 mixtures of both enantiomers) to patients. Two of many examples of how drastically different the effects of the two enantiomers can be include Methamphetamine and Naproxen (Figure 4). (*R*)-methamphetamine ***5*** is an over-the-counter nasal decongestant, while the (*S*)-methamphetamine ***4*** is the well-known addictive stimulant drug.[7] (*S*)-naproxen ***6***, on the other hand, is used as a pain reliever, but (*R*)-naproxen ***7*** is found to cause hepatotoxicity.[8] To avoid any unpredicted side effects, chemists have shifted their focus towards obtaining enantiopure chiral active pharmaceutical ingredients (APIs).

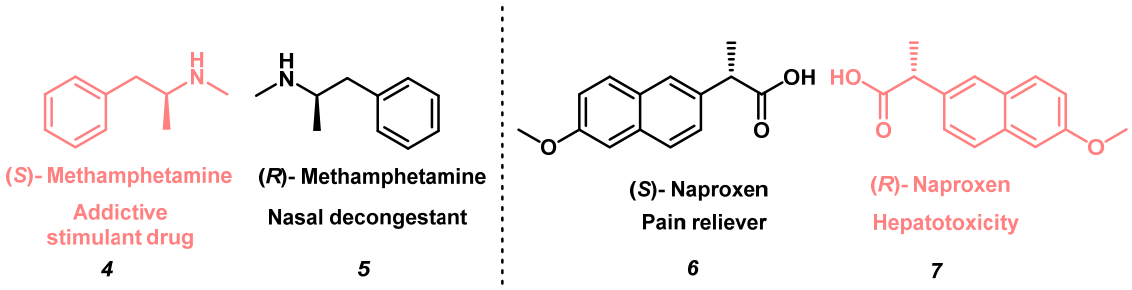

Figure 4. Examples of Enantiomers with Undesired Side Effects

1.4 Methods of Separating Enantiomers

Obtaining enantiopure (100:0 enantiomeric ratio) or enantioenriched (> 50:50 enantiomeric ratio) mixtures can be quite challenging as enantiomers have the same physical properties (melting point, boiling point, polarity etc.) and the same reactivity in achiral environments. Therefore, separation or purification through commonly used techniques such as column chromatography or distillation that rely solely on physical properties cannot be utilized. Single enantiomers are often obtained through specialized chromatography, crystallization or asymmetric synthesis.

1.4.1 Chromatography

The separation of enantiomers through chromatography can be possible through the design of chiral columns that take advantage of the specific spatial orientation of the chiral molecules. These columns are coated with a chiral stationary phase (CSP) that provides a chiral environment for the molecules that go through them. Examples of such coatings include oligosaccharides such as cyclodextrin,[9] polysaccharides, proteins, or macrocyclic antibiotics.[3] Even though most of these techniques are very efficient in separating enantiomers and providing a quantitative analysis of mixtures, large scale separations of drugs that will be released in the market are often done by much more sophisticated techniques. Two of the most effective ones are supercritical fluid chromatography (SFC) and simulated moving bed (SMB) chromatography.[6] While SFC utilizes carbon dioxide as a mobile phase, and SMB relies on the use of highly engineered systems of columns, they are both very expensive methods because of the cost of the chiral columns used on a preparative scale.

1.4.2 Crystallization

One other method of enantiomeric resolution is crystallization, and this technique has been explored since pioneered by Pasteur in 1848 via his observations of sodium ammonium tartrate.[10],[6] Enantiomers can be separated through fractional crystallization that follows the formation of diastereomeric salts or through preferential crystallization/enrichment where the preferred enantiomer is crystallized directly.[10] The development of efficient methods, however, can be quite challenging as phenomena related to nucleation and growth are still not well understood.[11] The formation and separation of diastereomeric salts depends on the chiral compound that introduces the new chiral center, the resolving agents, as well as the solvent system used to separate the pair.[12] On the other hand, the direct enrichment technique requires the determination of an ideal temperature and solvent system established through the analysis of binary and tertiary phase diagrams while taking into consideration key solubility data.[6]

1.4.3 Asymmetric synthesis

Alternatively, asymmetric synthesis or enantioselective synthesis enables chemists to design reactions that favor the formation of one of the enantiomers. From mimicking enzyme specificity to the synthesis of chiral auxiliaries, the introduction of biocatalysts[13] or enantioselective catalysis, asymmetric synthesis is a field that continues to grow.[14] The efficiency of these reactions depends on how enantiopure or enantioenriched the final products are as well as how tolerant the reactions are to different functional groups. The enantiopurity is assessed through enantiomeric excess (ee) which is calculated by subtracting the percentage of the minor enantiomer from the major enantiomer (ee= %major- %minor).

One form of asymmetric synthesis directly “borrows” from nature by using readily available biocatalysts to perform enantioselective reactions. Biocatalysts have been widely used in the biocatalytic asymmetric reductions of cyclic substrates.[13] One example is the use of baker’s yeast to selectively reduce 2,2- dimethylcyclohexane- 1,3-dione ***8*** to (*S*)- hydroxyketone ***9*** (Figure 5).[15] This was the first large scale synthesis of ***9***, and it allowed for the use of this compound as a chiral building block. Since then hydroxyketone ***9*** has been used in the synthesis of many naturally occurring biologically active compounds such as fregenedadiol ***10***, a natural bicyclic diterpene.[16]

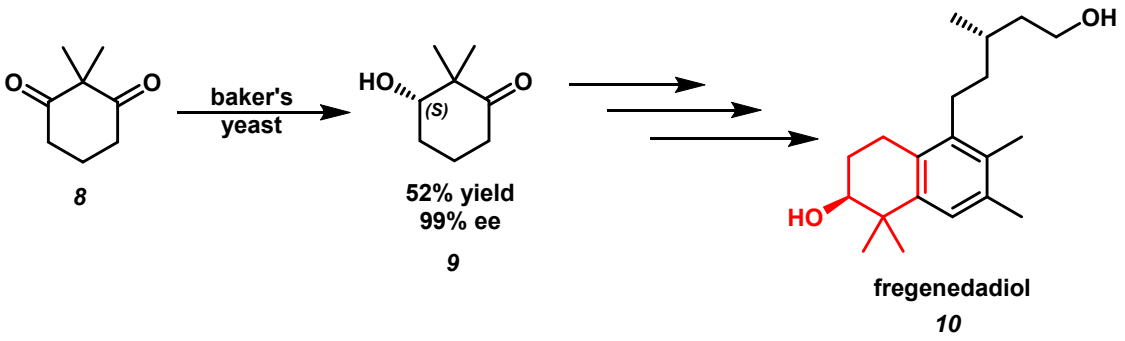

8

52% yield
99% ee

9

fregenedadiol

10

Figure 5. Biocatalytic Asymmetric Reduction with Baker’s Yeast

When not borrowing from nature, synthetic chemists often draw inspiration from mechanistic patterns observed in enzymes. The proline-catalyzed asymmetric aldol reaction is one example of such cases. Class I aldolases catalyze reactions of carbonyl compounds to synthesize β-hydroxyl carbonyl compounds via an enamine pathway.[17] List et al. then mimicked these aldolases to synthesize aldol products ***14*** in very good enantioselectivity by using *L*-proline ***12***.[18] This is a very important breakthrough as it is the first example of a nonmetallic small-molecule catalyst for direct intermolecular asymmetric aldol reactions (Figure 6).

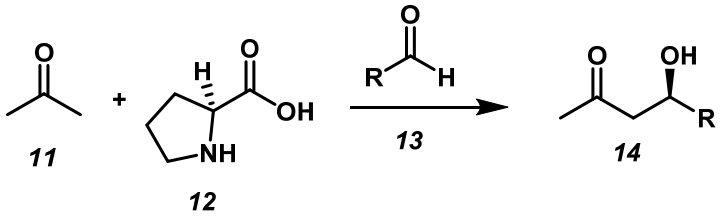

Figure 6. The First Example of Direct Intermolecular Asymmetric Aldol Reactions

In enantioselective catalysis chiral ligands and catalysts may or may not have a direct correlation to patterns observed in nature but provide a chiral environment for asymmetric synthesis to take place. For example, bis(oxazoline) ligands ***17***, inspired by the ligand framework of vitamin B_{12}, are found to catalyze Diels-Alder, Mukaiyama aldol, conjugate addition, cyclopropanation, and aziridation reactions. In contrast, BINOL ***2***, and BINAP ***3*** catalysts, completely synthetic molecules, have also been found to catalyze a variety of reactions. Salen complexes ***15***, TADDOL ***16***, and Cinchona alkaloid derivatives ***18***, are further examples of chiral ligands and catalysts that are used to catalyze enantioselective reactions (Figure7).[19]

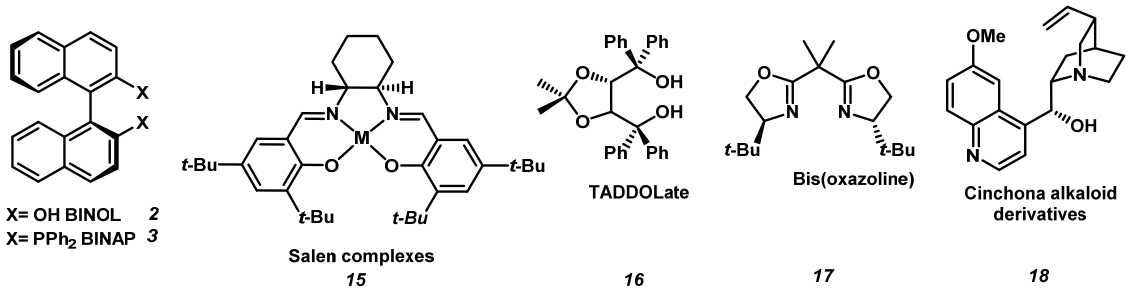

Figure 7. Chiral Ligands and Catalysts

1.5 Desymmetrization

One of the types of reactions that can be catalyzed by chiral catalysts is desymmetrization. This methodology has been very successful from the 1990s until now in synthesizing chiral molecules starting from meso anhydrides, meso ketones, divinyl carbinols, meso dienes, achiral epoxides, and even developing alcohol protection strategies.[20] The essence of this methodology lies in the plane of symmetry that exists in the prochiral intermediate (Figure 8). When this plane of symmetry is broken, a stereocenter is introduced. Ideally, when this process is catalyzed by chiral catalysts, the final product will be enantioenriched or enantiopure.

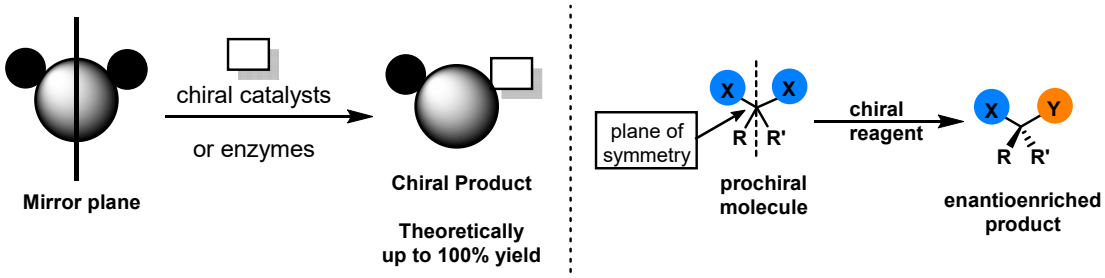

Figure 8. Desymmetrization

1.6 Conclusions

Chiral compounds are commonly found in nature and their purification as well as their synthesis can be very challenging. To overcome different obstacles chemists have tried to create chiral environments that would either differentiate between the enantiomers and aid in their separation, or help the reaction proceed in a certain direction to obtain enantiopure or enantioenriched compounds. The more tolerant to a wide substrate scope these reactions are and the better the enantioselectivity, the more successful the asymmetric synthesis. Therefore, it is very important that chemists

continue to develop methodologies and strive to synthesize complex and novel scaffolds through highly enantioselective reactions, and to test their applicability in a variety of substrates. The following chapter discusses the asymmetric synthesis of such scaffolds through a phosphoric acid catalyzed desymmetrization. This asymmetric internal cyclization methodology has been previously developed in the Petersen group, and this project aims to test its applicability in synthesizing enantioenriched spirocycles.

CHAPTER II

ASYMMETRIC SYNTHESIS OF SPIROCYCLES

2.1 Introduction

This project explores the asymmetric synthesis of spirocycles, cyclic compounds that are linked together by a common atom (Figure 9). The spirocyclic motif itself is very important as it can be found in many pharmaceuticals and natural products. Depending on the atoms attached to the central atom, these compounds can be classified into spirocycles with a non-quaternary carbon spiro center, or spirocycles with a quaternary carbon spiro center ***20***. Compounds such as ***19*** have heteroatoms attached to the spirocenter, while compounds like ***20*** have only carbon atoms attached to the central attom.

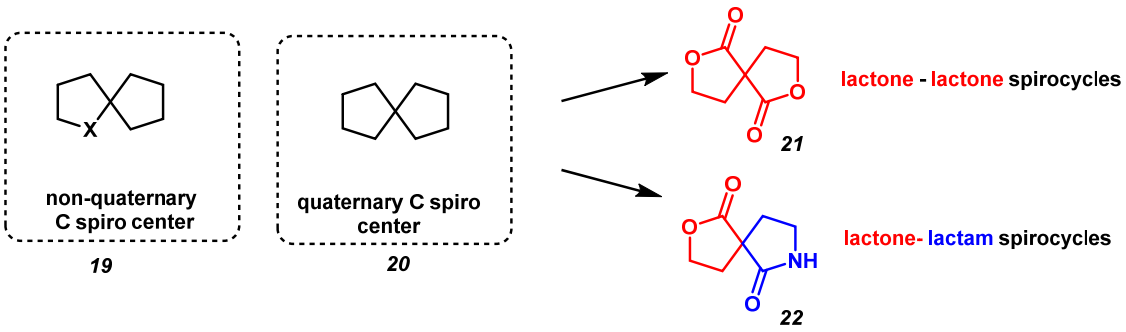

Figure 9. Types of Spirocycles

The project's main focus is the synthesis of spirocycles with quaternary C spiro centers, and even more specifically of spirolactones ***21*** or spirolactams ***22***. Important examples of spirolactams in nature include horsfiline ***23*** which is used as an analgesic[21] and azaspirene ***24*** which is used as an angiogenesis inhibitor (Figure 10).[22] Examples

of spirolactones with a tertiary C spiro centers include drospirenone ***25*** which is a synthetic compound used as an oral contraceptive[23] or abyssomycin C ***26*** which is used as an antimicrobial.[24] On the other hand, spirosesquiterpenes ***27*** and ***28*** are two of the very few examples of naturally occurring spirolactones with a quaternary C spiro center.[25] The scarcity of this motif in nature has been of great interest to the Petersen group. The 5 new spirocycles that this project introduces are scaffolds that have been underexplored and may have use for development in drug discovery projects. Therefore, this work not only presents an application of the previously developed enantioselective cyclization method by the Petersen group but introduces novel spirocyclic scaffolds that contain important motifs.

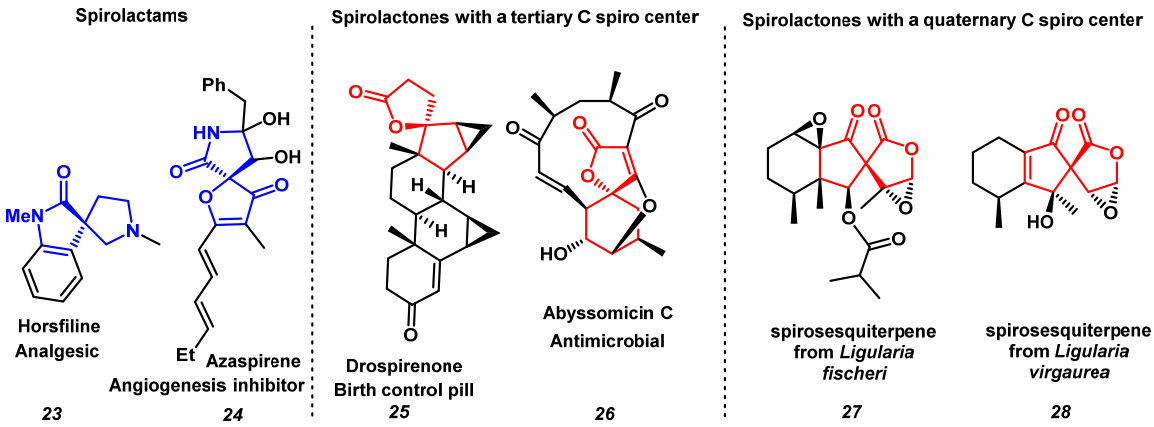

Figure 10. Biologically Active Spirocycles

2.2 Previous Results

As previously mentioned, the methodology used to synthesize the proposed spirolactone scaffolds has been previously developed in the Petersen lab and enables the enantioselective cyclization of prochiral intermediates via a chiral Brønsted acid catalyzed desymmetrization (Figure 11).[26] Prochiral diesters ***29*** are synthesized from

readily available starting materials and undergo a Brønsted acid catalyzed cyclization (5 mol% TRIP) that destroys the symmetry in the molecules to obtain chiral lactones ***31a-g*** in very good yield and enantiomeric excess. The catalyst used in this process is a BINOL phosphoric acid catalyst known as TRIP ***30*** which exhibits axial chirality and introduces a chiral environment in which the reaction can take place.

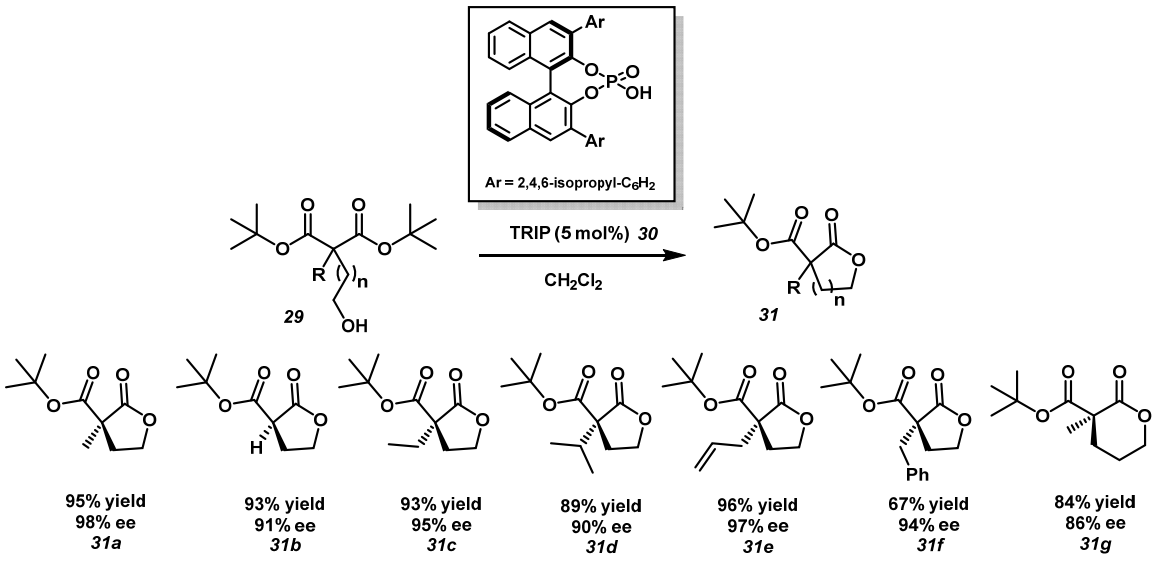

Figure 11. Previous Results

Density Functional Theory (DFT) calculations of an analogous kinetic resolution support a mechanism in which the reaction proceeds via a dual activation of the carbonyl and the hydroxyl group.[27] The acidic proton of the Brønsted acid activates the carbonyl while the Lewis basic oxygen hydrogen bonds to the hydroxyl group to lock the intermediate in a certain conformation and enable the cyclization (Figure 12). The bulky groups on both sides of the catalyst make it possible for the cyclization to be favored in one direction ***32*** as the other possible conformer ***33*** is disfavored because of steric clashes.

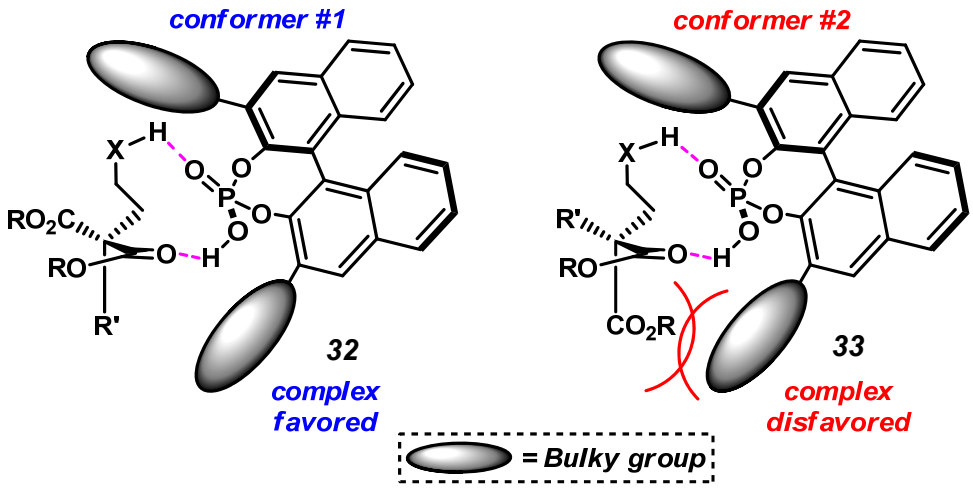

Figure 12. Proposed Activation

2.3 Application of the Methodology in Current Work

The Petersen group's interest in the asymmetric synthesis of novel small molecules led to the application of the above described desymmetrization in the preparation of enantioenriched spirocycles. Unlike the previous prochiral diesters ***29***, the new diesters ***34*** have two nucleophilic chains that would allow for consecutive cyclizations at the two electrophilic carbonyls (Figure 13). A desymmetrization is used to form the first ring which is depicted below in blue and set the stereocenter. The second cyclization (depicted in red) can then be performed via achiral acid catalysis or a coupling reaction. While the first cyclization is enantioselective, the second does not require the use of the chiral Brønsted acid as the absolute stereochemistry has already been set.

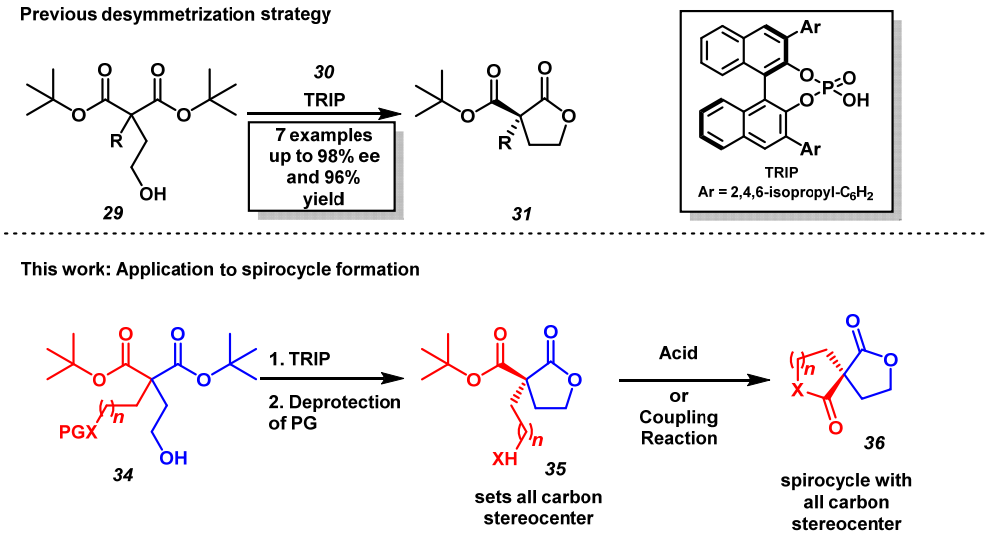

Figure 13. Applied Strategy

This strategy was used to synthesize seven different substrates (Figure 14). With the exception of compound ***21***, all the rest of the substrates had not been previously described in literature. Both compound ***21*** and ***37*** were first introduced in the group by Dr. Jennifer Wilent, a former PhD student. The combined efforts of her and Kyla Stingley (former M.S. student) on the synthesis of compound ***38*** provided data on the characterization of this compound. However, they both faced challenges in determining the enantiomeric excess of ***38***. Amber Kelley, a current PhD student, introduced compound ***39*** and ***42*** to the substrate scope, and was able to grow crystals of ***42*** that helped determine its absolute configuration. This work highlights the effort towards the determination of the enantiomeric excess of compound ***38*** and its precursor, as well as its enantioenrichment by recrystallization, and the synthesis of compounds ***40*** and ***41***. Attempts towards understanding the decrease in enantiomeric excess during the second cyclization will also be discussed.

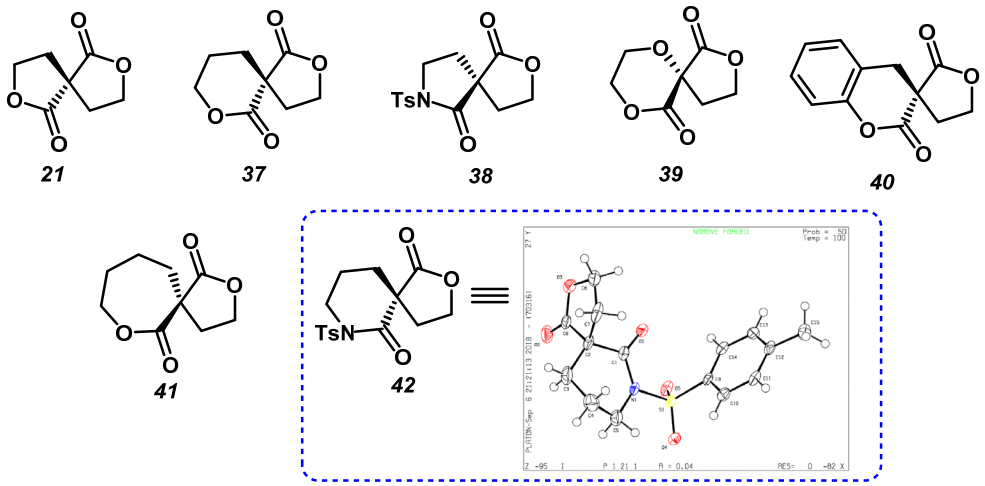

Figure 14. Substrate Scope

2.4 Results and Discussions

*2.4.1 Synthesis and recrystallization of compound **38***

Compound ***38*** was of great interest to the group as it was the second spirolactam scaffold introduced in the substrate scope. As previously mentioned, several members of the group have worked on obtaining the necessary data required for publishing this substrate.

Spirocycle ***38*** had been previously synthesized as a crystalline white solid by members of the Petersen group the readily available di-*tert*-butyl malonate ***43*** served as a starting material for all the substrates and underwent alkylation with sodium hydride (NaH), ***44*** and anhydrous tetrahydrofuran (THF) to obtain compound ***45*** in 68% yield (Figure 15). Intermediate ***45*** then underwent another alkylation with NaH, *N*-tosyl aziridine ***46*** and anhydrous THF to obtain compound ***47*** in 48% yield. The protected alcohol in this intermediate was then deprotected following a hydrogenolysis reaction with $Pd(OH)_2/C$ in ethyl acetate which yielded compound ***48*** in 96% yield. The prochiral diester ***48*** was used directly to perform the chiral cyclization with 10 mol% of (*S*)-TRIP

30a in dichloroethane for 9 days to yield compound ***49*** with 92% yield. While they were able to synthesize spirocycle ***38*** through cyclization with trifluoroacetic acid, the group was not able to obtain consisted results while determining the enantiomeric excess of lactone ***49*** or spirocycle ***38***. The first goal of this project was to address these issues by working on developing HPLC methods that would help determine the ee values.

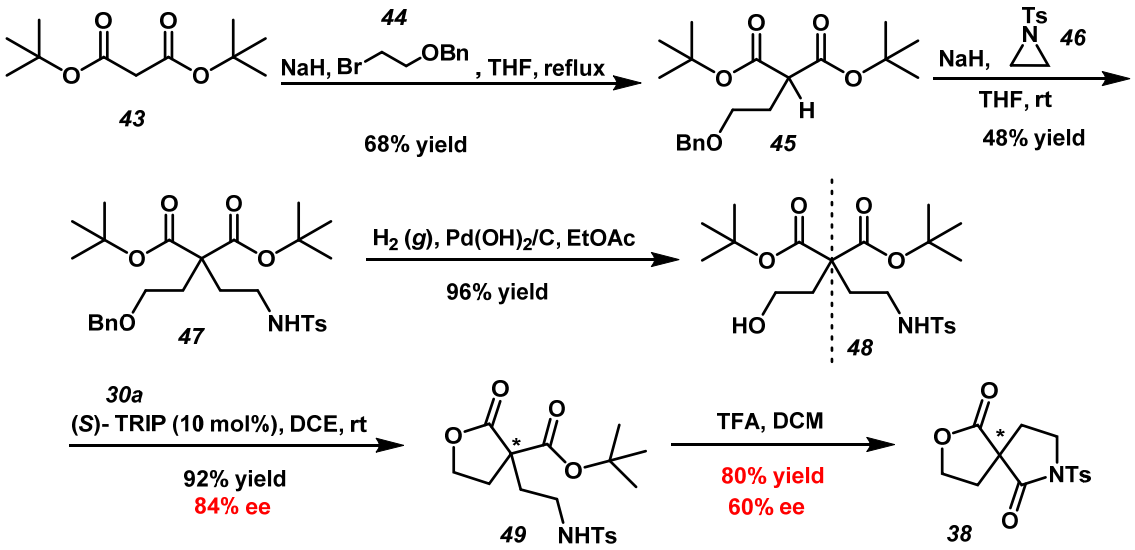

Figure 15. Steps Towards the Synthesis of Compound ***38***

After multiple attempts of resolving the issues faced before in separating the enantiomers of ***49*** an enantiomeric excess of 84% was obtained in a normal phase chiral HPLC, but with no complete baseline separation. Using the previously synthesized compound ***49***, the last cyclization was then performed in dichloromethane to obtain spirocycle ***38*** in 80% yield and 60% ee. A reverse phase chiral HPLC was used to separate these enantiomers and establish the ee values.

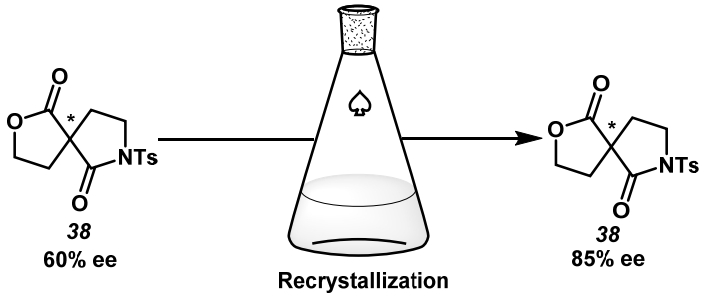

Figure 16. Recrystallization of Compound ***38***

The Petersen group was also interested in observing the effects of recrystallization in the enantiomeric excess since this compound was one of the few crystalline scaffolds that was synthesized. Several solvent systems were attempted and recrystallization with ethyl acetate and hexanes resulted in an enantiomeric excess of 85% after filtration with 87% recovery (Figure 16). This increase by 25% in ee values is a great example of how recrystallization can be used to for enantioenrichment of crystalline compounds with modest enantiomeric excess.

*2.4.2 Attempts towards the synthesis of compound **41***

Another interesting addition to the substrate scope would be the synthesis of spirocycle ***41*** which contains a seven membered lactone. Unlike the rest of the substrates, the synthesis of this compound was more challenging. Similar to the previous synthesis, di-*tert*-butyl malonate was used as a starting material to obtain the prochiral diester ***51*** which contains two protected nucleophilic chains (Figure 17). The first two alkylating steps were performed in dimethylformamide (DMF) while using NaH as a base. The first alkylation utilized ***44*** as an alkylating agent while the second one utilized ***50***. The different protecting groups on the two alcohols allows for the selective deprotection of only one of them by a hydrogenolysis reaction with $Pd(OH)_2$ on carbon. The accessible free alcohol was then utilized in the chiral cyclization with 10 mol% of

(*S*)-TRIP in dichloroethane to obtain ***53*** in 63% yield and 40% ee. The second alcohol was then deprotected with K_2CO_3 in methanol in 94% yield. Unlike the previous synthesis, reaction with trifluoroacetic acid in dichloromethane does not enable the second cyclization but removes the *tert*-butyl group and generates carboxylic acid ***55*** which is isolated in 99% yield.

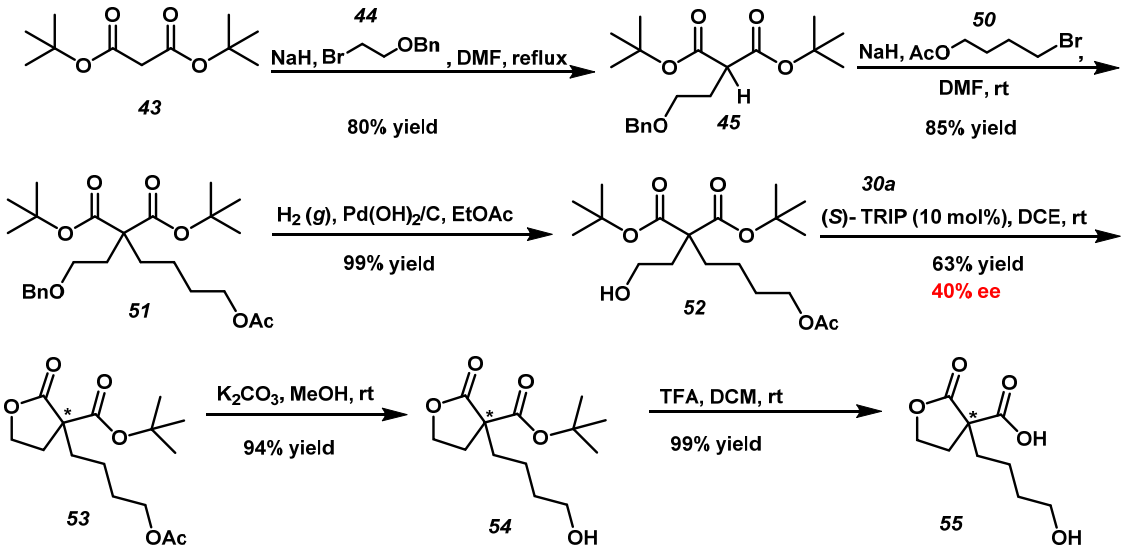

Figure 17. Steps Towards the Synthesis of Compound ***41***

An intramolecular transesterification of compound ***54*** is more challenging than the rest of the substrates as the formation of 7-membered ring is difficult. Common approaches towards the synthesis of macrocycles involve methods that allow the cyclization to proceed through intermediates where the carboxylate is decorated with an exceptionally good leaving group.[28] Such reactions are known as coupling reactions and can be used to form a macrocyclic ester from an alcohol and a carboxylic acid. The two different coupling reactions attempted in this synthesis were Steglich Esterification (DCC/DMAP) and the carbonyldiimidazole coupling (Figure 18). Even though traces of

what was believed to be the product were observed via NMR, compound ***41*** was not isolated using *N*, *N*'-dicyclohexylcarbodiimide ***56*** and 4-dimethylaminopyridine (DMAP). Dicyclohexylurea (DCU) ***59***, a biproduct of the reaction is a very soluble compound that has the tendency to travel with the solvent in column chromatography, making it difficult to obtain pure product, especially on small reaction scales. Even after attempts of precipitating DCU out of solution in cold acetonitrile, compound ***41*** was not isolated. Alternatively, coupling with CDI was the second approach used where what is believed to be spirocycle ***41*** was obtained in 18% yield. However, the enantiomeric excess of the final compound was only 25% and this coupled with the modest yield led to the exclusion of this substrate from the publication.

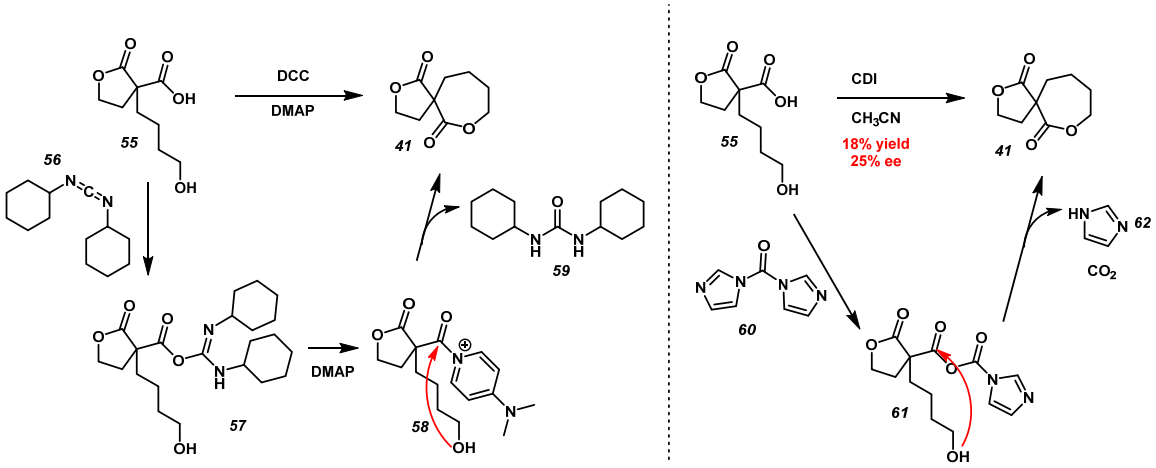

Figure 18. Coupling Reactions

*2.4.3 Synthesis of compound **40***

The first step towards the synthesis of compound ***40*** involved the alkylation of di-*tert*-butyl malonate with alkylating agent ***65***. Compound ***65*** was synthesized from *o*-cresol ***63*** which underwent a protecting step with *tert*-butyldimethylsilyl chloride (TBSCl)

and was brominated with azobisisobutyronitrile (AIBN) and *N*-bromosuccinimide (NBS) in benzene as previously published (Figure 19).[29]

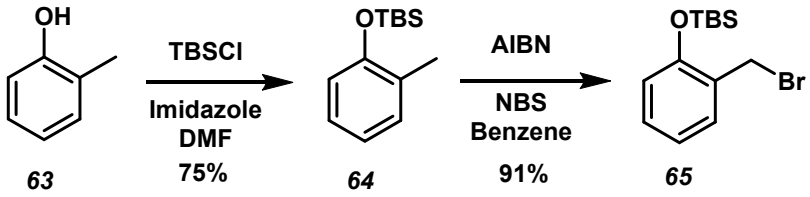

Figure 19. Synthesis of Alkylating Agent ***65***

The prochiral diester ***68*** that was synthesized after the second alkylation and the removal of the acetyl protecting group, underwent a cyclization with (*R*)- TRIP ***30b*** that yielded the TBS protected enantioenriched lactone ***69*** in 81% yield (Figure 20). The enantiomeric excess of the first cyclization was determined after the removal of the TBS group and was determined to be 76%. Upon cyclization with *p*-toluenesulfonic acid (*p*-TSA) in dichloroethane for 48 hours, the enantiomeric excess decreased to 72% with a low yield of 34%. Alternatively, when the reaction was heated to reflux, and a second equivalence of *p*-TSA was added to the mixture, the reaction went to completion but the spirocycle ***40*** resulted racemic (0% ee). Therefore, to avoid a decrease in enantiomeric excess, the yield of the reaction was sacrificed.

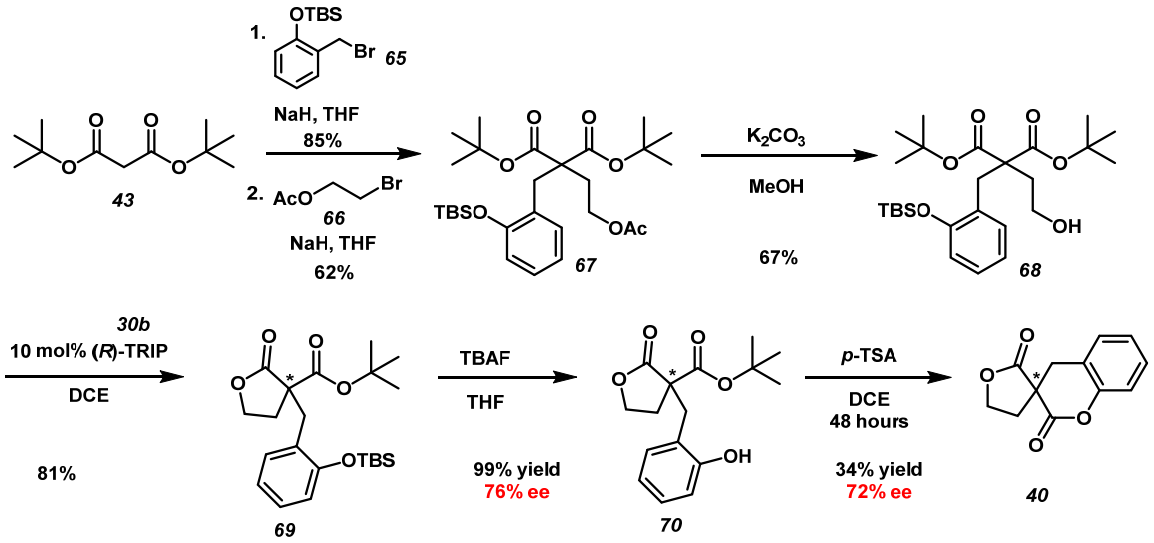

Figure 20. Steps Towards the Synthesis of Spirocycle ***40***

2.4.4 Attempts in understanding stereochemical retention

The decrease in enantiomeric excess that was observed in all the substrates upon the 2nd cyclization to form the spirocycles, led to the investigation of the mechanism of reaction via the cyclization of compound ***71*** (Figure 21). One possible explanation to this phenomenon lies in the fact that there are 2 possible electrophilic sites in ***71*** for cyclization. If the acid used in this step activates the ester carbonyl (red pathway) the synthesized spirocycle ***37*** will retain its stereochemistry and the enantiomeric excess will not decrease. However, if the acid activates the lactone carbonyl (blue pathway) the previously synthesized lactone will open to generate lactone ***72*** which will then yield spirocycle ***37*** with inverted stereochemistry.

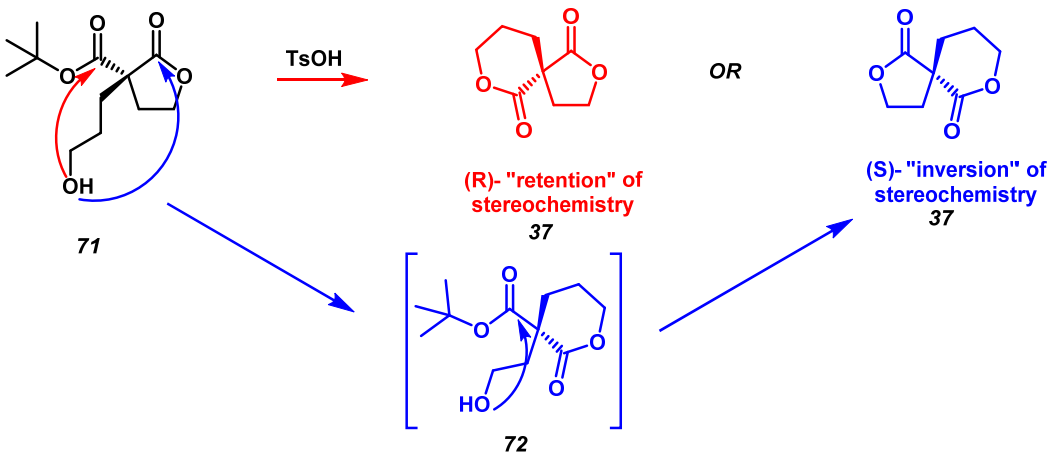

Figure 21. Pathway for Inversion of Stereochemistry

The question that arises after considering this pathway is whether the stereochemistry set during the first cyclization is retained and simply decreased because of this phenomenon or it is completely inverted to the opposite configuration. Two different approaches were strategized to give more insight into this matter (Figure 22). Approach A required the synthesis of compound ***72***. Assuming that a time dependent NMR study of the cyclization of compound ***71*** to ***37*** would show traces of compound ***72*** forming along the way if the blue “inversion” pathway was followed, the synthesis of compound ***72*** would be helpful in the accurate assignment of the collected NMR spectra. Approach B required the synthesis of compound ***37*** through a coupling reaction. Since the second ring of spirocycle ***37*** has been previously synthesized through acid catalysis, a coupling reaction would be able to bypass the issues that come with catalysis and yield a compound that retains the stereochemistry. Spirocycle ***37*** has been found to rotate plane-polarized light to the left (negative sign). Therefore, evidence in support of stereochemical retention could be provided if the newly synthesized spirocycle also rotates plane-polarized light to the left.

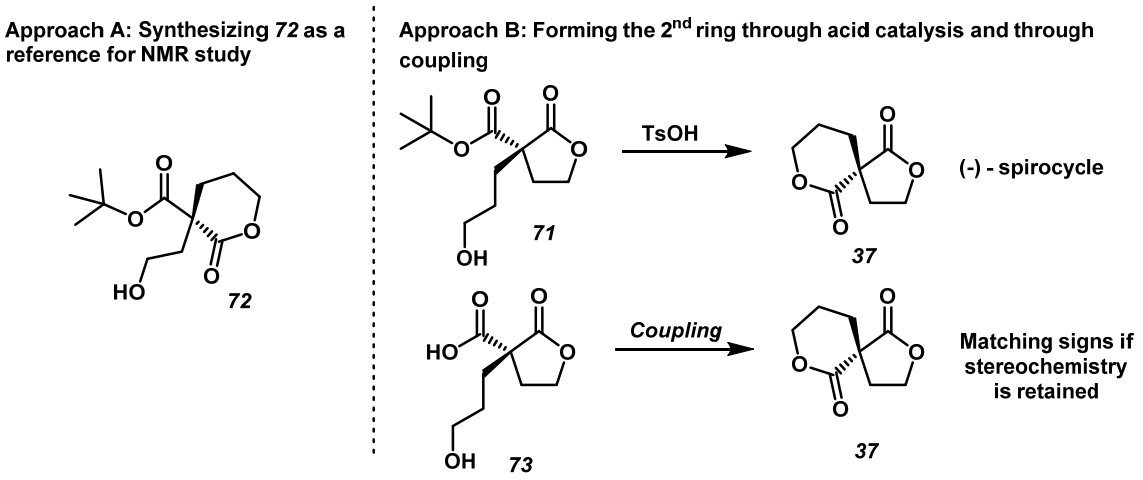

Figure 22. Approaches Towards Understanding Stereochemical Retention

However, even though intermediate ***76*** was successfully synthesized, lactone ***72*** was not isolable as it was immediately converted to lactone ***71*** (Figure 23). This indicates that the formation of the γ-lactone is more thermodynamically favorable. The reaction is also not reversible and the formed γ-lactone appears to be more stable. This can be due to the length of chain containing the alcohol as well as its spatial orientation that does not favor the addition to the lactone carbonyl without the presence of catalytic amounts of acid.

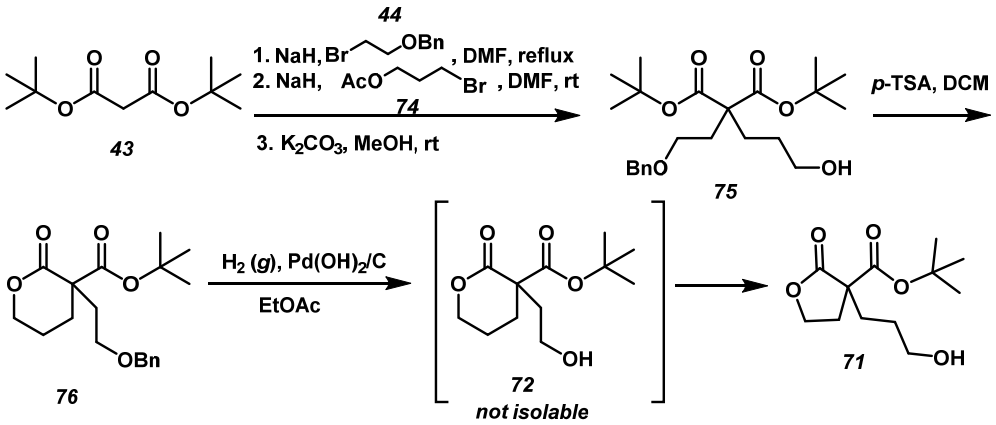

Figure 23. Attempts Towards the Synthesis of Compound ***72***

Approach B was also not fruitful as the deprotection of compound ***80*** resulted in the synthesis of spirocycle ***37*** (Figure 24). This undesired cyclization did not allow for a coupling reaction, and therefore the optical rotation of the final compound could not be compared to the previously synthesized spirocycle.

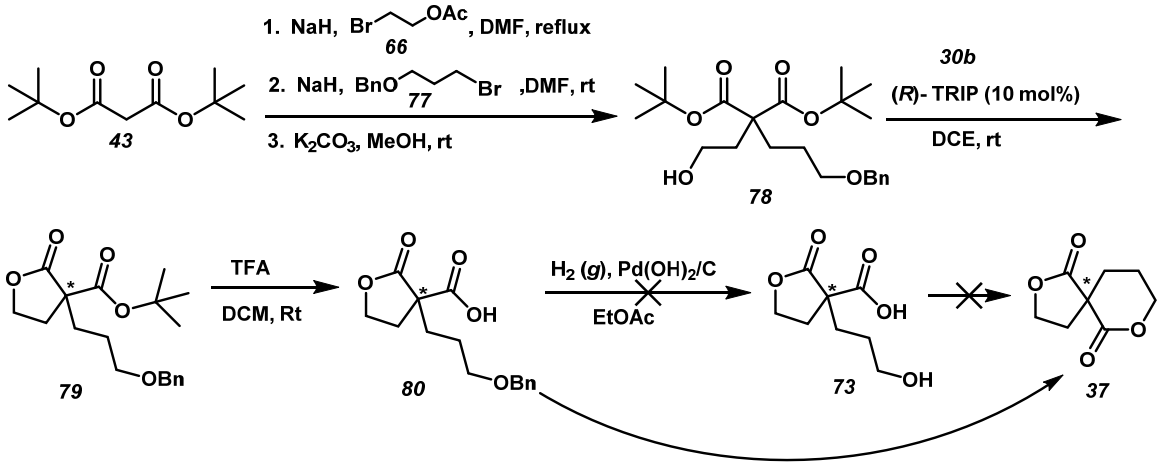

Figure 24. Attempts and Challenges Towards the Synthesis of Compound ***37***

2.4.5 Published results

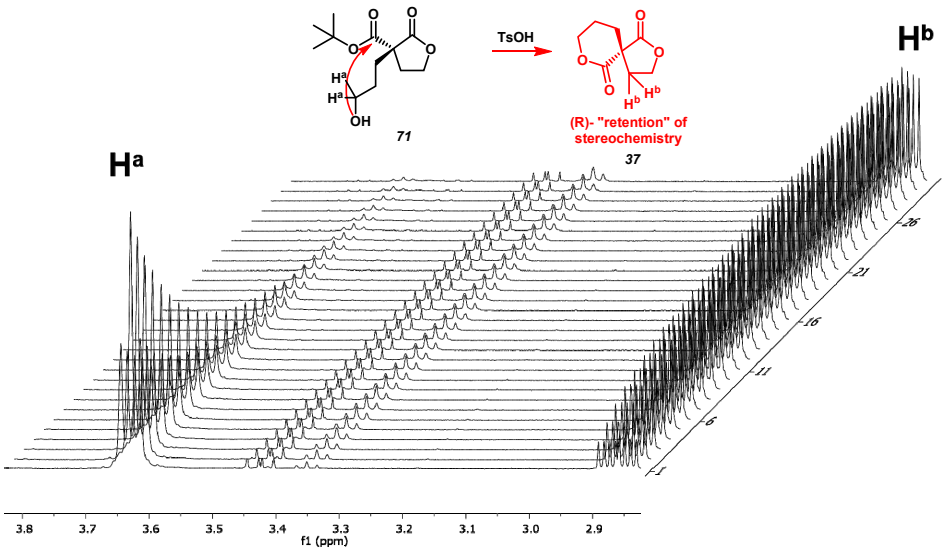

Figure 25. NMR Study

Even though the approaches mentioned above provided inconclusive results, previous work from Tyler Wilson, a former M.S. student, provided evidence in support of the retention of stereochemistry through NMR studies of the conversion of compound ***71*** to ***37*** (Figure 25).[30] In this study the rate of disappearance of protons H_a matches the rate of appearance of protons H_b, and no traces of the δ- hydroxy lactone were observed. The absence of substantial amounts of compound x, suggests that the major pathway is the red one (Figure 21), and the stereochemistry set during the first cyclization is preserved.

Additionally, four more substrates were introduced to the scope of this reaction by the rest of the Petersen group and X-ray crystallography of compound ***42*** was able to establish its absolute configuration (Figure 26). The rest of the stereochemistry was assigned to the molecules by analogy. Good to moderate ee values were also reported for all six of the published molecules.

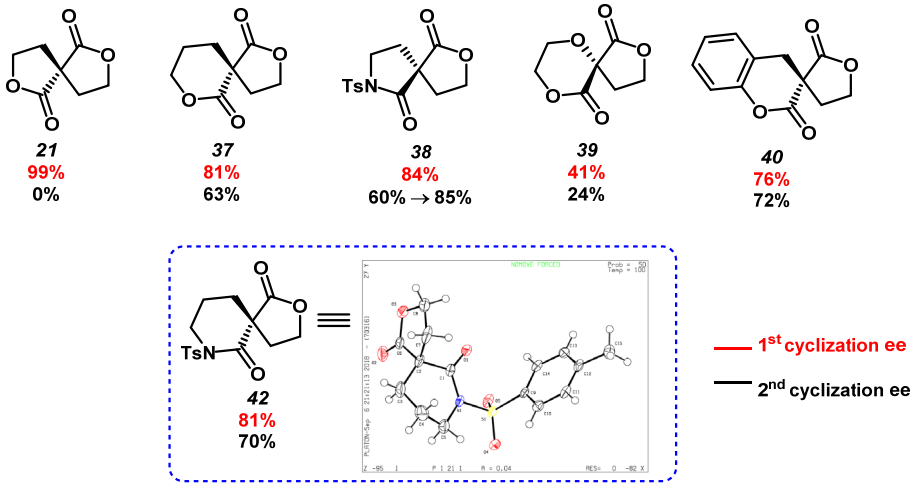

Figure 26. Published Results

2.5 Conclusions

This work focuses on the applications of a previously developed methodology on the synthesis of enantioenriched spirocycles, motifs that are present in many pharmaceuticals and natural products. The methodology is known as desymmetrization and enables the formation of enantioenriched molecules through a chiral Brønsted acid catalyzed internal cyclization. Six substrates were synthesized by the combined effort of several members of the group, and this work discussed the synthesis of some of them as well as challenges that were faces while trying to introduce a seventh substrate. Unfortunately, both approaches that would provide evidence towards the stereochemical retention of the substrates were not successful. Overall, this project introduces the synthesis of six novel and enantioenriched spirocyclic scaffolds, five of which had a quaternary carbon center.

CHAPTER III

EXPERIMENTAL

3.1 General Information

Unless noted, all solvents and reagents were obtained from commercial sources and used without further purification; anhydrous solvents were dried following standard procedures. The ^{1}H and ^{13}C nuclear magnetic resonance (NMR) spectra were plotted on 400 and 500 MHz spectrometer using $CDCl_3$ as a solvent at room temperature. The NMR chemical shifts (δ) are reported in ppm. Abbreviations for ^{1}H NMR: s = singlet, d = doublet, m = multiplet, b = broad, t = triplet, q = quartet, quint = quintet. The reactions were monitored by TLC using silica G F254 precoated plates. Flash chromatography was performed using flash grade silica gel (particle size: 40-63 μm, 230 × 400 mesh). Enantiomeric excess was determined by GC analysis and HPLC analysis. IR data was obtained with a FTIR spectrometer one with frequencies reported in cm^{-1}. High Resolution Mass Spectra were acquired on an Orbitrap XL MS system. The specific rotations were acquired on an analytical polarimeter.

3.2 Synthesis of Compound *38*

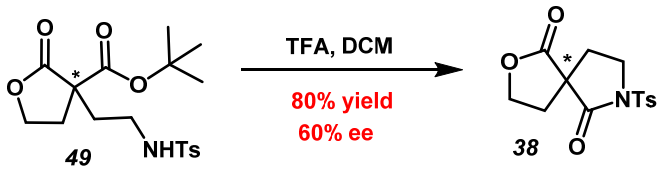

Figure 27. Compound ***38***

To a solution of lactone intermediate ***49*** (42.0 mg, 0.110 mmol) in CH_2Cl_2 (2 mL) was added excess trifluoroacetic acid (2 mL) and the solution was stirred until reaction completion was determined by TLC analysis. The reaction was extracted with ethyl acetate (2 x 10 mL) and H_2O (1 x 10 mL). The organic phase was dried over $MgSO_4$ and concentrated to afford compound ***38*** as white solid (29 mg, 85% yield, 60% ee). The compound was then dissolved in ethyl acetate and hot hexanes and let to cool down to room temperature. The recrystallized material was filtered and rinsed with cold hexanes to result in 85% ee and 87% recovery. ^{1}H NMR (500 MHz, $CDCl_3$) δ 7.88 (d, *J* = 8 Hz, 2H), 7.34 (d, *J* = 8 Hz , 2H), 4.48 (m, 1H), 4.32 (m, 1H), 4.07 (m, 2H), 2.73 (m, 1H), 2.52 (m, 1H), 2.43 (s, 3H), 2.16 (m, 2H); ^{13}C NMR (126 MHz, $CDCl_3$) δ 174.3, 170.1, 145.9, 134.2, 130.0, 128.2, 66.9, 53.1, 45.1, 32.1, 28.9, 21.9; IR (neat) cm^{-1} 2923, 1765, 1716, 1358, 1348, 1167, 1105, 1024, 668, 585; HRMS ($C_{14}H_{15}NO_5S$, ESI): calculated 310.0744 $[M+Na]^{+1}$, found 310.0745, $[\alpha]_D^{21}$ = –35.2° (c = 0.25, $CHCl_3$); mp = 134.2 - 136.6°C.

3.3 Synthesis of Compound *41*

*3.3.1 Synthesis of intermediate **45***

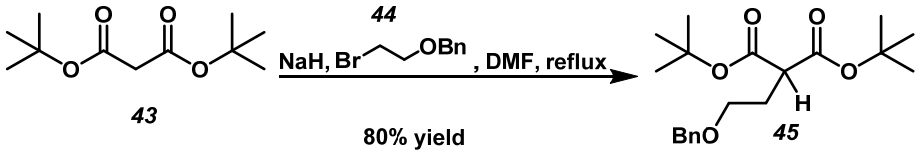

Figure 28. Intermediate ***45***

Di-*tert*-butyl malonate (500 mg, 2.3 mmol) was added dropwise to a solution of sodium hydride (60% in mineral oil, 138mg, 3.5 mmol) in DMF (23 mL), and the solution was stirred until gas evolution was complete. Benzyl 2-bromoethyl ether ***44*** (497 mg, 2.3 mmol), was added to the reaction mixture and the solution was stirred until reaction completion was determined by TLC analysis (24 hours). The reaction was quenched with saturated NH_4Cl (10 mL) at 0°C, phases were separated, and aqueous phase was extracted with ethyl acetate (2 x 10 mL). The organic phase was dried over anhydrous $MgSO_4$ and concentrated. The residue was purified by flash chromatography on silica gel (5→20 % ethyl acetate /hexanes) to obtain monoalkylated malonate as a colorless oil (648 mg, 80% yield). ^{1}H NMR (500 MHz, $CDCl_3$) δ 7.33 (m, 5H), 4.48 (s, 2H), 3.50 (t, *J* = 6.2 Hz, 2H), 3.39 (t, *J* = 7.4 Hz, 1H), 2.12 (dt, *J* = 7.4, 6.2 Hz, 2H), 1.44 (s, 18H).^{13}C NMR (126 MHz, $CDCl_3$) δ 168.9, 138.4, 128.5, 127.8, 127.7, 81.5, 73.1, 67.6, 51.0, 28.9, 28.0

*3.3.2 Synthesis of intermediate **51***

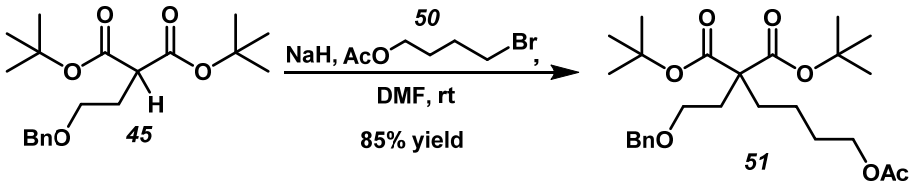

Figure 29. Intermediate ***51***

The monoalkylated malonate ***45*** (250 mg, 0.71 mmol) was added to a solution of sodium hydride (60% mineral oil, 43 mg, 1.1 mmol) in DMF (7 mL). The solution was stirred until gas evolution was complete. To the reaction mixture was added 4-bromobutyl acetate ***50*** (209 mg, 1.1 mmol) at 0°C, and the solution was stirred until reaction completion was determined by TLC analysis (24 hours). The reaction was quenched with saturated NH_4Cl (10 mL) at 0 °C, phases were separated, and aqueous phase was extracted with ethyl acetate (2 x 10 mL). The organic phase was dried over anhydrous $MgSO_4$ and concentrated. The residue was purified by flash chromatography on silica gel (5→ 20% ethyl acetate/hexanes) to obtain the dialkylated malonate ***51*** as a colorless liquid (281 mg, 85% yield). ^{1}H NMR (500 MHz, $CDCl_3$) δ 7.10 (m, 5H), 4.46 (s, 2H), 4.01 (t, *J* = 6.6 Hz, 2H), 3.42 (t, *J* = 7.0 Hz, 2H), 2.16 (t, *J* = 7.0 Hz, 2H), 2.01 (s, 3H), 1.82 (m, 2H), 1.59 (m, 2H), 1.41 (s, 18H), 1.23 (m, 2H); ^{13}C NMR (126 MHz, $CDCl_3$) δ 171.2, 170.7, 138.3, 128.4, 127.8, 127.7, 81.2, 73.0, 66.2, 64.2, 57.0, 31.6, 29.0, 27.9, 21.1, 20.6; IR (neat) cm^{-1} 2975, 1722, 1366, 1239, 1147, 1111; HRMS ($C_{26}H_{40}O_7$, ESI): calculated 487.2666 $[M+Na]^{+1}$, found 487.2656.

*3.3.3 Synthesis of intermediate **52***

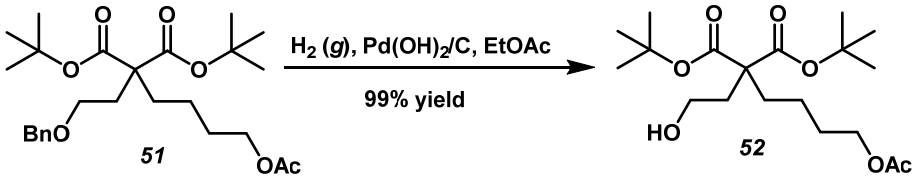

Figure 30. Intermediate ***52***

To a solution of the dialkylated intermediate ***51*** (250 mg, 0.54 mmol) in ethyl acetate (11 mL) was added $Pd(OH)_2$ (20% on carbon, 38 mg, 0.27 mmol) and the solution was stirred under hydrogen pressure using a balloon filled with hydrogen gas at room temperature until reaction completion was determined by TLC analysis. The reaction mixture was filtered through a plug of Celite® and the filtrate was concentrated under vacuum, to afford compound ***52*** as colorless oil (198 mg, 99% yield). ^{1}H NMR (500 MHz, $CDCl_3$) δ 4.04 (t, *J* = 6.5 Hz, 2H), 3.65 (t, *J* = 6.6 Hz, 2H), 2.07 (t, *J* = 6.6 Hz, 2H), 2.01 (s, 3H), 1.84 (m, 2H), 1.62 (m, *J* = 6.6 Hz, 2H), 1.44 (s, 18H), 1.26 (m, 2H); ^{13}C NMR (126 MHz, $CDCl_3$) δ 171.2, 81.7, 64.2, 59.1, 57.3, 35.2, 32.9, 29.0, 27.9, 21.1, 20.7; IR (neat) cm^{-1} 3451, 2974, 1720, 1366, 1238, 1034, 846; HRMS ($C_{19}H_{34}O_7$, ESI): calculated 375.2383 $[M+Na]^{+1}$, found 375.2368.

*3.3.4 Synthesis of intermediate **53***

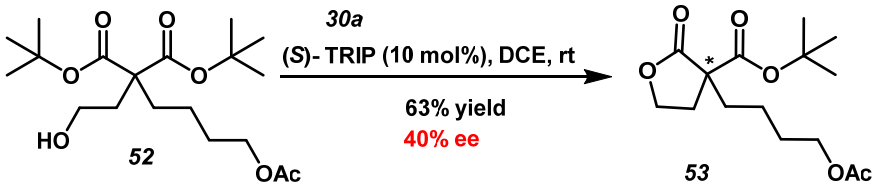

Figure 31. Intermediate ***53***

To a solution of acid ***52*** (190 mg, 0.50 mmol) in dichloroethane (5 mL) was added compound *(S)*- TRIP ***30a*** (38 mg, 0.050 mmol) and the solution was stirred for 10 days at room temperature. The reaction was extracted with ethyl acetate (2 x 10 mL) and H_2O (1 x 10 mL). The organic phase was dried over $MgSO_4$ and concentrated to afford lactone intermediate ***53*** as a colorless liquid (95.8 mg, 63% yield).^{1}H NMR (500 MHz, $CDCl_3$) δ 4.31 (m, 2H), 4.06 (t, *J* = 6.5 Hz, 2H), 2.66 (m, 1H), 2.19 (m, 1H), 2.05 (m, 1H) 2.03 (s, 3H), 1.75 (m, 1H), 1.66 (m, 2H), 1.48 (m, 1H), 1.47 (s, 9H), 1.33 (m, 1H); ^{13}C NMR (126 MHz, $CDCl_3$) δ 175.2, 171.2, 168.6, 83.1, 66.2, 64.1, 54.8, 33.7, 32.0, 28.8, 27.90, 27.89, 27.88, 21.4, 21.1; IR (neat) cm^{-1} 2976, 1772, 1728, 1242, 1028; HRMS ($C_{15}H_{24}O_6$, ESI): calculated 323.1465 $[M+Na]^{+1}$, found 323.1451.

*3.3.5 Synthesis of intermediate **54***

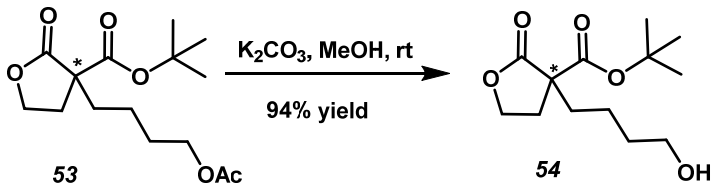

Figure 32. Compound ***54***

To a solution of intermediate ***53*** (100 mg, 0.41 mmol) in methanol (8 mL) was added K_2CO_3 (226 mg, 1.6 mmol), and the solution was stirred at room temperature until reaction completion was determined by TLC analysis. The reaction mixture was diluted with CH_2Cl_2 and was extracted with CH_2Cl_2 (2 x 15 mL) and H_2O (1 x 10 mL). The organic layer was dried over $MgSO_4$ and concentrated to afford compound ***54*** as a colorless oil (78 mg, 94% yield, 40% ee). ^{1}H NMR (500 MHz, $CDCl_3$) δ 4.3 (m, 2H), 3.66 (t, *J* = 5 Hz, 2H), 2.65 (m, 1H), 2.22 (m, 1H), 2.05 (td, *J* = 10, 5 Hz, 1H), 1.75 (td, *J* = 15, 10 Hz 1H), 1.59 (m, 4H), 1.47 (s, 9H), 1.33 (m, 1H); ^{13}C NMR (126 MHz, $CDCl_3$) δ 175.4, 168.7, 83.1, 66.3, 62.3, 54.9, 33.5, 32.6, 31.9, 27.9, 21.0; HRMS ($C_{13}H_{22}O_5$, ESI): calculated 259.154 $[M+H]^{+1}$, found 259.1539.

*3.3.6 Synthesis of compound **41***

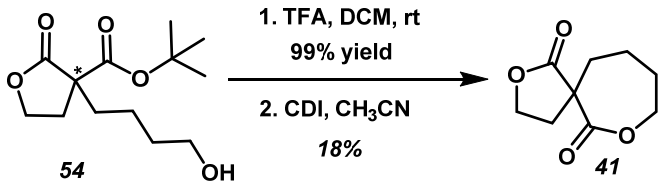

Figure 33. Compound ***41***

To a solution of alcohol ***54*** (125 mg, 0.42 mmol) in CH_2Cl_2 (1 mL) was added 0.2 mL of trifluoroacetic acid (excess). The reaction mixture was stirred at room temperature until reaction completion was determined by TLC analysis. The reaction was diluted with CH_2Cl_2 and was extracted with CH_2Cl_2 (2 x 15 mL) and acidic aqueous layer (1 x 10 mL). The organic layer was dried over $MgSO_4$ and concentrated to afford a carboxylic acid intermediate ***55*** as a colorless oil (100 mg, 99% yield). ^{1}H NMR (400 MHz, $CDCl_3$) δ 8.38 (bs, 1H), 4.38 (m, 4H), 2.78 (m, 1H), 2.27 (m, 1H), 212 (m, 1H), 2.81 (m, 1H), 1.55 (m, 1H), 1.40 (m, 1H).

The carboxylic acid (43 mg, 0.22 mmol) was concentrated in a scintillation vial which was later purged with argon. Acetonitrile (4.3 mL, 0.05M) and carbonyldiimidazole (38 mg, 0.24 mmol) were then added to the vial, and the reaction was stirred overnight. The mixture was concentrated and purified via column chromatography (60% ethyl acetate/hexanes) to obtain the product ***41*** as a white solid (7 mg, 18%). ^{1}H NMR (500 MHz, $CDCl_3$) δ 4.83 (m, 1H), 4.36 (m, 2H), 4.24 (m, 1H), 2.96 (m, 1H), 2.24 (m, 2H), 2.07 (m, 1H), 1.93 (m, 2H), 1.80 (m, 1H), 1.73 (m, 1H); ^{13}C NMR (126 MHz, $CDCl_3$) δ 174.5, 170.7, 69.8, 65.7, 56.0, 34.7, 32.0, 28.8, 24.1.

3.4 Synthesis of Compound *40*

*3.4.1 Synthesis of intermediate **65***

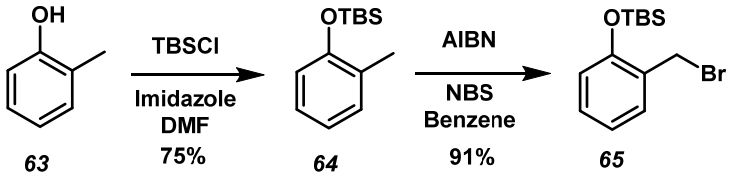

Figure 34. Intermediate ***65***

Dry DMF (10 mL, 0.1 M) was added to a 50 mL flask followed by *o*-cresol ***63*** (1.0 mL, 10 mmol). Imidazole (1.50 g, 22 mmol) was added next followed by *tert*-butyldimethylsilyl chloride (1.66 g, 11 mmol). The reaction was left stirring overnight and quenched with water after 21 hours. The mixture was extracted with ethyl acetate, dried over $MgSO_4$ and concentrated in vacuo. The mixture was purified via column chromatography (10% ethyl acetate /hexanes) to obtain ***64*** as a colorless oil (1.65 g, 75% yield). ^{1}H NMR (500 MHz, $CDCl_3$) δ 7.13 (d, *J*= 10 Hz, 1H), 7.05 (t, *J* = 10 Hz, 1H), 6.85 (t, *J* = 10 Hz, 1H), 6.77 (d, *J*= 5 Hz, 1H), 2.21 (s, 3H), 1.02 (s, 9H), 0.22 (s, 6H); ^{13}C NMR (126 MHz, $CDCl_3$) δ 154.0, 131.0, 129.0, 126.7, 121.1, 118.6, 25.9, 18.4, 17.0, -4.1.

To a 100 mL round bottom flask was added benzene (20 mL) followed by compound ***64*** (1.65 g, 7.4 mmol). azobisisobutyronitrile (183 mg, 1.1 mmol) and *N*-bromosuccinimide (1.45 g, 8.2 mmol) were added next, and the reaction was left stirring for 4 hours under reflux (90^{o}C). After 4 hours the reaction mixture was cooled to room temperature and filtered through a fritted funnel with 1 inch of silica while being rinsed with hexanes. Compound ***65*** was obtained as a colorless oil without the need of purification (1.99 g, 91% yield). ^{1}H NMR (500 MHz, $CDCl_3$) δ 7.32 (d, *J* = 10 Hz, 1H),

7.17 (t, J = 10 Hz, 1H), 6.91 (t, *J* = 15 Hz, 1H), 6.80 (d, *J* = 15 Hz, 1H), 4.52 (s, 2H), 1.04 (s, 9H), 0.28 (s, 6H); ^{13}C NMR (126 MHz, $CDCl_3$) δ 154.0, 131.0, 130.0, 128.5, 121.4, 118.7, 29.5, 25.9, 18.4, -4.0.

*3.4.2 Synthesis of intermediate **81***

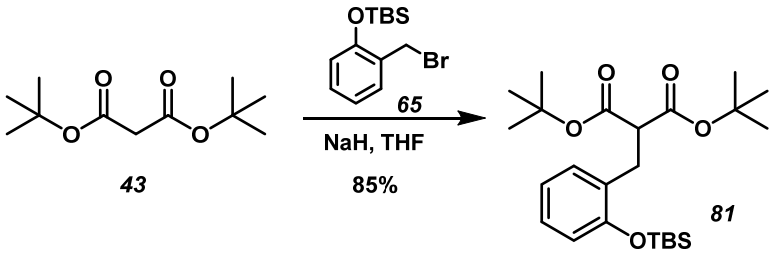

Figure 35. Intermediate ***81***

To a 50 mL round bottom flask containing NaH (60% dispersion, 94 mg, 2.3 mmol), was added di-*tert*-butyl malonate (0.35 mL, 1.6 mmol), THF (16 mL), and ***65*** (570 mg, 1.9 mmol). The mixture was stirred overnight at room temperature, then quenched with H_2O (10 mL) and diluted with ethyl acetate (30 mL). The layers were separated, and the organic layer was washed with water (10 mL), dried over $MgSO_4$, and concentrated in vacuo. The resulting crude material was purified using silica gel column chromatography (10% ethyl acetate/hexanes) to afford the mono alkylated intermediate ***81*** as a white solid (580 mg, 85% yield) which was taken directly on to the next step. ^{1}H NMR (500 MHz, $CDCl_3$) δ 7.11 (m, 1H), 7.08 (m, 1H), 6.82 (m, 1H), 6.76 (m, 1H), 3.60 (t, *J* = 7.9 Hz, 1H), 3.07 (d, *J* = 7.9 Hz, 2H), 1.39 (s, 18H), 1.00 (s, 9H), 0.25 (s, 6H); ^{13}C NMR (126 MHz, $CDCl_3$) δ 168.6, 153.9, 131.4, 128.7, 127.8, 120.8, 118.2, 81.3, 53.4, 30.5, 28.0, 25.9, 18.3, -4.0; HRMS ($C_{24}H_{40}O_5Si$, ESI): calculated 437.2723 $[M+H]^{+1}$, found 437.2718; mp= 67.8- 69.5°C.

*3.4.3 Synthesis of intermediate **67***

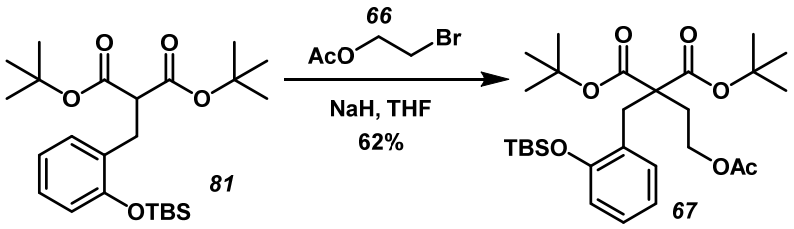

Figure 36. Intermediate ***67***

To a 50 mL round bottom flask containing NaH (60% dispersion, 93 mg, 2.3 mmol), was added ***81*** (340 mg, 0.78 mmol), THF (8 mL), and 2-bromoethylacetate ***66*** (0.26 mL, 2.3 mmol). The mixture was stirred overnight at room temperature, then quenched with H_2O (10 mL) and diluted with ethyl acetate (30 mL). The layers were separated, and the organic layer was washed with water (10 mL), dried over $MgSO_4$, and concentrated in vacuo. The resulting crude material was purified using silica gel column chromatography (10% ethyl acetate/hexanes) to afford the dialkylated intermediate ***67*** as a colorless oil (254 mg, 62% yield). ^{1}H NMR (400 MHz, $CDCl_3$) δ 7.15 (m, 1H), 7.06 (m, 1H), 6.82 (m, 1H), 6.77 (m, 1H), 4.11 (t, *J* = 8.0 Hz, 2H), 3.26 (s, 2H), 2.04 (t, *J*= 8.0 Hz, 2H), 1.95 (s, 3H), 1.44 (s, 18H), 1.00 (s, 9H), 0.21 (s, 6H); ^{13}C NMR (101 MHz, $CDCl_3$) δ 170.9, 170.4, 154.3, 131.1, 127.6, 127.4, 119.0, 81.8, 61.4, 58.1, 32.1, 31.8, 27.9, 26.0, 21.1, 18.4, -4.0; HRMS ($C_{28}H_{46}O_7Si$, ESI): calculated 523.3091 $[M+H]^{+1}$, found 523.3087.

*3.4.4 Synthesis of intermediate **68***

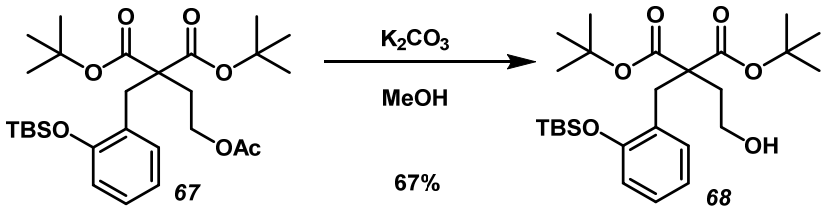

Figure 37. Intermediate ***68***

To a 50 mL round bottom flask, was added compound ***67*** (190 mg, 0.36 mmol) in methanol (7 mL), followed by K_2CO_3 (150 mg, 1.1 mmol). The mixture was stirred at room temperature for 30 min and then separated with H_2O and Ethyl acetate. The aqueous layer was extracted with ethyl acetate (3 x 7 mL) and the combined organic layers were dried with $MgSO_4$, filtered and concentrated in vacuo. The mixture was purified via column chromatography (20% Ethyl acetate/hexanes) to obtain the product ***68*** as a colorless oil (117 mg, 67% yield). ^{1}H NMR (400 MHz, $CDCl_3$) δ 7.15 (m, 1H), 7.06 (m, 1H), 6.82 (m, 1H), 6.77 (m, 1H), 3.66 (t, *J* = 6.5 Hz, 2H), 3.27 (s, 2H), 1.98 (t, *J* = 6.5 Hz, 2H), 1.45 (s, 18H), 1.00 (s, 9H), 0.21 (s, 6H); ^{13}C NMR (126 MHz, $CDCl_3$) δ 171.2, 130.9, 127.6, 127.6, 121.1, 119.2, 81.9, 59.4, 59.0, 36.2, 32.4, 28.0, 26.0, 18.5, -4.0; HRMS ($C_{26}H_{44}O_6Si$, ESI): calculated 503.2805 $[M+Na]^{+1}$, found 503.2799.

*3.4.5 Synthesis of intermediate **69***

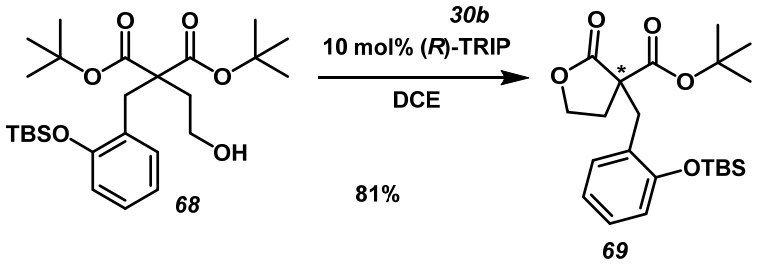

Figure 38. Intermediate ***69***

To a solution of (*R*)-TRIP ***30b*** (29.8 mg, 0.040 mmol) in CH_2Cl_2 (4 mL) was added compound ***68*** (190 mg, 0.40 mmol) and the solution was stirred for 11 days at room temperature. The reaction was extracted with ethyl acetate (2 x 10 mL) and H_2O (1 x 10 mL). The organic phase was dried over $MgSO_4$ and concentrated to afford after purification (20% ethyl acetate/hexanes) the lactone intermediate ***69*** as a white solid (130 mg, 81% yield). ^{1}H NMR (400 MHz, $CDCl_3$) δ 7.21 (m, 1H), 7.11 (m, 1H), 6.87 (m, 1H), 6.79 (m, 1H), 4.17 (q, *J* = 8.5 Hz, 1H), 3.83 (td, *J* = 8.5, 4.0 Hz, 1H), 3.51 (d, *J* = 12.0 Hz, 1H), 3.11 (d, *J* = 12.0 Hz, 1H), 2.46 (m, 1H), 2.24 (m, 1H), 1.48 (s, 9H), 0.99 (s, 9H), 0.22 (d, *J* = 19.7 Hz, 6H); ^{13}C NMR (101 MHz, $CDCl^3$) δ 175.8, 169.1, 154.3, 131.8, 128.4, 126.6, 121.8, 118.6, 83.0, 66.4, 56.4, 31.8, 30.1, 27.9, 25.9, 18.3, -3.8, -4.3; HRMS ($C_{26}H_{44}O_6Si$, ESI): calculated 407.2253 $[M+H]^{+1}$, found 407.2248; mp= 91.5°C-93.2°C

*3.4.6 Synthesis of intermediate **70***

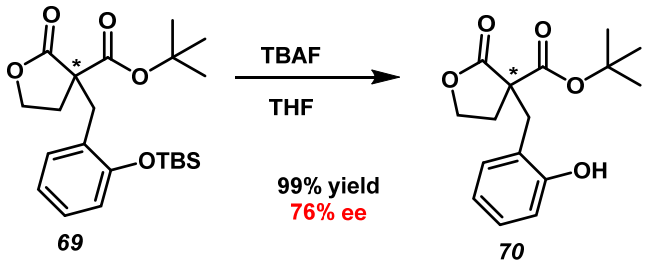

Figure 39. Intermediate ***70***

To a 10 mL round bottom flask was added compound ***69*** (115 mg, 0.28 mmol) and dry THF (4 mL). Tetra- *n*- butylammonium fluoride (0.85 mL. 0.85 mmol) was then added to the solution and the reaction was left stirring at 0°C for 2 hours. The mixture was separated with H_2O (1x 10 mL) and ethyl acetate (2x 10 mL) and dried over $MgSO_4$. The crude material underwent column chromatography (30% ethyl acetate/hexanes) to obtain ***70*** as a yellow oil (80 mg, 97% yield, 75% ee). ^{1}H NMR (500 MHz, $CDCl_3$) δ 7.16 (m, 1H), 7.09 (bs, 1H), 7.06 (m, 1H), 6.89 (m, 1H), 6.85 (m, 1H), 4.31 (m, 1H), 4.22 (td, *J* = 8.0, 4.0 Hz, 1H), 3.30 (d, *J* = 14.7 Hz, 1H), 3.17 (d, *J* = 14.7 Hz, 1H), 2.58 (m, 1H), 2.47 (m, 1H), 1.45 (s, 9H); ^{13}C NMR (126 MHz, $CDCl_3$) δ 177.1, 169.5, 155.1, 121.9, 120.7, 117.8, 84.4, 56.6, 32.6, 31.3, 27.8; HRMS ($C_{16}H_{20}O_5$, ESI): calculated 293.1389 $[M+H]^{+1}$, found 293.1380.

*3.4.7 Synthesis of compound **40***

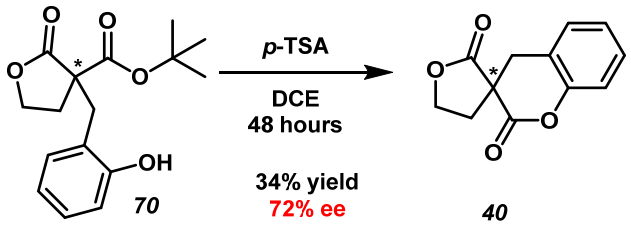

Figure 40. Compound ***40***

To a 10 mL round bottom flask was added compound ***70*** (70 mg, 0.24 mmol) dissolved in dry dichloroethane (2.5 mL) followed by *p*-toluenesulfonic acid (41 mg, 0.24 mmol). The reaction was left stirring at room temperature for 36 hours. The mixture was separated with H_2O (1x 10 mL) and ethyl acetate (2x 10 mL) and dried over $MgSO_4$. The crude material underwent column chromatography (30% ethyl acetate/hexanes) to obtain ***40*** as a white solid (18 mg, 35% yield, 72% ee). ^{1}H NMR (500 MHz, $CDCl_3$) δ 7.32 (m, 1H), 7.23 (m, 1H), 7.16 (m, 1H), 7.10 (m, 1H), 4.45 (m, 2H), 3.62 (d, *J* = 16.2 Hz, 1H), 2.93 (d, *J* = 16.2 Hz, 1H), 2.62 (m, 1H), 2.23 (m, 1H); ^{13}C NMR (126 MHz, $CDCl_3$) δ 173.2, 165.7, 151.0, 128.6, 125.3, 119.6, 116.8, 65.7, 49.2, 33.8, 33.0; HRMS ($C_{12}H_{10}O_4$, ESI): calculated 219.0657 [M+H]+1, found 219.0651; $[\alpha]_D^{21}$= – 9.09° (c = 0.22, $CHCl_3$); mp= 140.1 - 141.8°C.

3.5 Synthesis of Compound *71*

*3.5.1 Synthesis of intermediate **82***

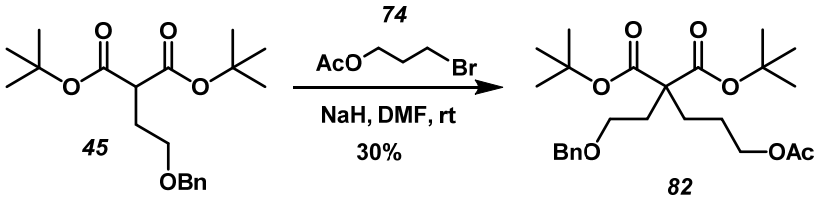

Figure 41. Intermediate ***82***

To a 25 mL round bottom flask containing NaH (60% dispersion, 83 mg, 2.1 mmol), was added ***45*** (365 mg, 1.0 mmol), DMF (10 mL), and 3-bromopropylacetate ***74*** (282 mg, 1.6 mmol). The mixture was stirred overnight at room temperature, then quenched with H_2O (10 mL) and diluted with Ethyl acetate (30 mL). The layers were separated, and the organic layer was washed with water (10 mL), dried over $MgSO_4$, and concentrated in vacuo. The resulting crude material was purified using silica gel column chromatography (20% ethyl acetate/hexanes) to afford the dialkylated intermediate ***82*** as a colorless oil (135 mg, 30% yield). ^1H NMR (500 MHz, $CDCl_3$) δ 7.31 (m, 5 H), 4.46 (s, 2H), 4.00 (t, *J*= 5Hz, 2H), 3.42 (t, *J*= 5Hz, 2H), 2.16 (t, *J*= 5Hz, 2H), 2.01 (s, 3H), 1.87 (m, 2H), 1.41 (s, 18H).

*3.5.2 Synthesis of intermediate **76***

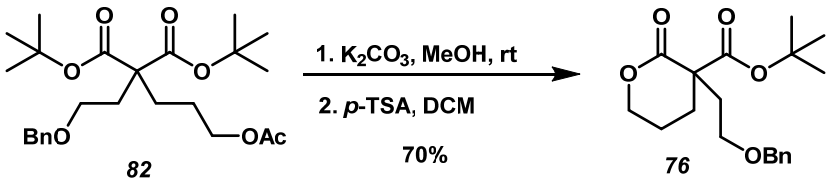

Figure 42. Intermediate ***76***

To a 10 mL round bottom flask, was added compound ***82*** (135 mg, 0.30 mmol) in MeOH (7 mL), followed by K_2CO_3 (150 mg, 1.1 mmol). The mixture was stirred at room temperature for hour and then separated with H_2O and ethyl acetate. The aqueous layer was extracted with ethyl acetate (3 x 7 mL) and the combined organic layers were dried with $MgSO_4$, filtered and concentrated in vacuo. The intermediate alcohol was isolated without purification as a colorless oil (122 mg, 99% yield).

To a 10 mL round bottom flask was added the alcohol intermediate (122 mg, 0.30 mmol) dissolved in dry dichloromethane (3 mL) followed by *p*-toluenesulfonic acid (57 mg, 0.33 mmol). The reaction was left stirring at room temperature for 24 hours. The mixture was separated with H_2O (1x 10 mL) and ethyl acetate (2x 10 mL) and dried over $MgSO_4$. The product was obtained as a colorless oil ***76*** (72 mg, 70% yield) ^{1}H NMR (500 MHz, $CDCl_3$) δ 7.31 (m, 5H), 4.46 (q, *J*= 15, 5 Hz, 2H), 4.25 (m, 2H), 3.61 (m, 2H), 2.32 (m, 2H), 2.17 (m, 1H), 1.94 (m, 2H), 1.84 (m, 1H), 1.44 (s, 9H); ^{13}C NMR (126 MHz, $CDCl_3$) δ 170.6, 170.4, 138.3, 128.5, 127.8, 127.7, 83.0, 73.1, 68.7, 66.6, 53.7, 35.8, 28.5, 27.9, 20.7.

*3.5.3 Synthesis of compound **71***

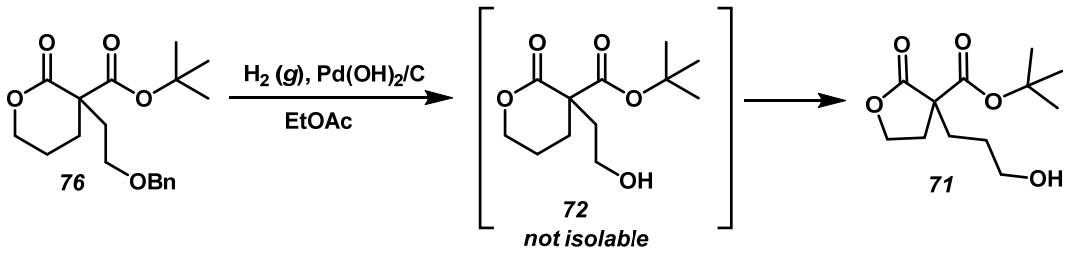

Figure 43. Compound ***71***

To a solution of compound ***76*** (77 mg, 0.23 mmol) in ethyl acetate (5 mL) was added $Pd(OH)_2$ (20% on carbon, 16 mg, 0.12 mmol) and the solution was stirred under hydrogen pressure using a balloon filled with hydrogen gas at room temperature until reaction completion was determined by TLC analysis. The reaction mixture was filtered through a plug of Celite® and the filtrate was concentrated under vacuum, to afford compound ***71*** as colorless oil (56 mg, 99% yield). ^{1}H NMR (400 MHz, $CDCl_3$) δ 4.30 (m, 2H), 3.63 (m, 2H), 2.63 (m, 1H), 2.21 (m, 1H), 2.05(m, 1H), 1.88 (bs, 1H), 1.81 (m, 1H), 1.67 (m, 1H), 1.53 (m, 1H), 1.44 (s, 9H); ^{13}C NMR (101 MHz, $CDCl_3$) δ 175.5, 168.8, 98.9, 83.3, 66.3, 62.4, 54.6, 32.2, 30.3, 27.9.

3.6 Synthesis of Compound *80*

*3.6.1 Synthesis of intermediate **83***

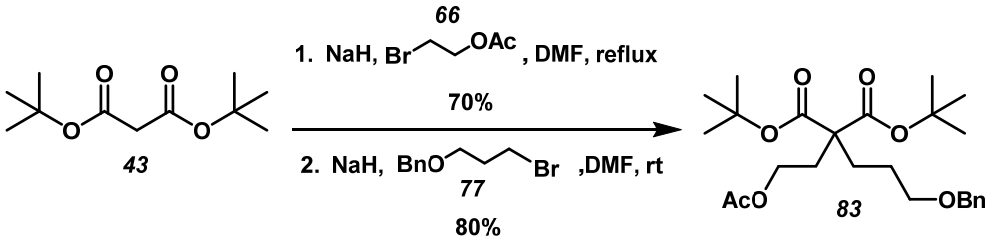

Figure 44. Intermediate ***83***

To a 50 mL round bottom flask containing NaH (60% dispersion, 92 mg, 2.3 mmol), was added di-*tert*-butyl malonate ***43*** (0.518 mL, 2.3 mmol), dry DMF (23 mL) and 2-bromoethyl acetate ***66*** (0.280 mL, 2.5 mmol). The mixture was stirred overnight at room temperature, then quenched with saturated NH_4Cl (10 mL) and diluted with ethyl acetate (30 mL). The layers were separated, the organic layer was washed with water (10 mL), dried over $MgSO_4$, and concentrated in vacuo. The resulting crude material was purified using silica gel column chromatography (10% ethyl acetate/hexanes) to afford the mono-alkylated intermediate as a colorless oil (487 mg, 70% yield) which was used directly in the next step.

The mono-alkylated intermediate (500 mg, 1.7 mmol), was added to a 25 mL round bottom flask containing NaH (60% dispersion, 132 mg, 3.3 mmol) and DMF (17 mL). Next, 3- bromopropylbenzylether ***77*** (0.440 mL, 2.48 mmol) was added to the solution. The mixture was stirred overnight at rt then quenched with H_2O (10 mL) and diluted with ethyl acetate (30 mL). The layers were separated, the organic layer was washed with water (10 mL), dried over $MgSO_4$, and concentrated in vacuo. The resulting crude material was purified using silica gel column chromatography (10% ethyl

acetate/hexanes) to afford ***83*** as a colorless oil (600 mg, 80% yield). ^{1}H NMR (500 MHz, $CDCl_3$) δ 7.31 (m, 5H), 4.48 (s, 2H), 4.06 (t, *J* = 7.2 Hz, 2H), 3.45 (t, *J* = 6.6 Hz, 2H), 2.16 (t, *J* = 7.2 Hz, 2H), 1.99 (s, 3H), 1.88 (m, 2H), 1.49 (m, 2H), 1.44 (s, 18H); ^{13}C NMR (126 MHz, $CDCl_3$) δ 171.0, 170.4, 138.6, 128.4, 127.7, 127.6, 81.6, 72.9, 70.3, 60.8, 56.6, 30.6, 29.1, 27.9, 24.5, 21.0; IR (neat) cm^{-1} 2975, 1720, 1367, 1235, 1147; HRMS ($C_{25}H_{38}O_7$, ESI): calculated 473.2516 $[M+Na]^{+1}$, found 473.2499.

3.6.2 Synthesis of intermediate ***79***

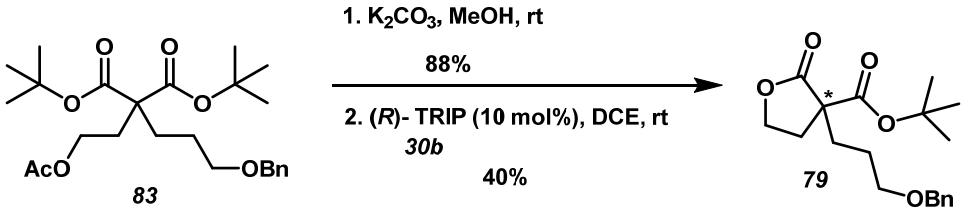

Figure 45. Intermediate ***79***

To a 25 mL round bottom flask, was added compound ***83*** (260 mg, 0.58 mmol) in MeOH (12 mL), followed by K_2CO_3 (160 mg, 1.2 mmol). The mixture was stirred at room temperature for 1 hour and then added to H_2O (2 mL) and diluted with Ethyl acetate (5 mL). HCl was added until the solution was neutralized. The layers were separated, and the aqueous layer was extracted with ethyl acetate (3 x 10 mL). The combined organic layers were dried with $MgSO_4$, filtered and concentrated in vacuo. The resulting crude material did not need any further purification and was isolated as a colorless oil (206 mg, 88% yield) which was used directly in the next step. To a 10 mL round bottom flask, was added the above alcohol (206 mg, 0.50 mmol) in dichloroethane (5 mL), followed by *R*-TRIP ***30b*** (38 mg, 0.050 mmol). The reaction was stirred at room temperature for 10 days then diluted with CH_2Cl_2 (10 mL) and added H_2O (5 mL). The layers were

separated, and the aqueous layer was extracted with ethyl acetate (3 x 5 mL). The combined organic layers were dried over $MgSO_4$, filtered, and concentrated in vacuo. The crude material was purified by silica gel column chromatography (20% to 30% ethyl acetate/hexanes) to afford ***79*** as a colorless oil (68 mg, 40% yield). ^{1}H NMR (500 MHz, $CDCl_3$) δ 7.32 (m, 5H), 4.48 (s, 2H), 4.30 (m, 2H), 3.49 (m, 2H), 2.66 (m, 1H), 2.22 (m, 1H), 2.11 (m, 1H), 1.82 (m, 1H), 1.74 (m, 1H), 1.56 (m, 1H), 1.45 (s, 9H); ^{13}C NMR (126 MHz, $CDCl_3$) δ 175.3, 168.6, 138.4, 128.5, 127.8, 127.8, 83.1, 73.0, 69.9, 66.2, 54.6, 31.9, 30.8, 27.9, 25.2; IR (neat) cm^{-1} 2976, 2342, 1770, 1721, 1368; HRMS ($C_{19}H_{26}O_5$, ESI) calculated 357.1678 $[M+Na]^{+1}$, found 357.1661.

*3.6.3 Synthesis of compound **80***

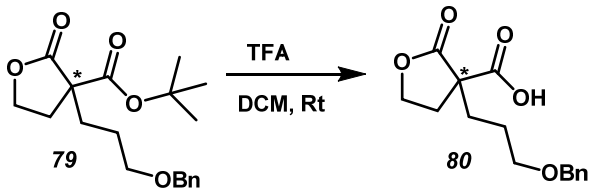

Figure 46. Compound ***80***

To a 10 mL round bottom flask was added compound ***79*** (68 mg, 0.20 mmol) dissolved in CH_2Cl_2 (2 mL). Trifluoroacetic acid was added in excess (0.5 mL) and the reaction was left stirring for 1 hour. The mixture was then concentrated under vacuum to remove any residual trifluoroacetic acid and the product ***80*** was obtained without purification as a colorless oil (56 mg, 99% yield). ^{1}H NMR (500 MHz, $CDCl_3$) δ 10.27 (bs, 1H), 7.32 (m, 5H), 4.51 (s, 2H), 4.35 (m, 2H), 3.52 (m, 2H), 2.74 (m, 1H), 2.25 (m, 1H), 2.17 (m, 1H), 1.88 (m, 1H), 1.76 (m, 1H), 1.61 (m, 1H

REFERENCES

1. Cahn, R. S.; Ingold, C. K.; Prelog, V. *Experientia* **1956**, *12*, 81−94
2. Hoye, T. R.; Jeffrey, C. S.; Shao, F. *Nat. Protoc*. **2007**, *2*, 2451-2458
3. Calcaterra, A.; D'Acquarica, I. *J. Pharm. Biomed. Anal*. **2018**, *147*, 323–340
4. Ji, N.; Shen, Y. *Chirality* **2006**, *18*, 146–158
5. Brooks, W. H.; Guida, W. C.; Daniel, K.G. *Curr. Top. Med. Chem*. **2011,** *11*, 760–770
6. Wang, Y.; Chen, A. M. *Org. Process Res. Dev.* **2008**, *12*, 282-290
7. Ward, L. F.; Enders, J. R.; Bell, D. S.; Cramer, H. M.; Wallace, F. N.; McIntire, G. L. *J. Anal. Toxicol*. **2016**, *40*, 255–263
8. Caballo, C.; Sicilia, M. D.; Rubio, S. *Anal. Bioanal. Chem*. **2015**, *407*, 4721−4731
9. Wang, R. Q; Ong, T. T.; Ng, S. C. *J. Chromatogr. A*. **2008**, *1203*, 185–192
10. Hein, J. E.; Cao, B. H.; Viedma, C.; Kellog, R. M.; Blackmond, D. G. *J. Am. Chem. Soc.* **2012**, *30*, 12629–12636;
11. Lorenz, H.; Capla, F.; Polenske, D.; Elsner, M. P.; Seidel- Morgenstern, *A. J. Chem. Technol. Metall.* **2007**, *42*, 5-16
12. Ceccato, A.; Reus, E.; Brione, W.; Vanderweyen, A.; Flament, A.; Caliaro, G.; Tilstam, U. *Org. Process Res. Dev*. **2007**, *11*, 223−228
13. Sugai, T.; Higashibayashi, S.; Hanaya, K. *Tetrahedron* **2018**, *74*, 3469-3487
14. Scott, J. W.; Valentine, D. Jr. *Science* **1974**, *184*, 943-952
15. Mori, K.; Mori, H. *Org. Synth*. **1990**, *68*, 56
16. (a) Mori, K. *Synlett*. **1995**, *11*, 1097-1109; (b) Philkhana, S. C.; Reddy, D.S. *Tetrahedron Lett.* **2017**, *58*, 1262–1264

17. Fessner, W.D.; Schneider, A.; Held, H.; Sinerius, G.; Walter, C.; Hixon, M.; Schloss J. V. *Angew. Chem. Int. Ed. Engl.* **1996**, *35*, 2219–2221

18. List, B.; Lerner, R. A.; Barbas, C. F. *J. Am. Chem. Soc.* **2000**, *122*, 2395–2396

19. Yoon, T. P.; Jacobsen, E.N; *Science* **2003**, *299*, 1691-1693

20. (a) Magnuson, S.R. *Tetrahedron* **1995**, *51*, 2167-2213; (b) Hodgson, D. M.; Gibbs, A. R.; Lee, J. P. *Tetrahedron* **1996**, *52*, 14361- 14384; (c) Willis, M.C. *J. Chem. Soc., Perkin Trans.* **1999**, *1*, 1765-1784

21. Jossang, A.; Jossang, P.; Hadi, H. A.; Sévenet. T.; Bodo, B. *J. Org. Chem.* **1991**, *56*, 6527-6530

22. Asami, Y.; Kakeya, H.; Onose, R.; Yoshida, A.; Matsuzaki, H.; Osada, H. *Org. Lett.* **2002**, *4*, 2845-2848

23. Krattenmacher, R. *Contraception* **2000**, *62*, 29–38

24. Bister, B.; Bischoff, D.; Ströbele, M.; Riedlinger, J.; Reicke, A.; Wolter, F.; Bull, A. T.; Zähner, H.; Fiedler, H. P.; Süssmuth, R. D. *Angew. Chem. Int. Ed.* **2004**, *43*, 2574–2576

25. Zhang, W. J.; Li, X. H.; Shi, Y. P. *J. Nat. Prod*. **2010**, *73*, 143–146

Wu, Q. X.; Shi, Y. P.; Yang, L. *Org. Lett.* **2004**, *6*, 2313–2316

26. Wilent, J. E.; Qabaja, G.; Kimberly, K. S. *Org. Synth*. **2016**, *93*, 75–87

Wilent, J. E.; Kimberly, K. S. *J. Org. Chem.* **2014**, *79,* 2303-2307

27. Changotra, A.; Sunoj, R. B. *Org. Lett.* **2016**, *18*, 3730-3733

28. Parenty, A.; Moreau, X.; Campagne, J.M. *Chem. Rev*. **2006**, *106*, 911- 939

29. Zhang, Q.; Takacs, J. M. *Org. Lett.* **2008**, *10*, 4, 545-548

30. Kelley, A. M., Minerali, E., Wilent J. E., Chambers, N. J., Stingley K. J., Wilson, G. T., Petersen K. S.; *Tetrahedron Lett.* **2019**, *60*, 1262–1264

APPENDIX A

NMR SPECTRA

The ^{1}H and ^{13}C nuclear magnetic resonance (NMR) spectra were plotted on 400 and 500 MHz spectrometer using $CDCl_3$ as a solvent at room temperature. The NMR chemical shifts (δ) are reported in ppm.

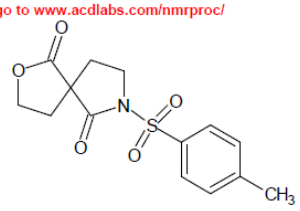

38

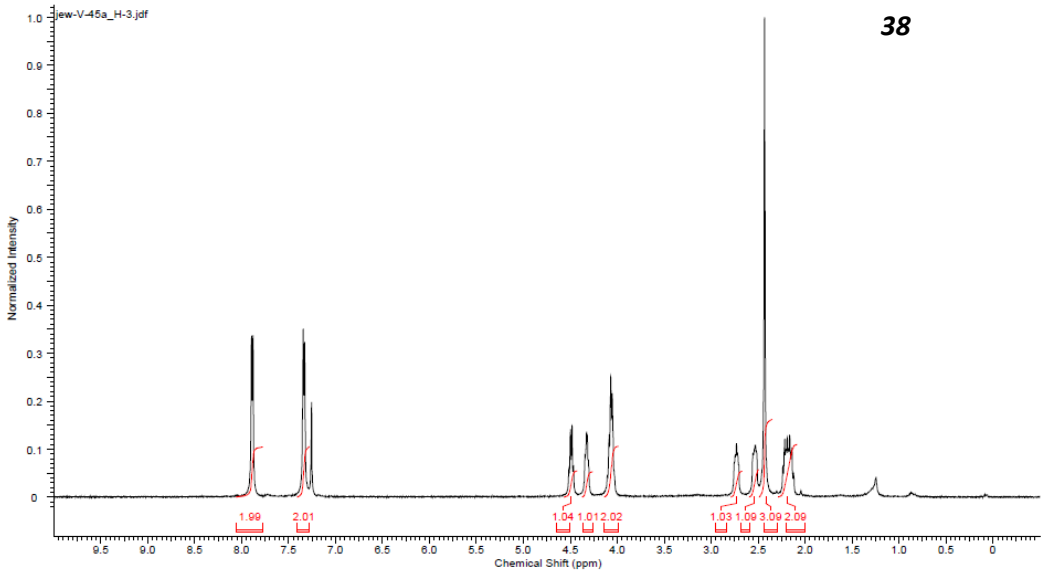

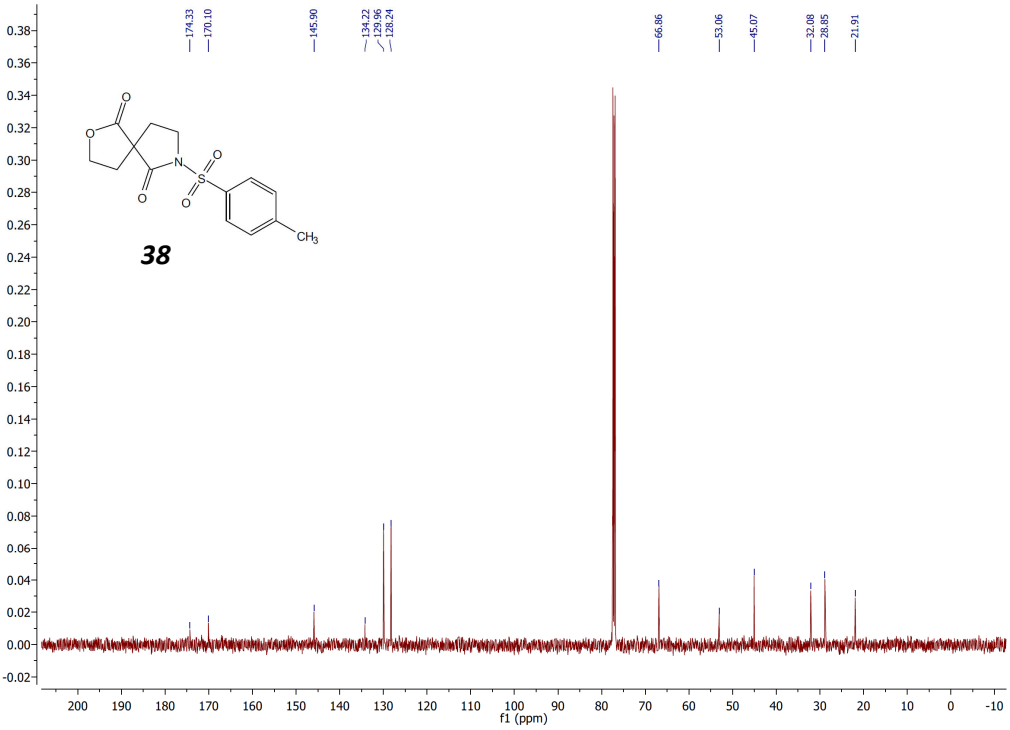

38

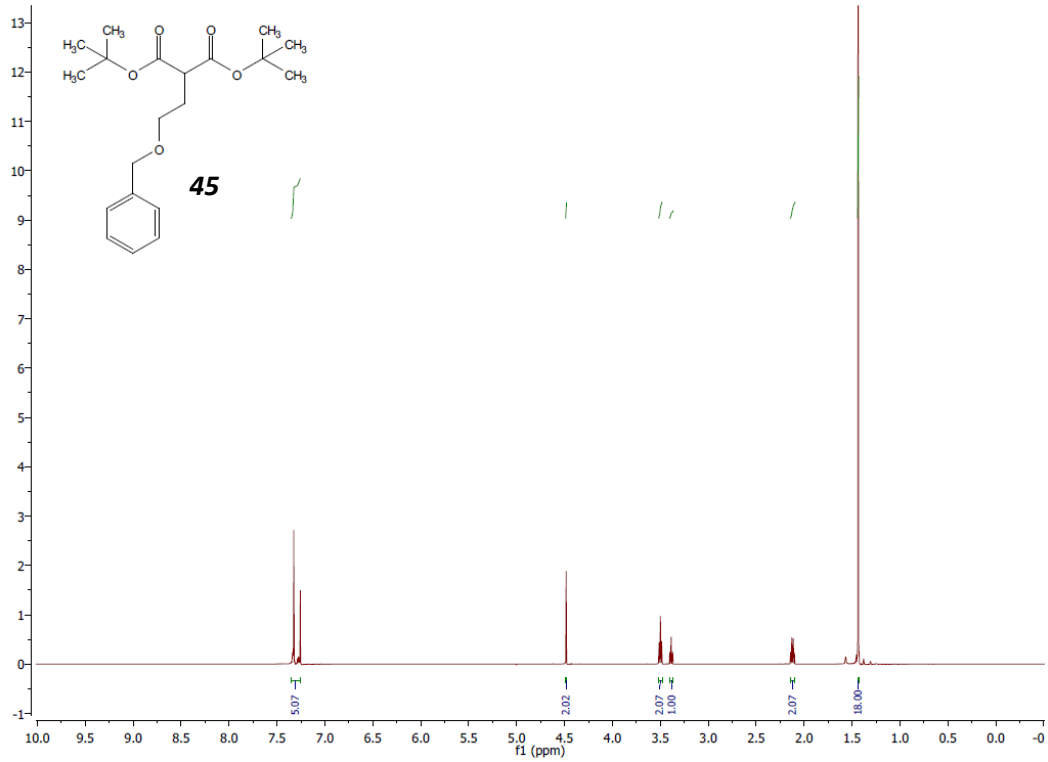
45
5.07
2.02
2.07
1.00
2.07
18.00
f1 (ppm)

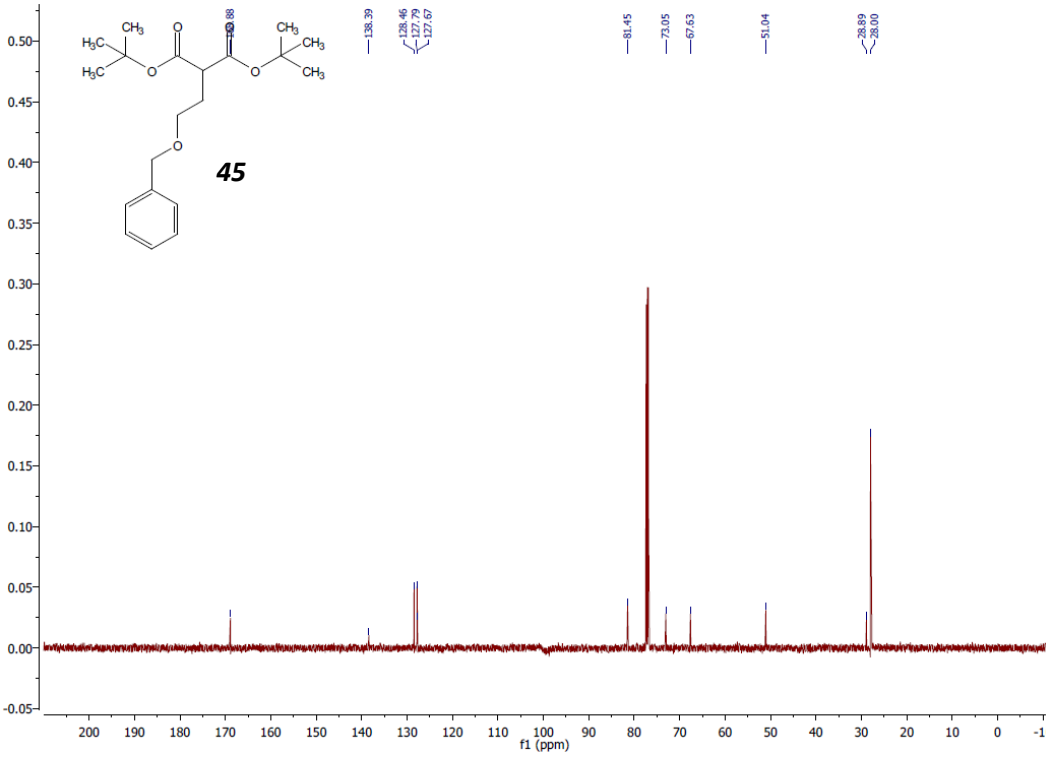
45
138.39
128.46
127.79
127.67
81.45
73.05
67.63
51.04
28.89
28.00
f1 (ppm)

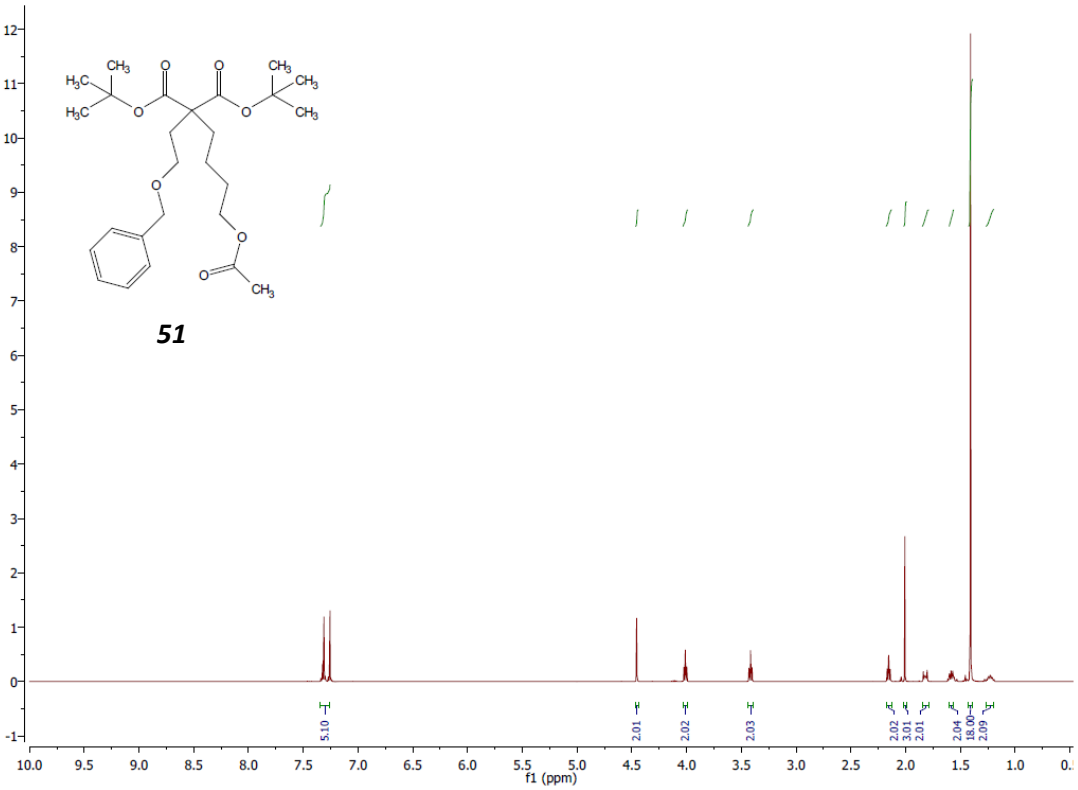

51

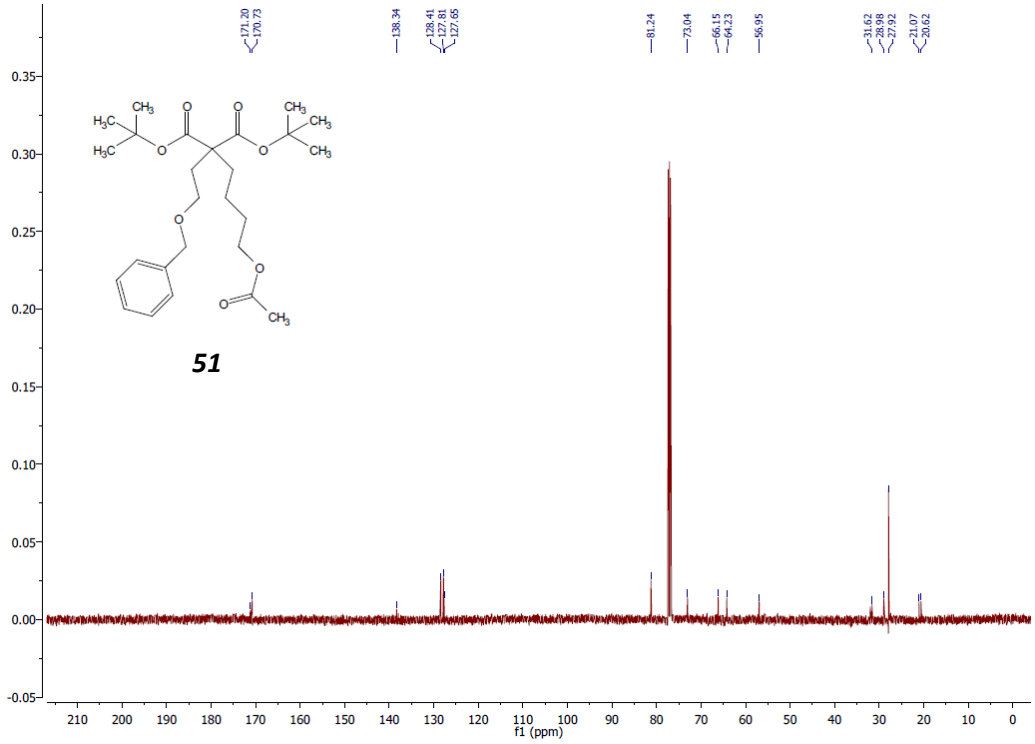

51

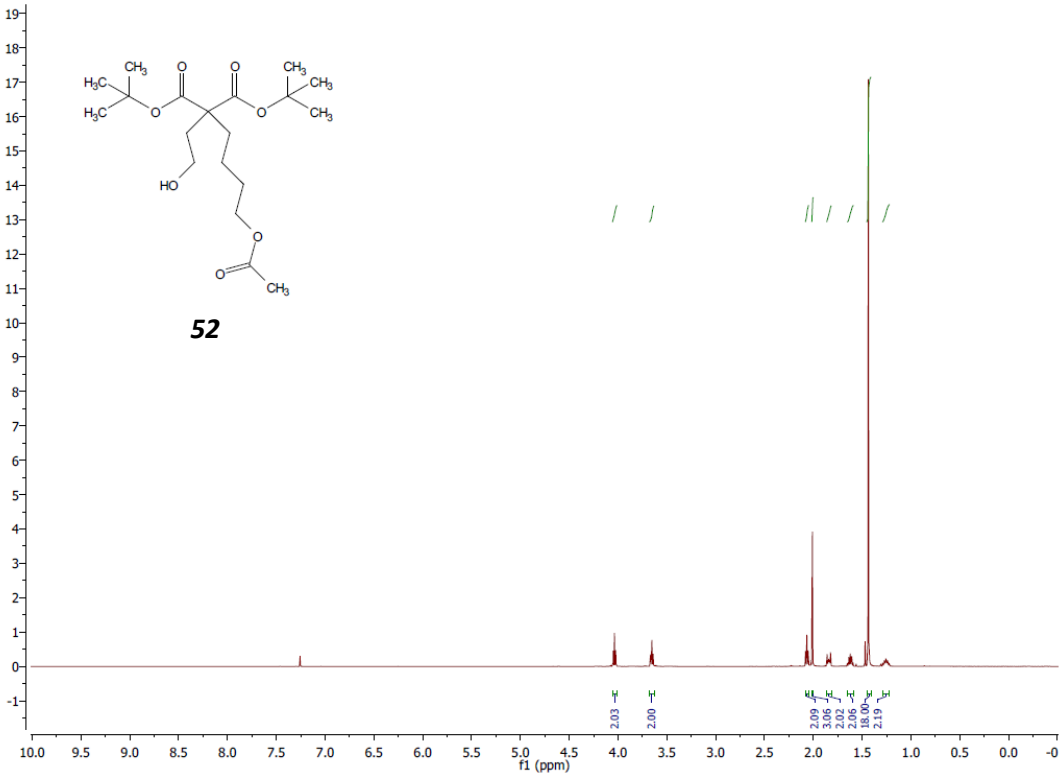
HO
O
O
O
O
O
O
CH3
H3C
H3C
CH3
CH3
CH3
f1 (ppm)

52

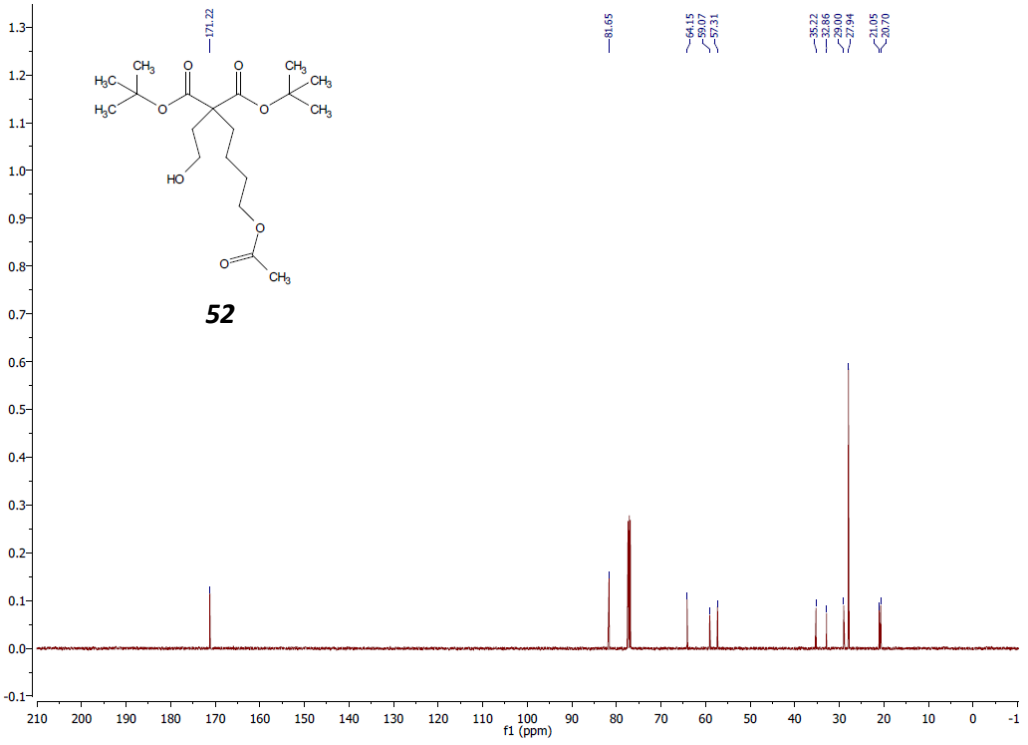
171.22
81.65
64.15
59.07
57.31
35.22
32.66
29.00
27.94
21.05
20.70
HO
O
O
O
O
O
CH3
H3C
H3C
CH3
CH3
CH3
f1 (ppm)

52

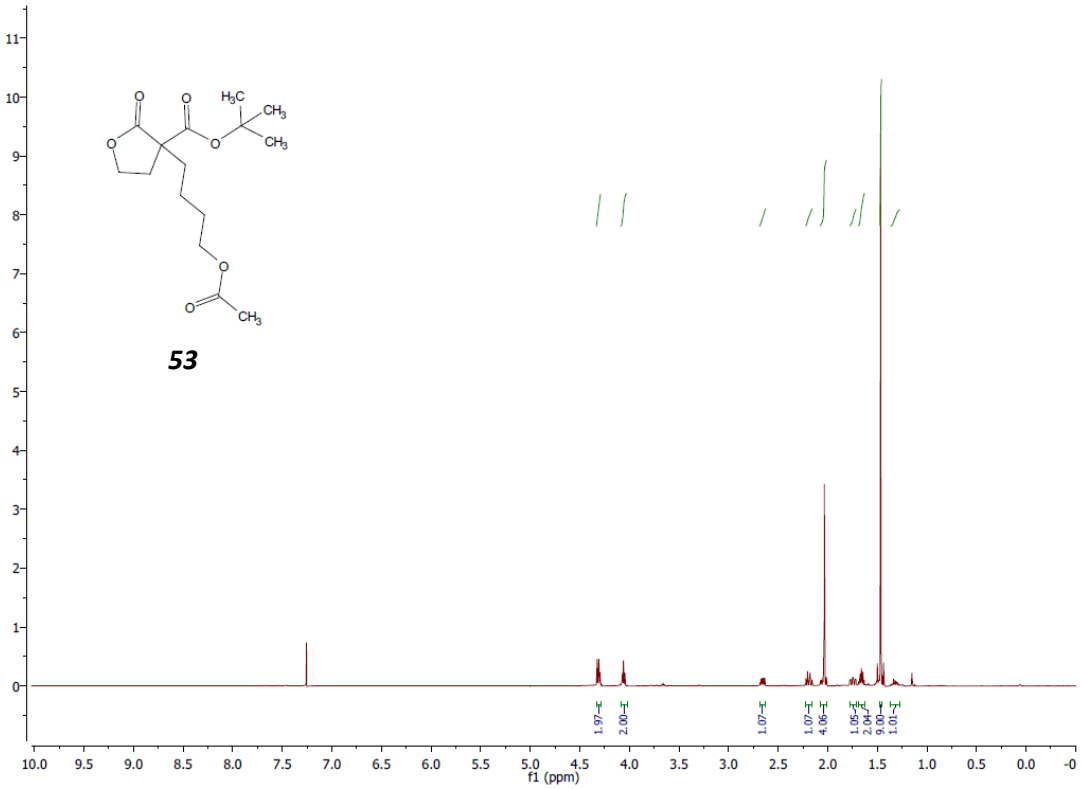

53

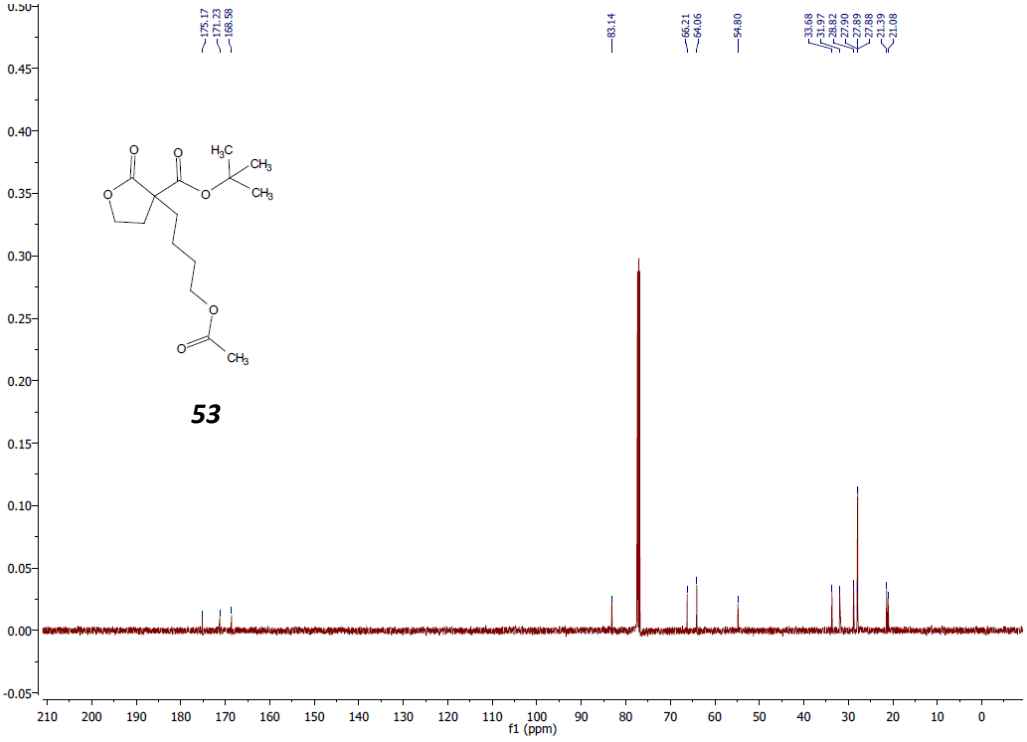

53

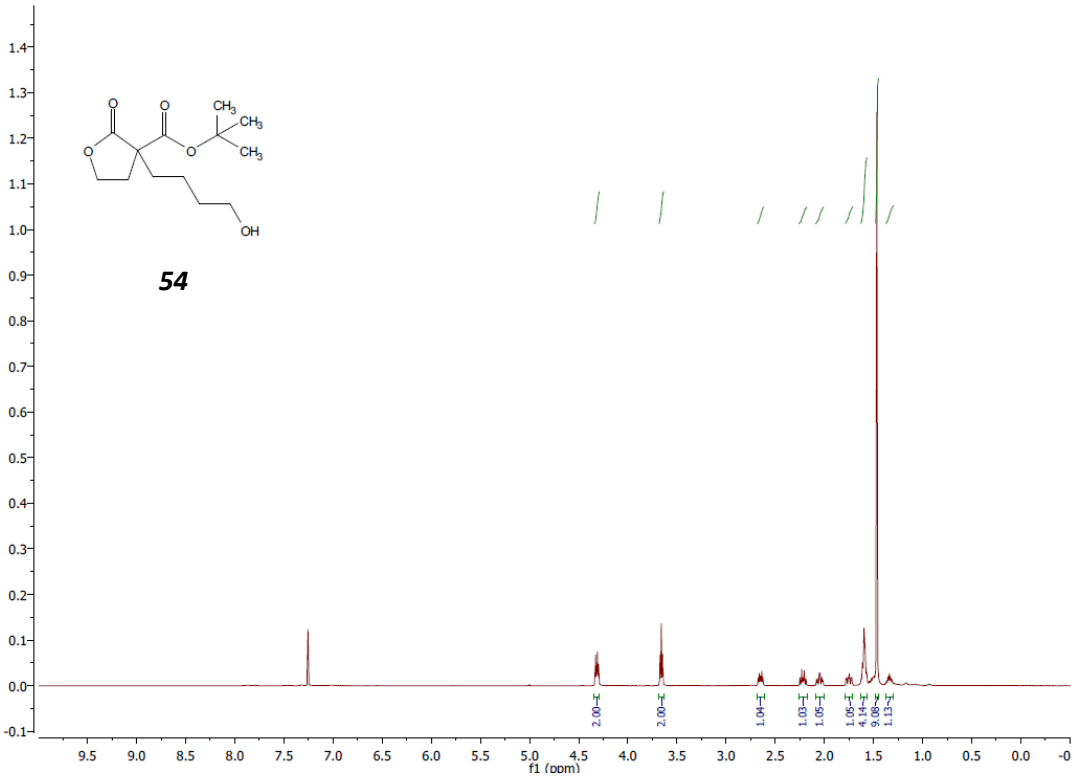
54
f1 (ppm)

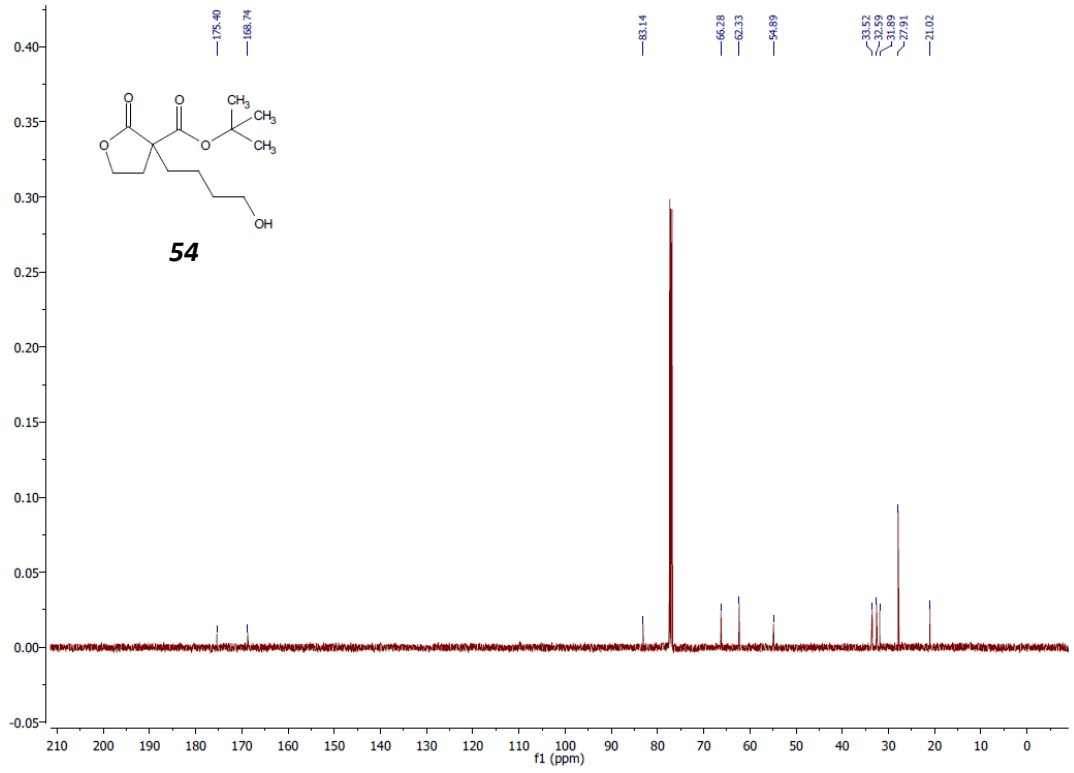
175.40
168.74
83.14
66.28
62.33
54.89
33.52
32.59
31.89
27.91
21.02
54
f1 (ppm)

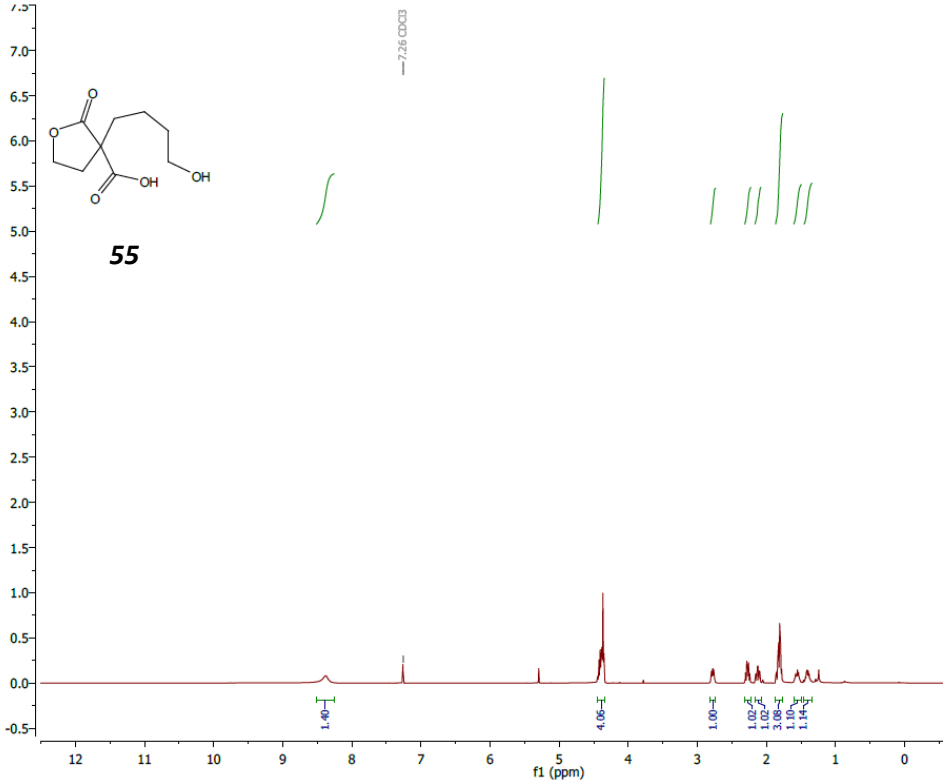

55

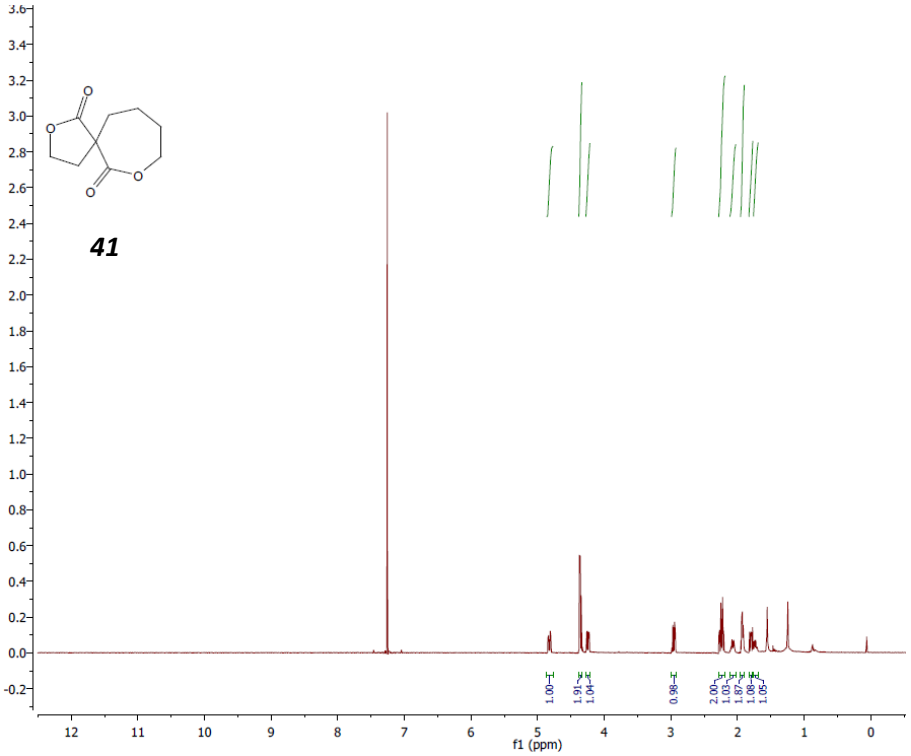

41

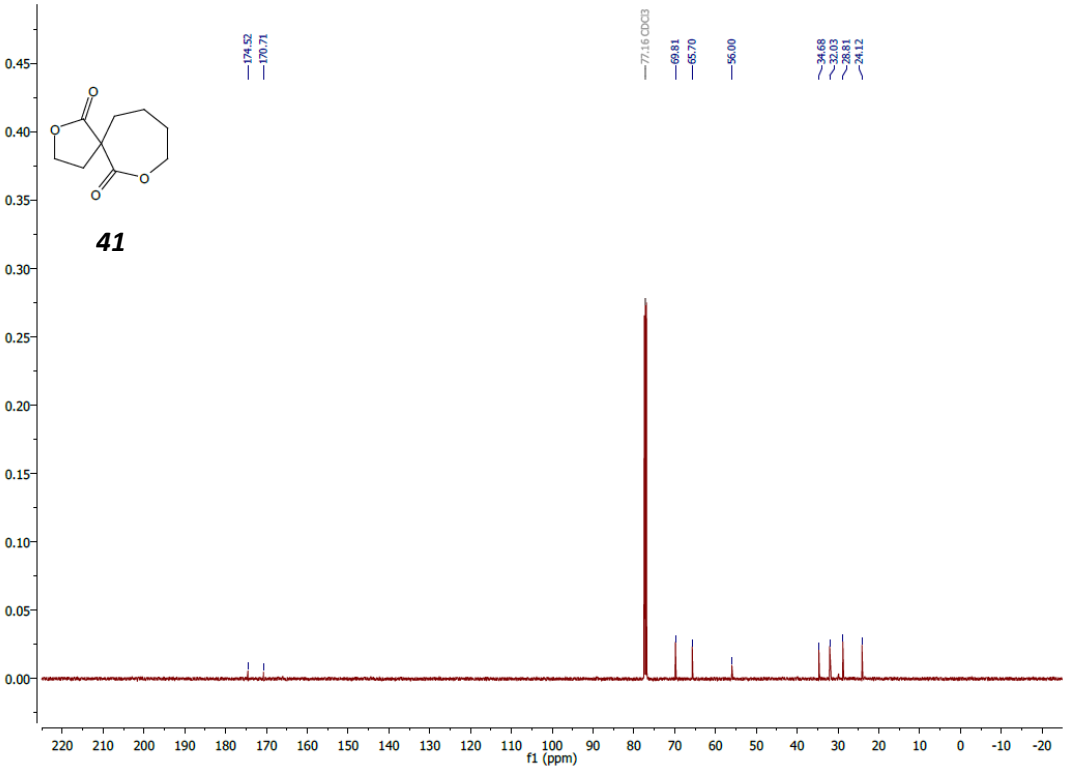
174.52
170.71
77.16 CDCl3
69.81
65.70
56.00
34.68
32.03
28.81
24.12
f1 (ppm)

41

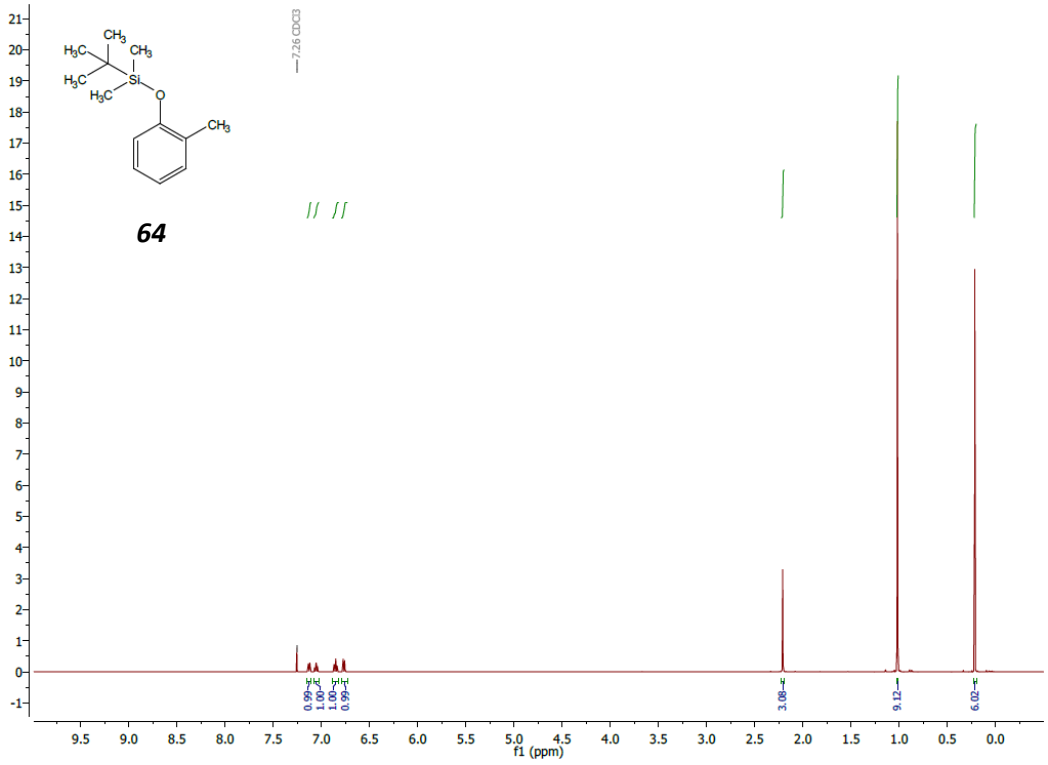
7.26 CDCl3
0.99
1.00
1.08
0.99
3.08
9.12
6.02
f1 (ppm)

64

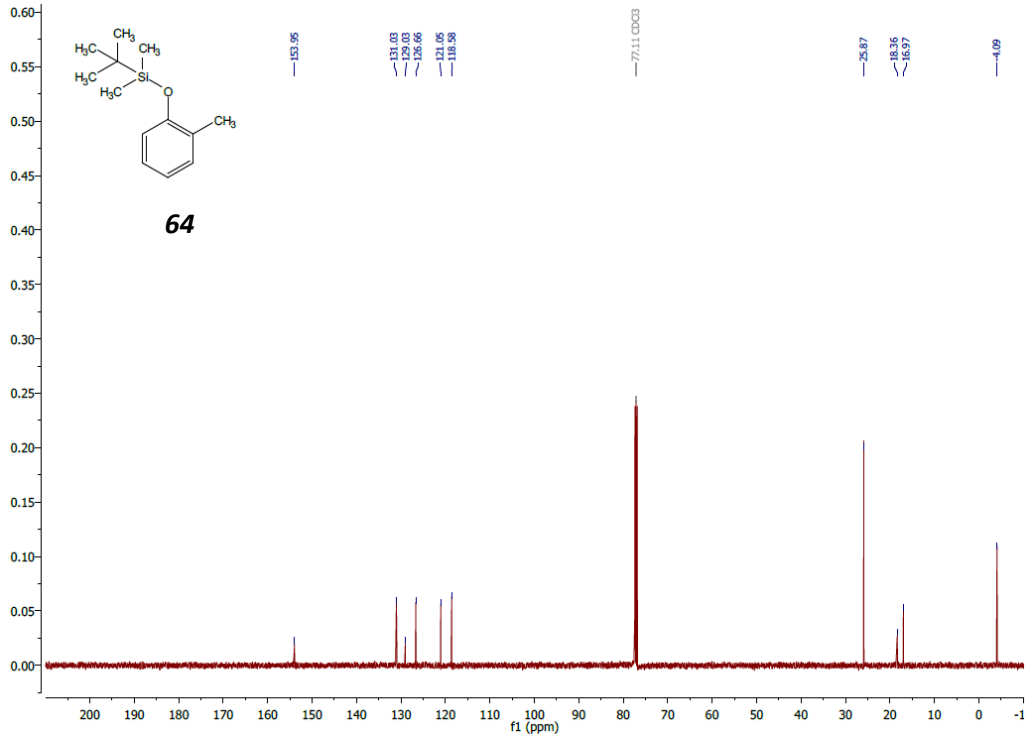
153.95
131.03
129.03
126.66
121.05
118.58
77.11 CDCl3
25.87
18.36
16.97
-4.09
f1 (ppm)

64

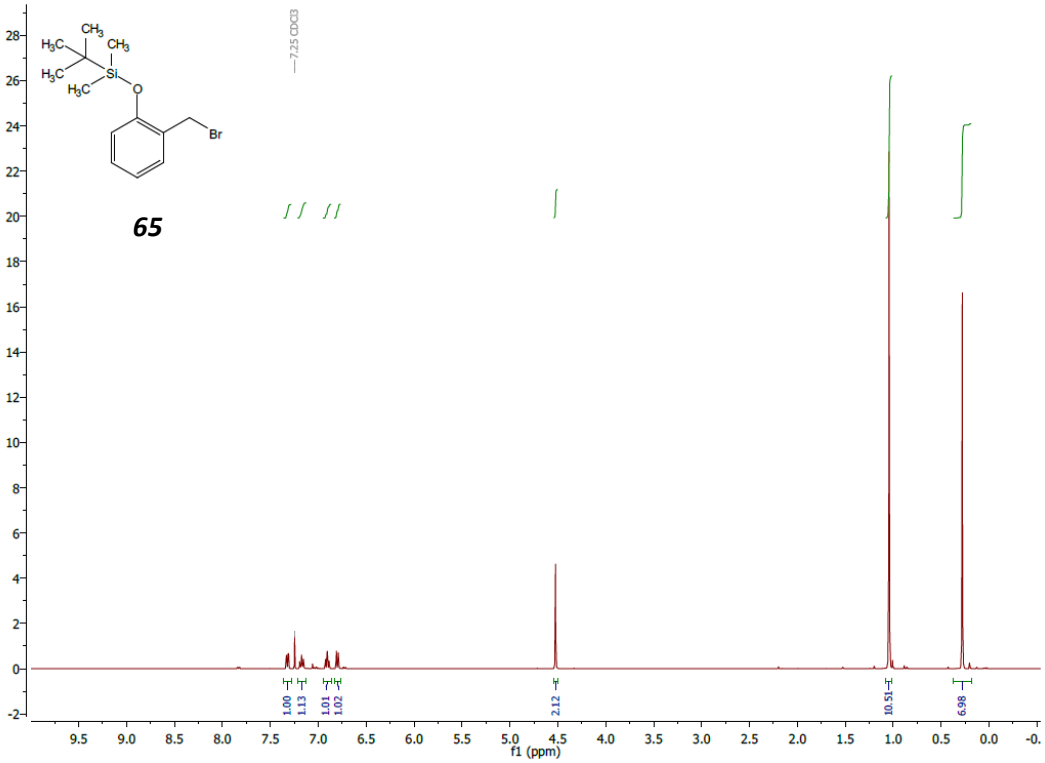
7.25 CDCl3
1.00
1.13
1.01
1.02
2.12
10.51
6.98
f1 (ppm)

65

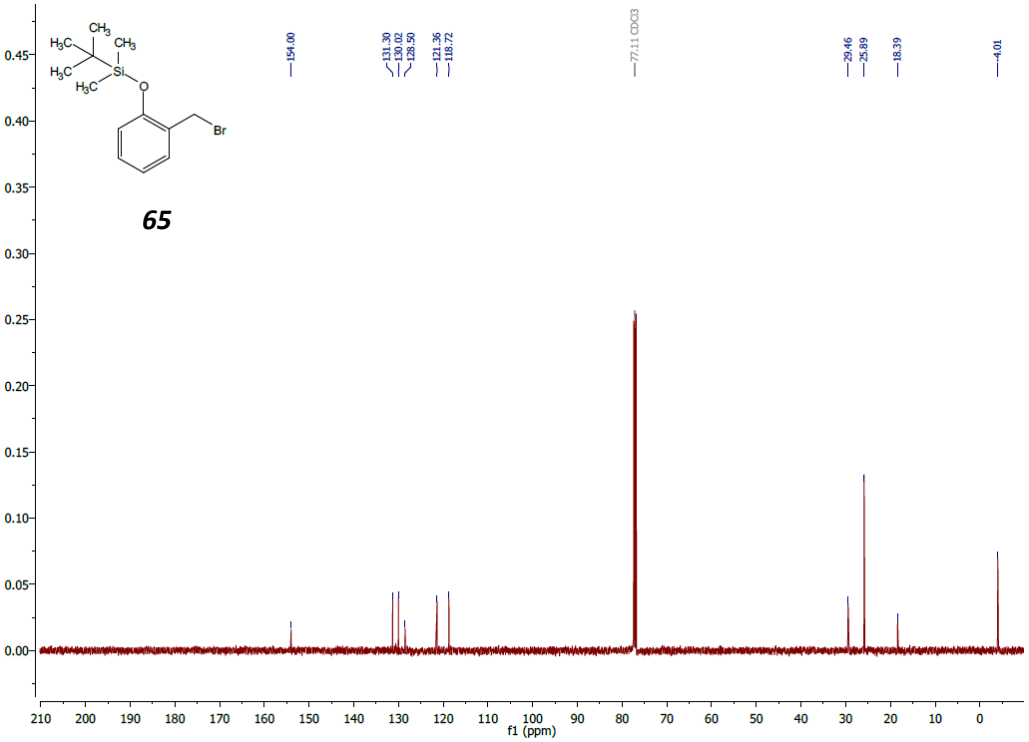
154.00
131.30
130.02
128.50
121.36
118.72
77.11 CDCl3
29.46
25.89
18.39
-4.01
Br
f1 (ppm)

65

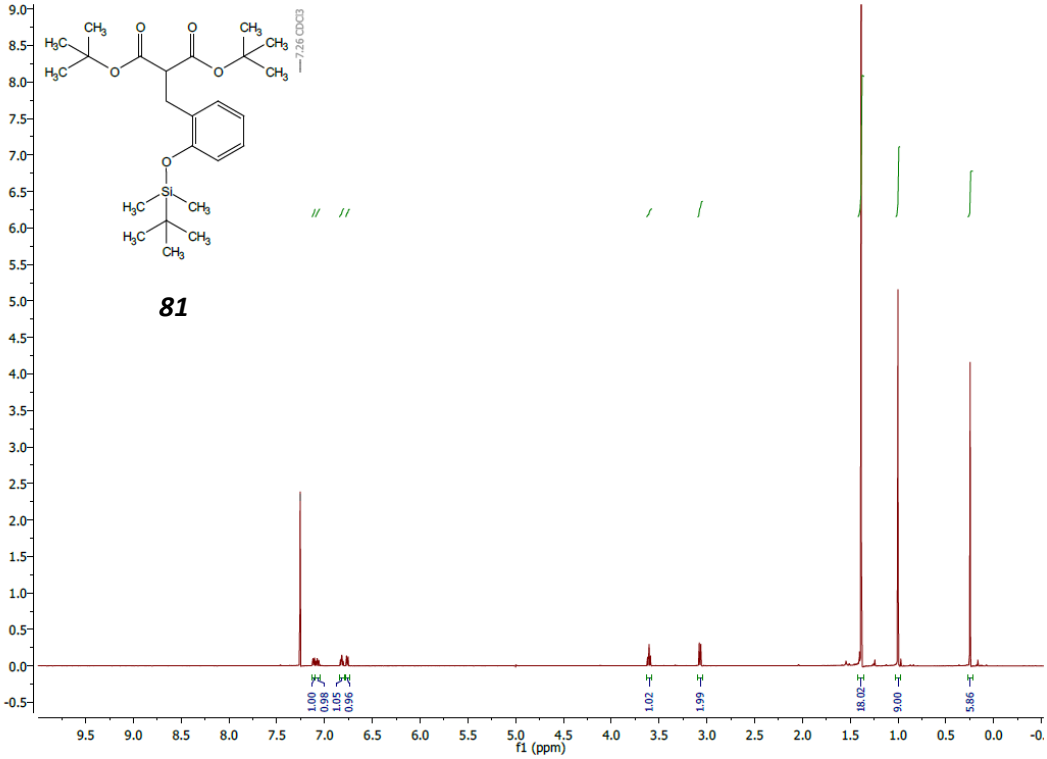
7.26 CDCl3
1.00
0.98
1.05
0.96
1.02
1.99
18.02
9.00
5.86
f1 (ppm)

81

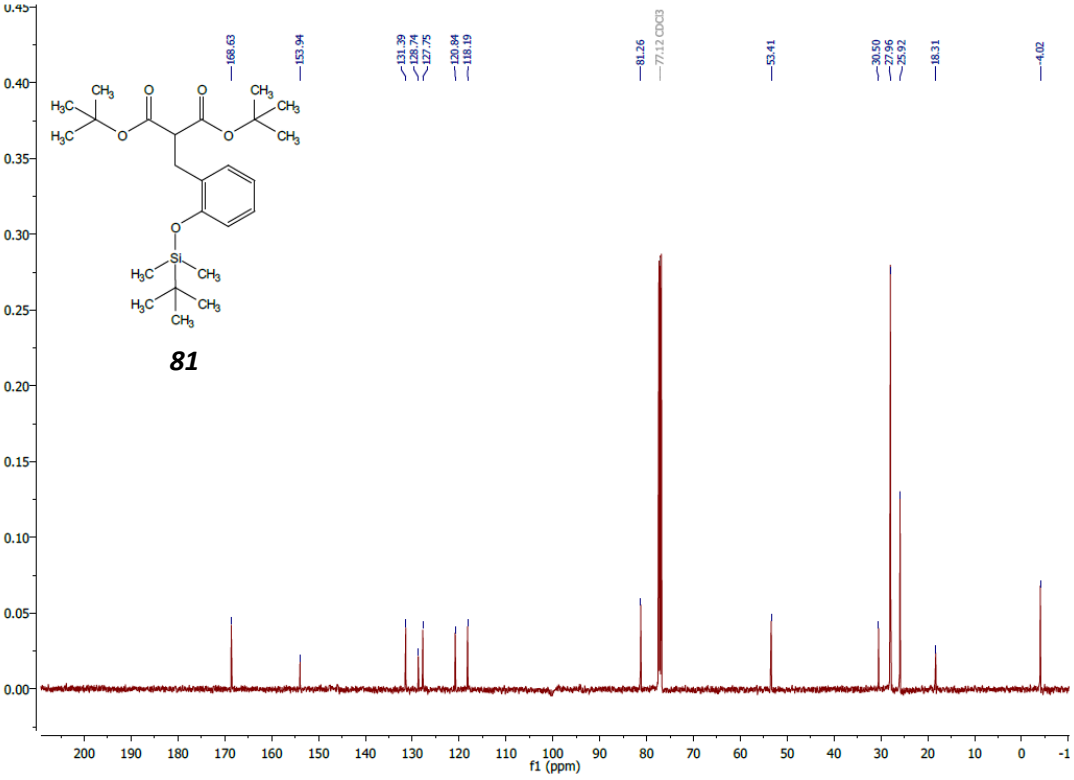
168.63
153.94
131.39
128.74
127.75
120.84
118.19
81.26
77.12 CDCl3
53.41
30.50
27.96
25.92
18.31
-4.02
f1 (ppm)

81

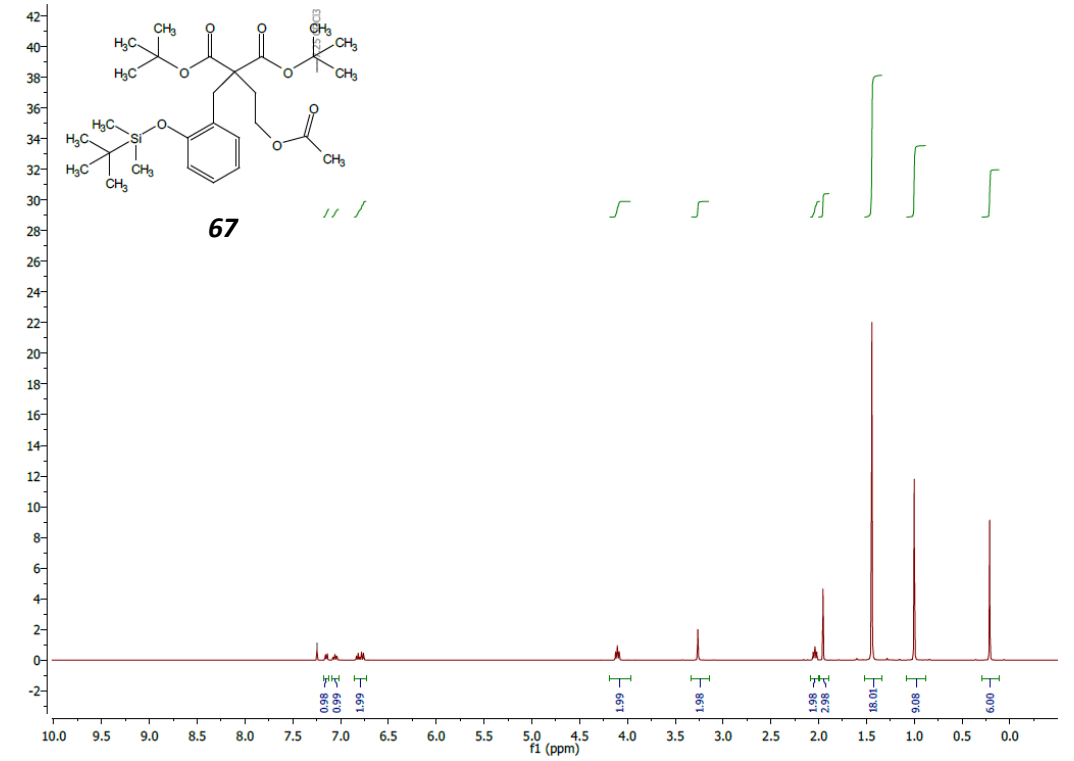
0.98
0.99
1.99
1.99
1.98
1.98
2.98
18.01
9.08
6.00
f1 (ppm)

67

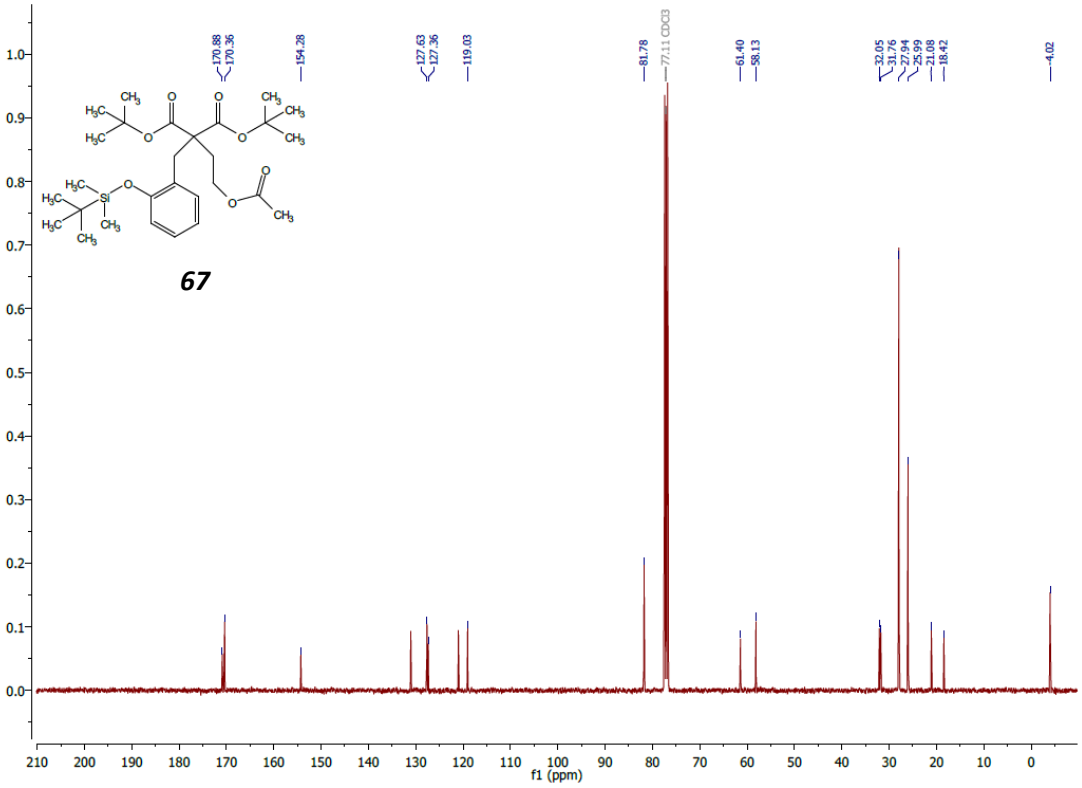
170.88
170.36
154.28
127.63
127.36
119.03
81.78
77.11 CDCl3
61.40
58.13
32.05
31.76
27.04
25.99
21.08
18.42
-4.02
f1 (ppm)

67

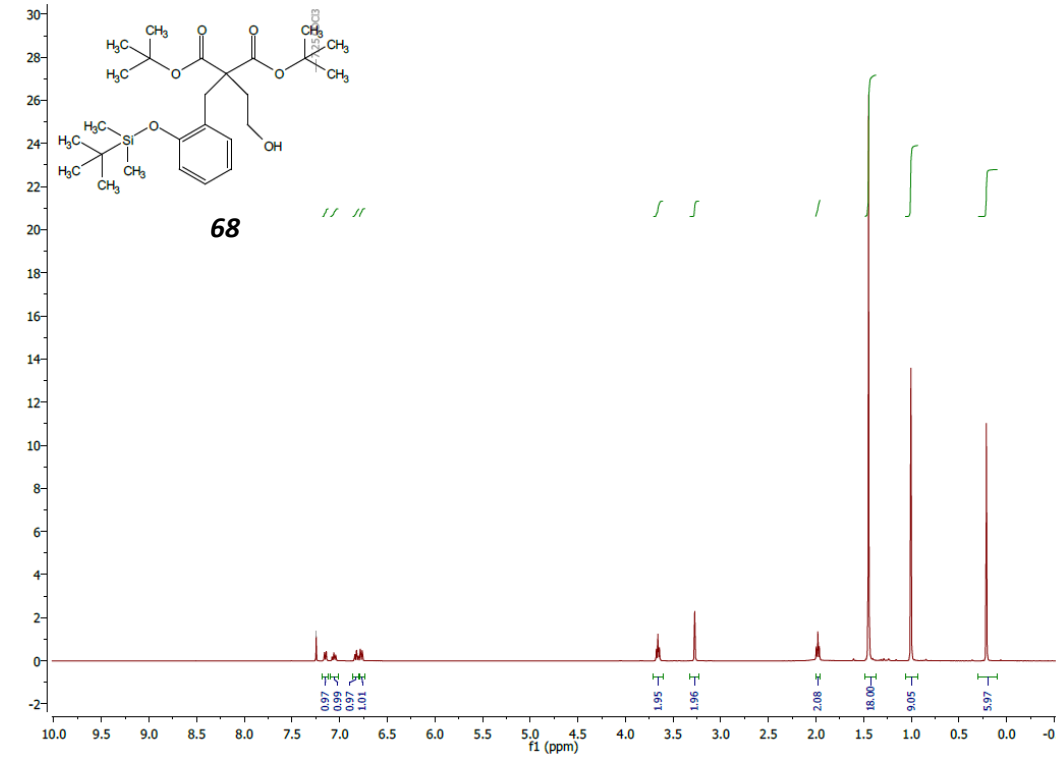
OH
0.97
0.99
0.97
1.01
1.95
1.96
2.08
18.00
9.05
5.97
f1 (ppm)

68

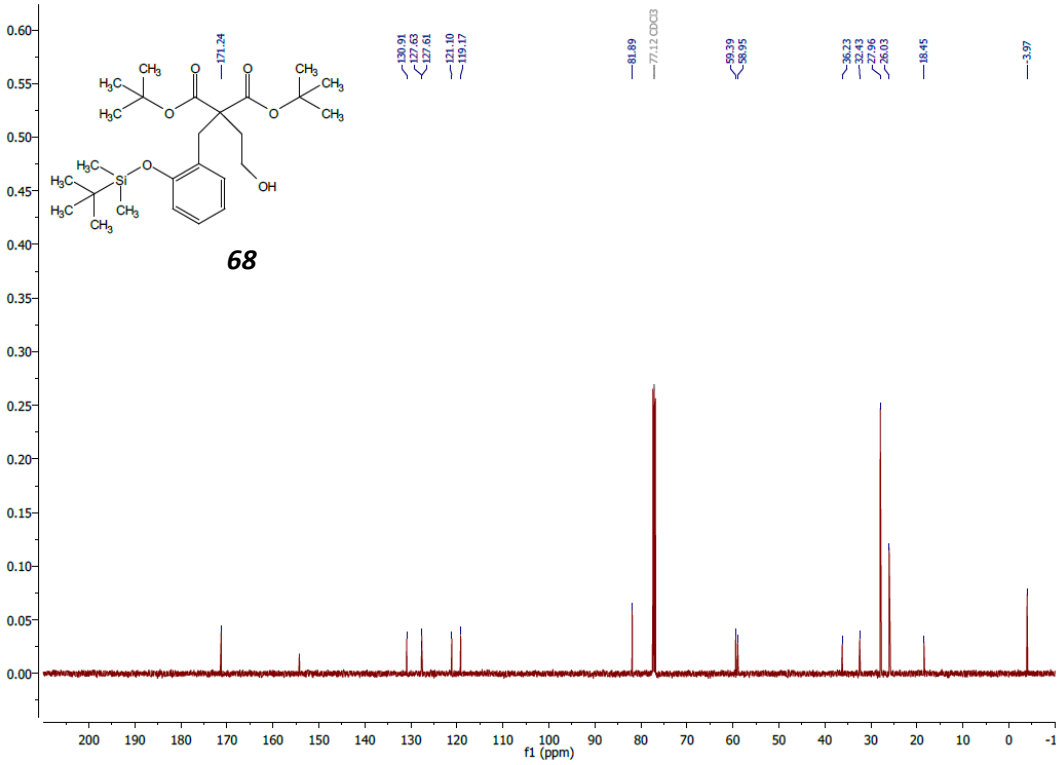
171.24
130.91
127.63
127.61
121.10
119.17
81.89
77.12 CDCl3
59.39
58.95
26.23
24.43
22.96
18.45
-3.97
f1 (ppm)

68

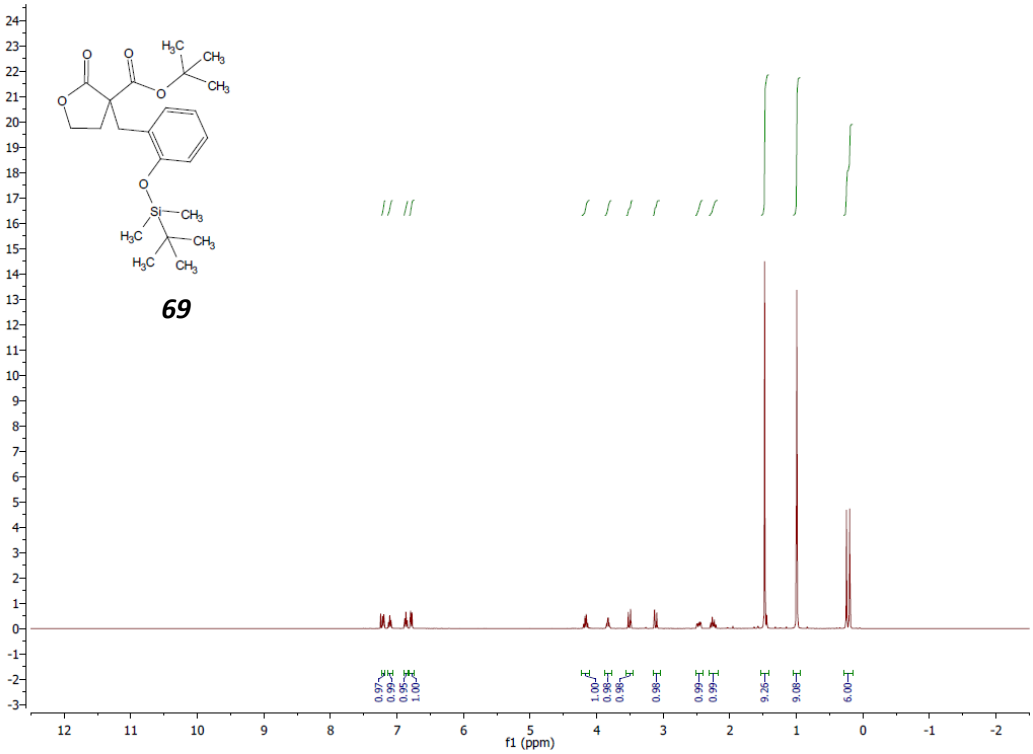
0.97
0.99
0.95
1.00
1.00
0.98
0.98
0.98
0.99
0.99
9.26
9.08
6.00
f1 (ppm)

69

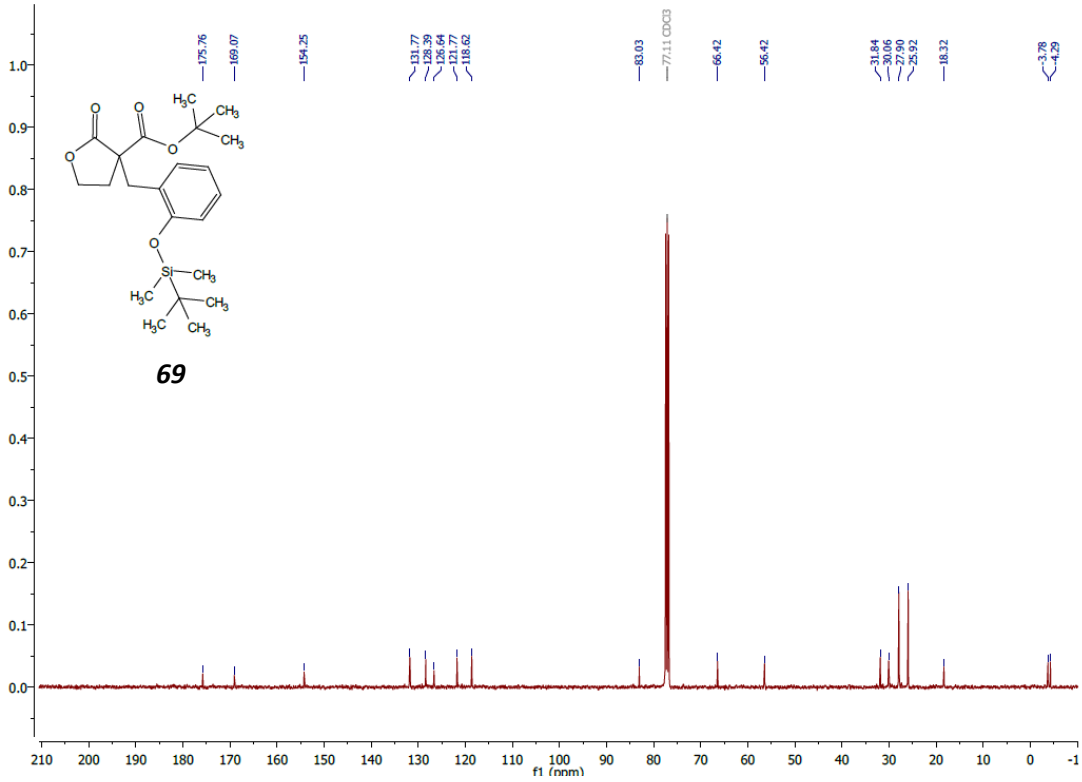
175.76
169.07
154.25
131.77
128.39
126.64
121.77
118.62
83.03
77.11 CDCl3
66.42
56.42
31.84
30.06
27.90
25.92
18.32
-3.78
-4.29
f1 (ppm)

69

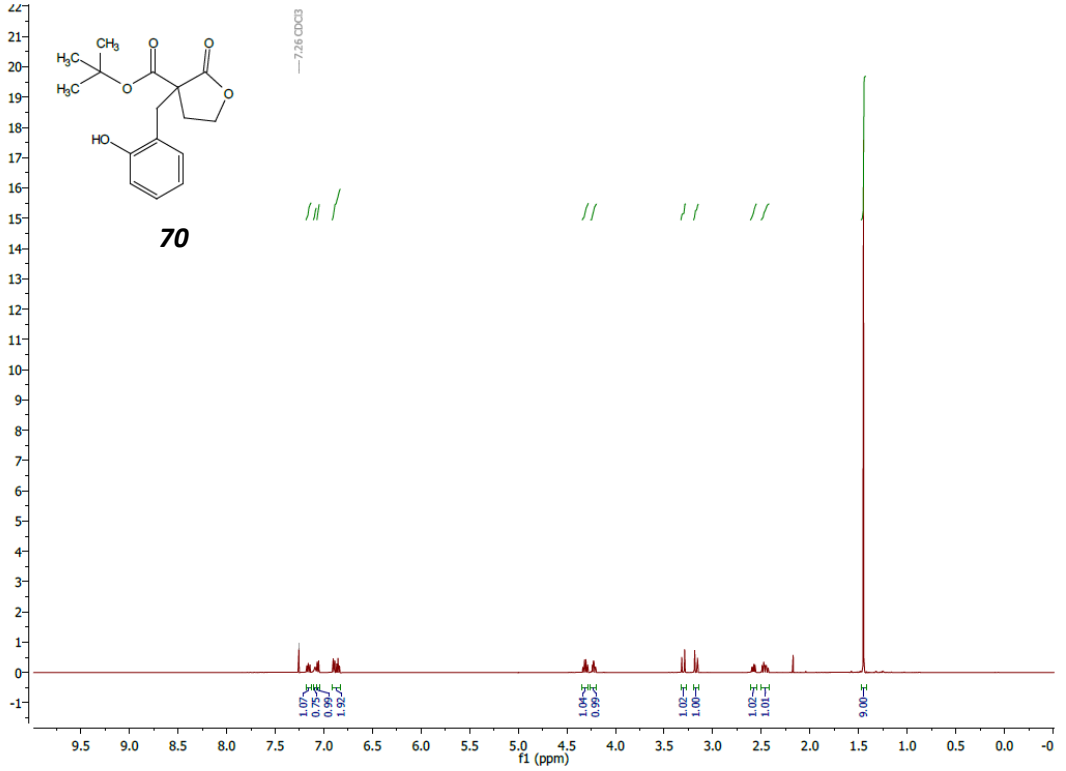
7.26 CDCl3
1.07
0.75
0.99
1.92
1.04
0.99
1.02
1.00
1.02
1.01
9.00
f1 (ppm)

70

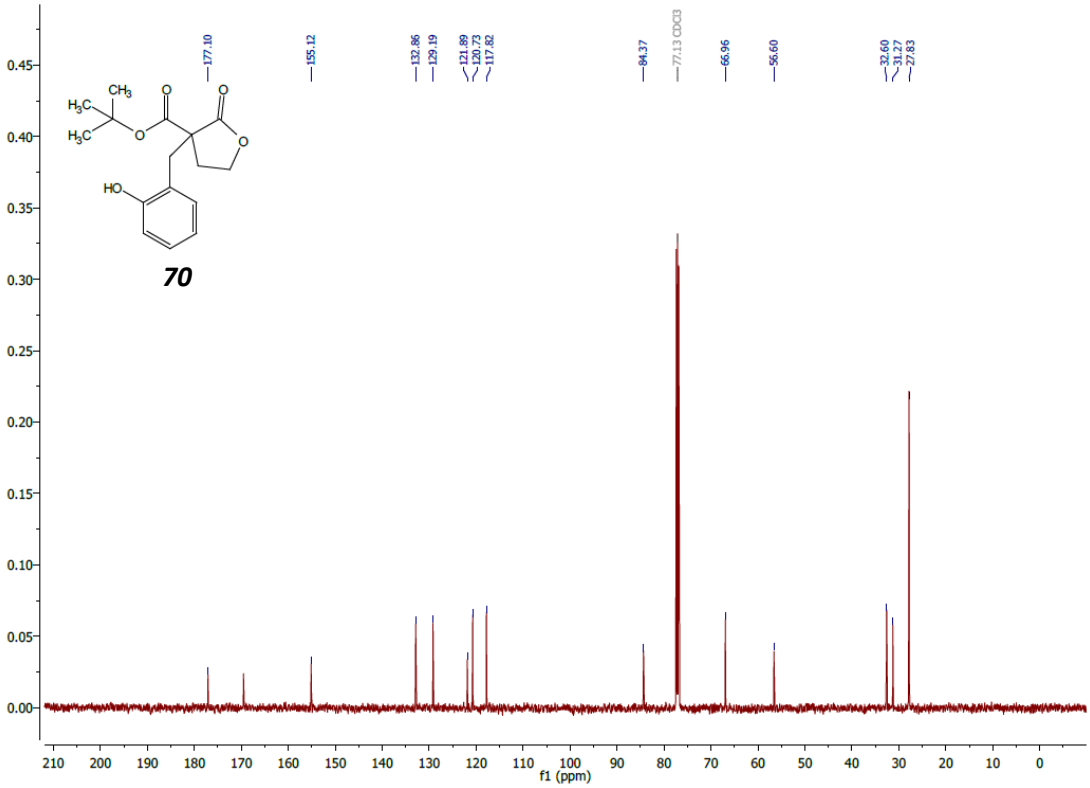
177.10
155.12
132.86
129.19
121.89
120.73
117.82
84.37
77.13 CDCl3
66.96
56.60
32.60
31.27
27.83
f1 (ppm)

70

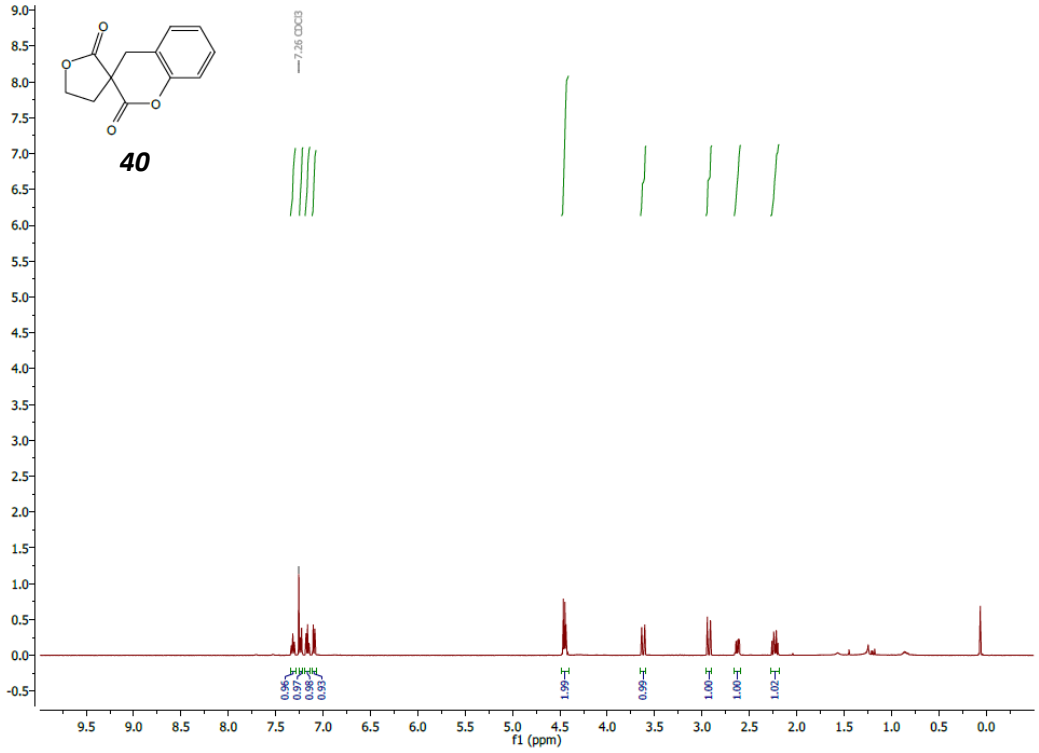
7.26 CDCl3
0.96
0.97
0.98
0.93
1.99
0.99
1.00
1.00
1.02
f1 (ppm)

40

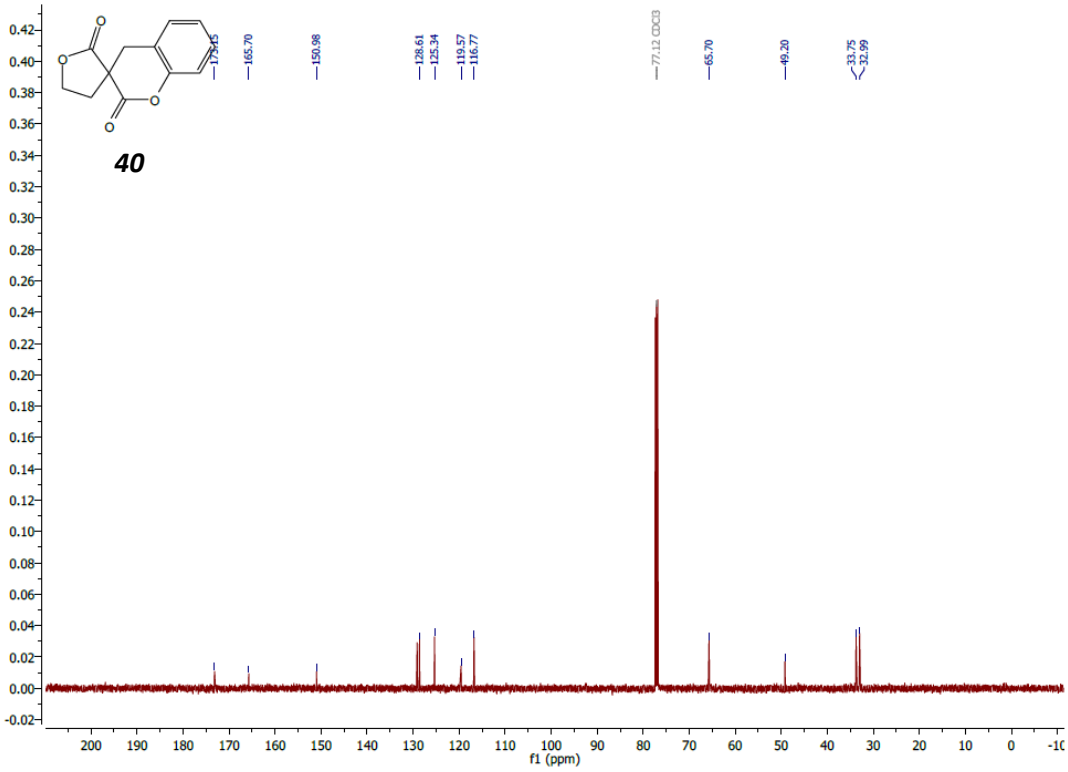
40
173.45
165.70
150.98
128.61
125.34
119.57
116.77
77.12 CDCl3
65.70
49.20
33.75
32.99
f1 (ppm)

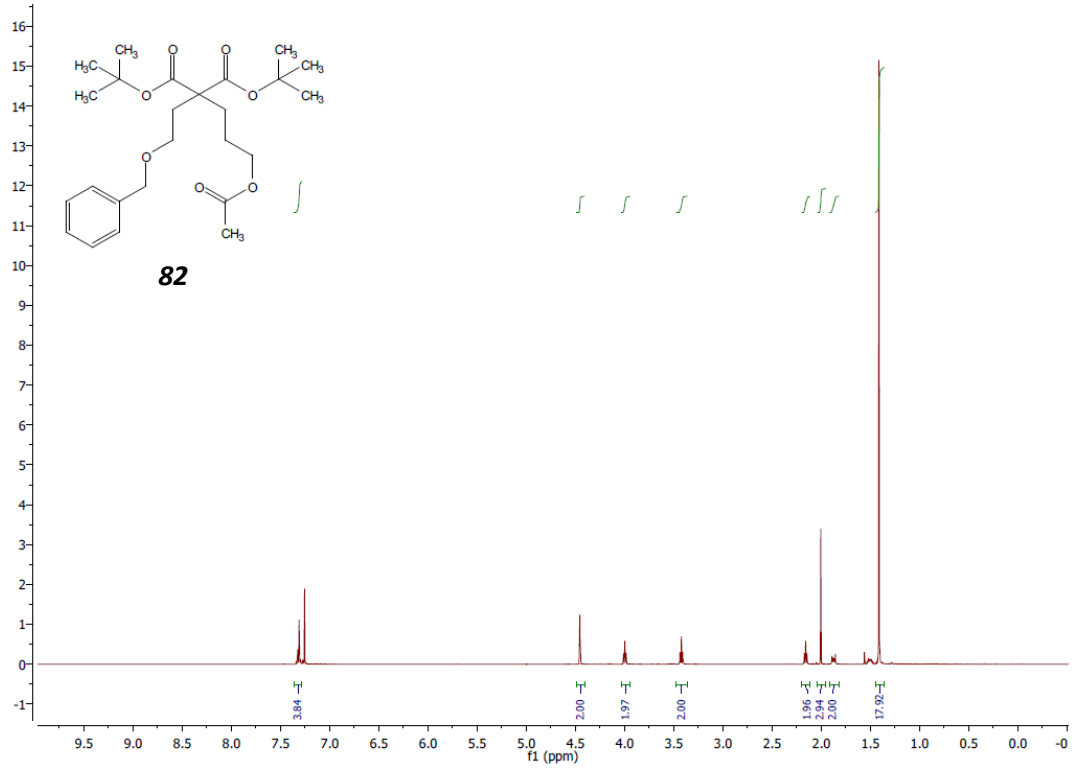
82
3.84
2.00
1.97
2.00
1.96
2.94
2.00
17.92
f1 (ppm)

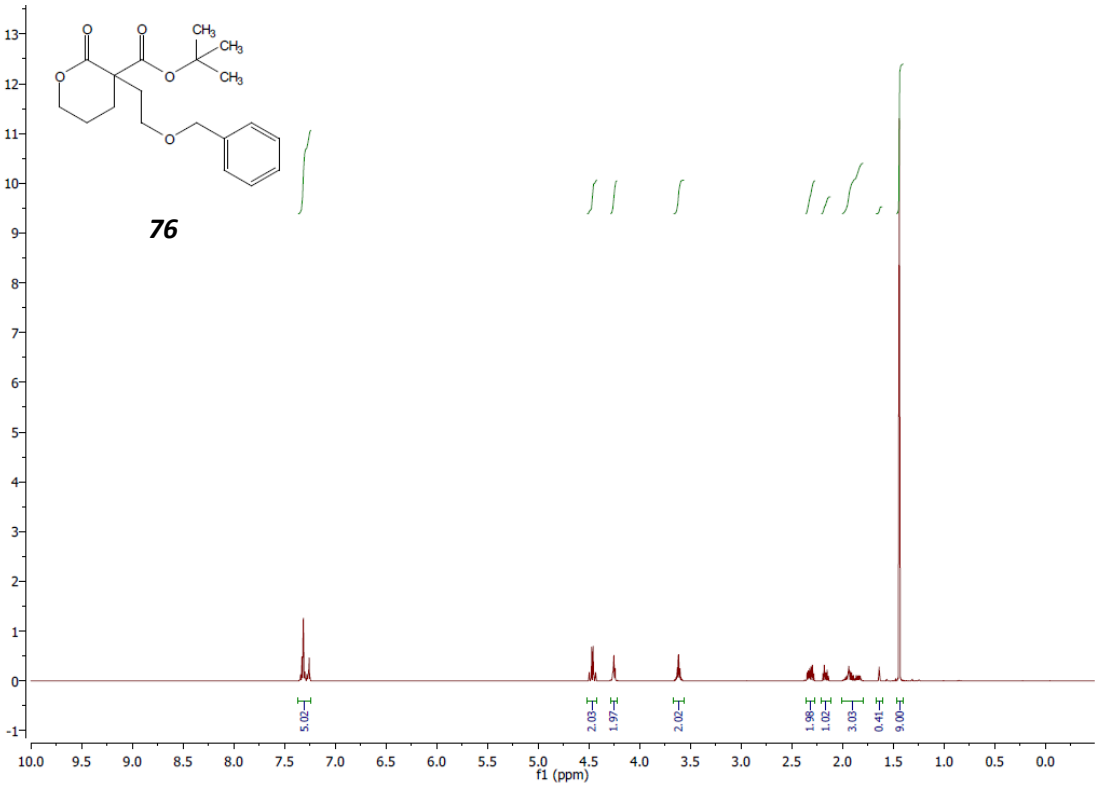
76
5.02
2.03
1.97
2.02
1.98
1.02
3.03
0.41
9.00
f1 (ppm)

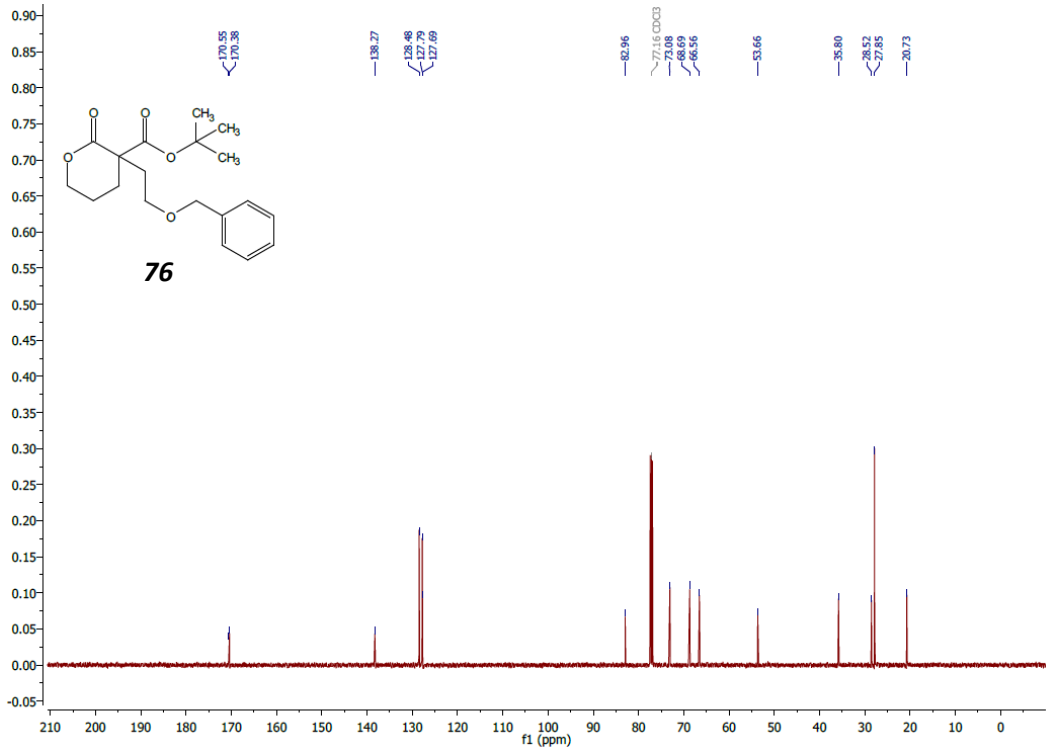
76
170.55
170.38
138.27
128.48
127.79
127.69
82.96
77.16 CDCl3
73.08
68.69
66.56
53.66
35.80
28.52
27.85
20.73
f1 (ppm)

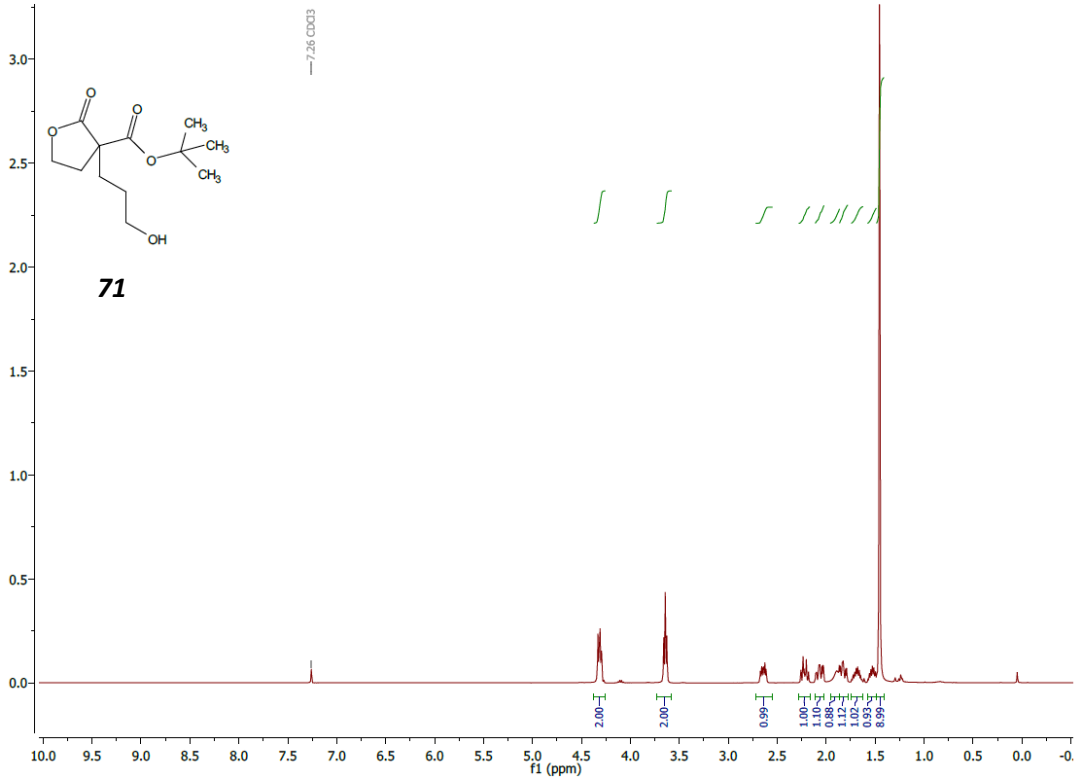
7.26 CDCl3
71
2.00
2.00
0.99
1.00
1.10
0.88
1.12
1.02
0.93
8.99
f1 (ppm)

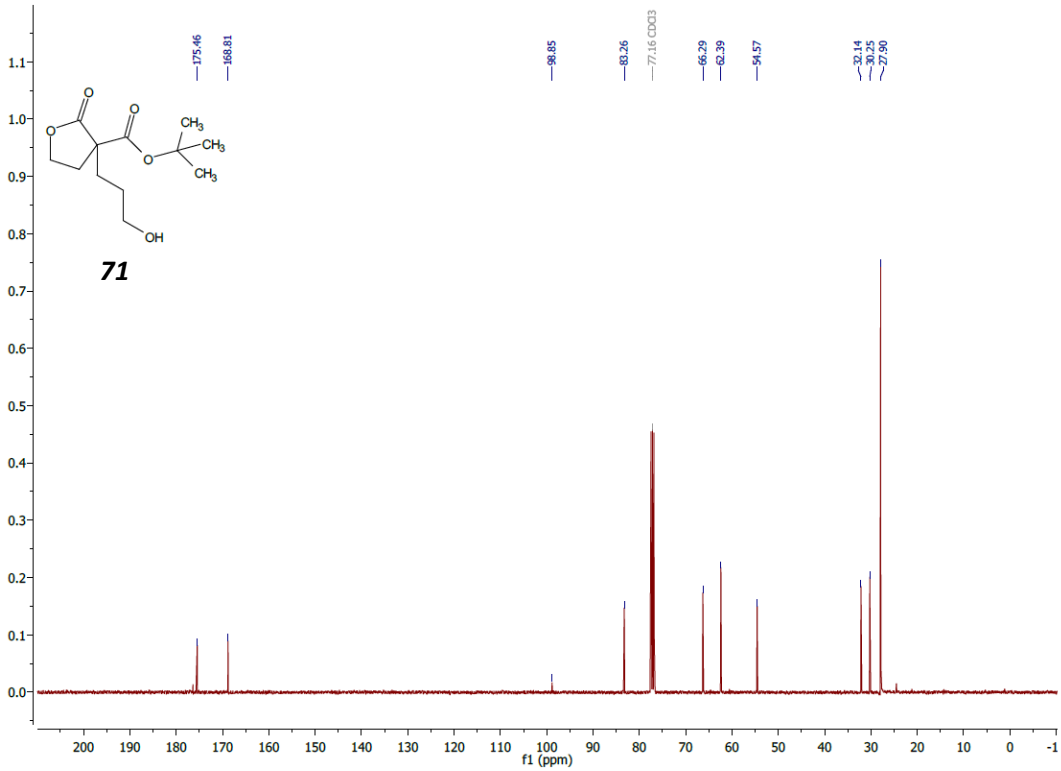
175.46
168.81
88.85
83.26
77.16 CDCl3
66.29
62.39
54.57
32.14
30.25
27.90
71
f1 (ppm)

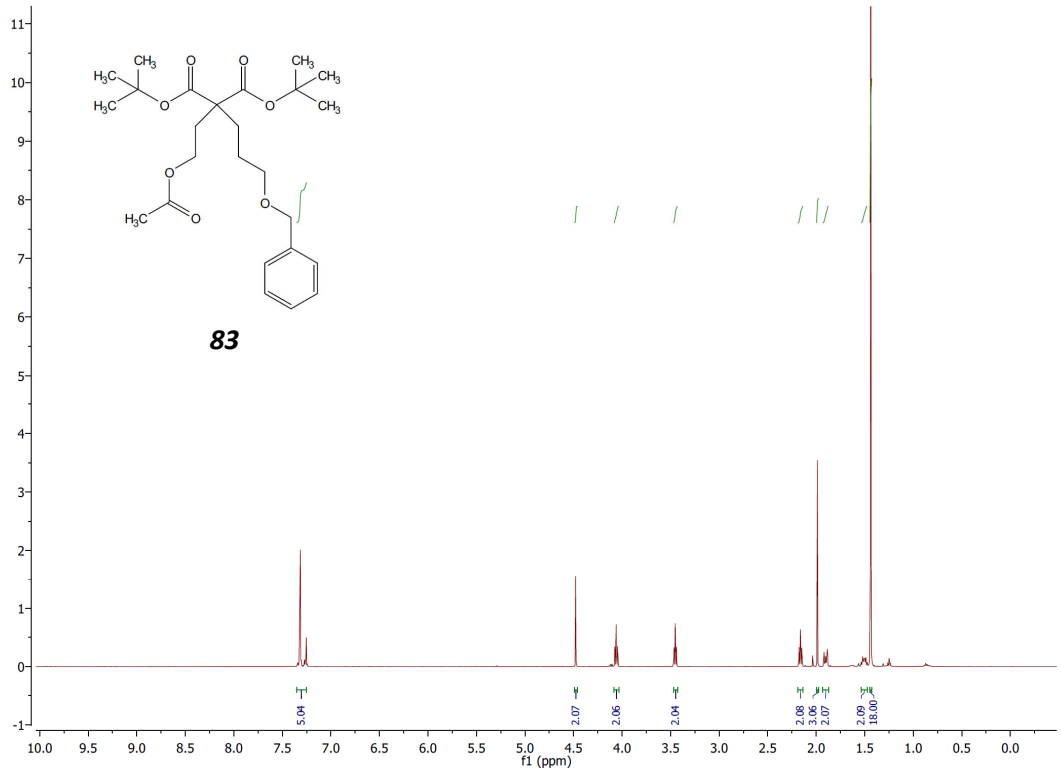
83
5.04
2.07
2.06
2.04
2.08
3.06
2.07
2.09
18.00
f1 (ppm)

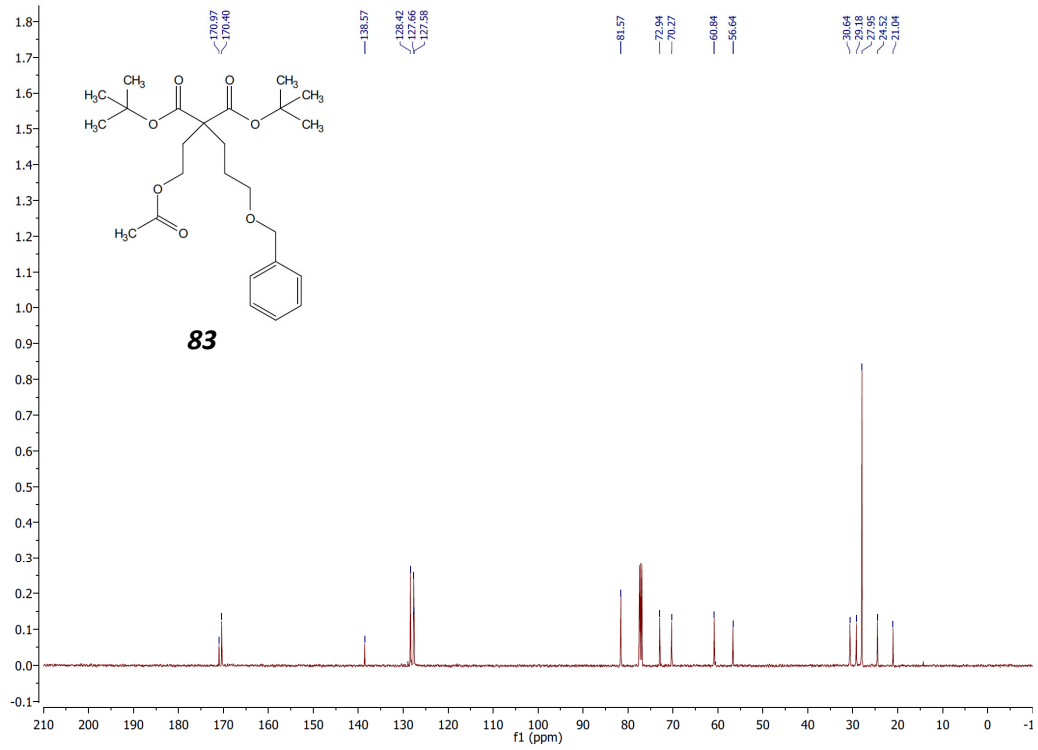
170.97
170.40
138.57
128.42
127.66
127.58
81.57
72.94
70.27
60.84
56.64
30.64
29.18
27.95
24.52
21.04
83
f1 (ppm)

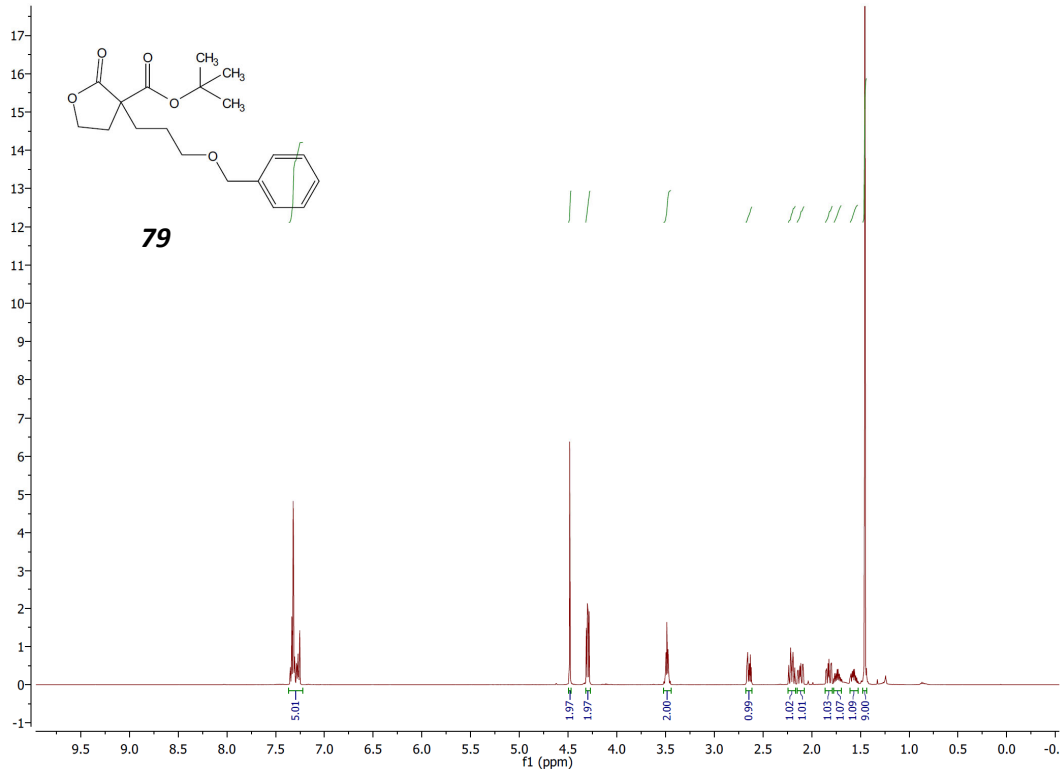
79
5.01
1.97
1.97
2.00
0.99
1.02
1.01
1.03
1.07
1.09
9.00
f1 (ppm)

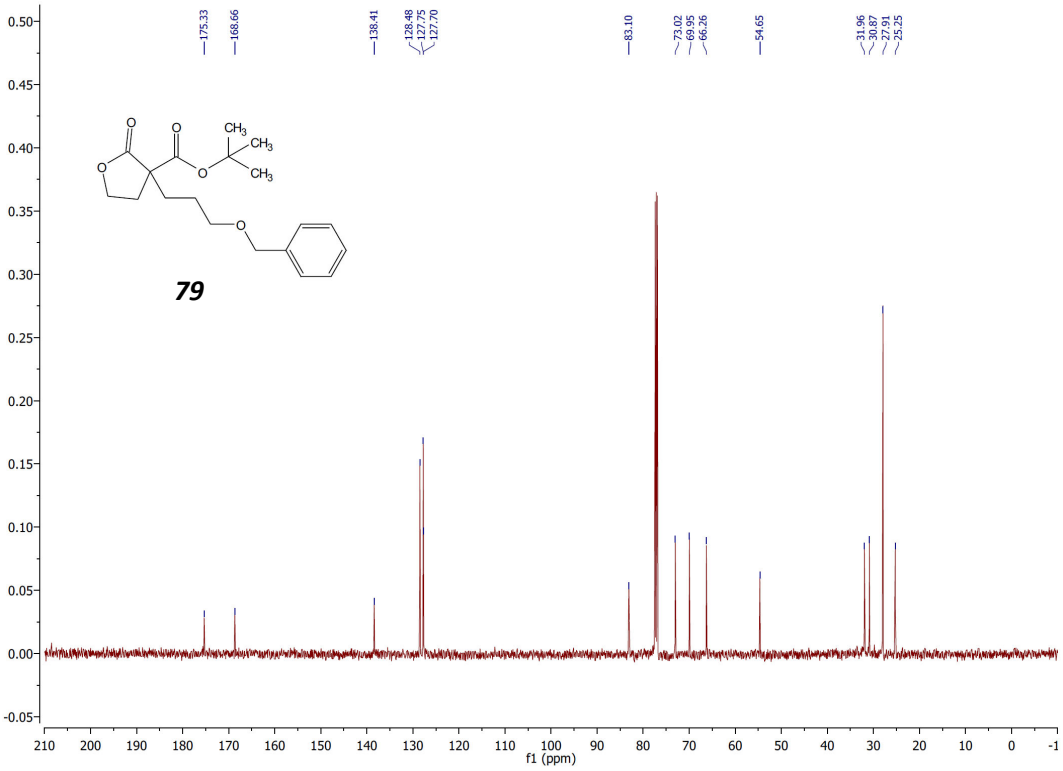
175.33
168.66
138.41
128.48
127.75
127.70
83.10
73.02
69.95
66.26
54.65
31.96
30.87
27.91
25.25
79
f1 (ppm)

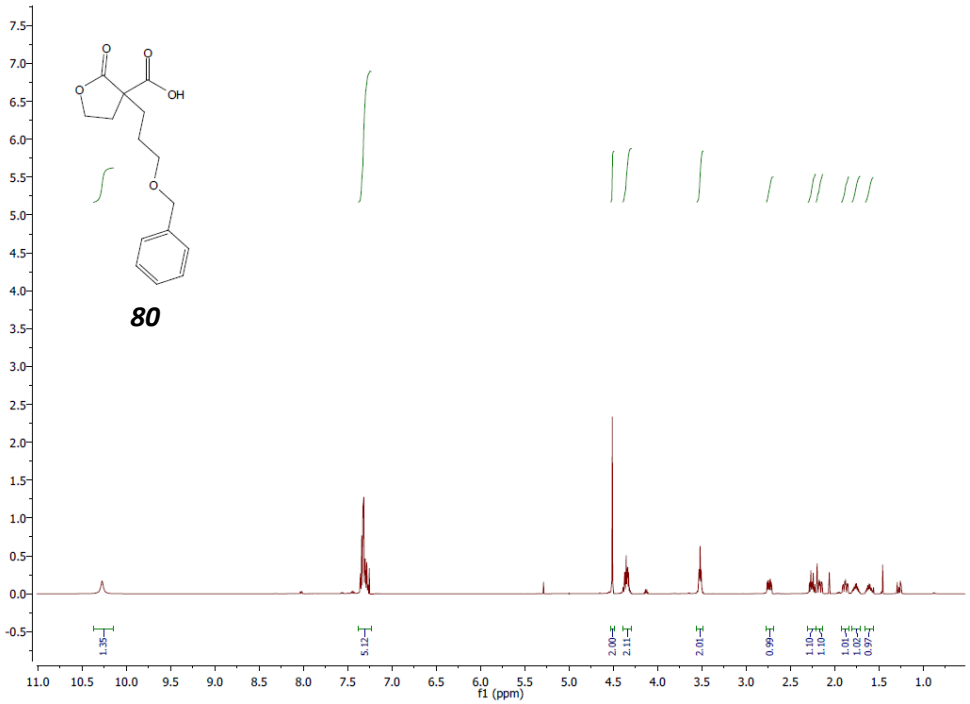
O
O
O
OH
O
80
7.5
7.0
6.5
6.0
5.5
5.0
4.5
4.0
3.5
3.0
2.5
2.0
1.5
1.0
0.5
0.0
-0.5
1.35
5.12
2.00
2.11
2.01
0.99
1.10
1.10
1.01
1.02
0.97
11.0
10.5
10.0
9.5
9.0
8.5
8.0
7.5
7.0
6.5
6.0
5.5
5.0
4.5
4.0
3.5
3.0
2.5
2.0
1.5
1.0
f1 (ppm)

APPENDIX B

CHROMATOGRAMS

HPLC chromatograms were obtained using an Agilent 1260 Infinity and Varian Prostar HPLC systems.

The Agilent 1260 Infinity HPLC system is equipped with an Agilent 1260 autosampler, an Agilent 1260 quaternary pump, Agilent 1260 diode array detectors (DAD), and the data analysis software used was Agilent ChemStation.

The Varien Prostar HPLC system is equipped with Prostar 210 pumps and a Prostar 335 photodiode array detector (PDA), with the collection and analysis of data using Galaxie Chromatography Workstation software instrument.

Analysis details can be found with each chromatogram.

Compound *49*- Racemic

HPLC Conditions: Column: HPLC OD-H 4.6 mm x 250 mm x 5 µm; Eluent Rate: 1mL/min; Eluent: 10% IPA/hexane; Monitoring wave: 210 nm

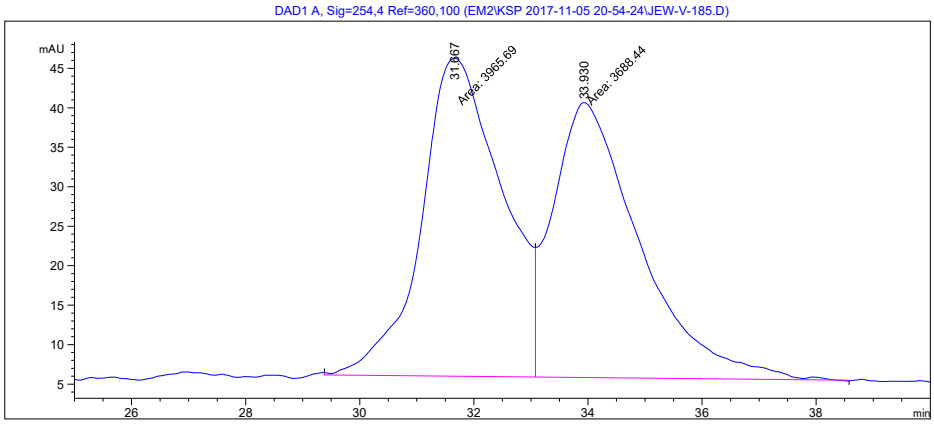

Peak #	RetTime [min]	Sig	Type	Area [mAU*s]	Height [mAU]	Area %
1	31.667	1	MF	3965.68652	40.27905	51.8111
2	33.930	1	FM	3688.44409	34.82159	48.1889

Compound *49*- Enantioenriched

HPLC Conditions: Column: HPLC OD-H 4.6 mm x 250 mm x 5 µm; Eluent Rate: 1mL/min; Eluent: 10% IPA/hexane; Monitoring wave: 210 nm

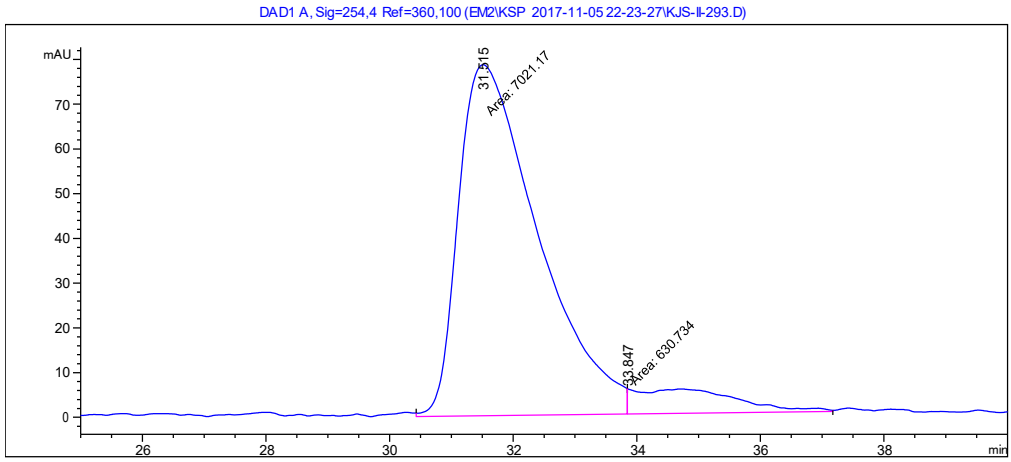

Peak #	RetTime [min]	Sig	Type	Area [mAU*s]	Height [mAU]	Area %
1	31.515	1	MF	7021.16748	78.45442	91.7572
2	33.847	1	FM	630.73370	5.70773	8.2428

Compound *38*- Racemic

HPLC Conditions: Column: HPLC OD-RH; Eluent Rate: 1mL/min; Eluent: 40% Acetonitrile/Aqueous; Monitoring wave: 254 nm

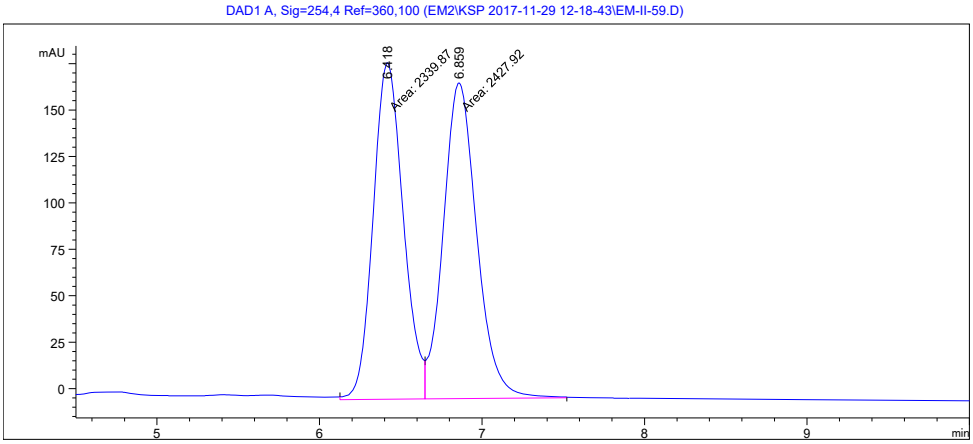

Peak #	RetTime [min]	Sig	Type	Area [mAU*s]	Height [mAU]	Area %
1	6.418	1	MF	2339.87256	181.26688	49.0767
2	6.859	1	FM	2427.91797	170.05028	50.9233

Compound *38*- Enantioenriched (before recrystallization)

HPLC Conditions: Column: HPLC OD-RH; Eluent Rate: 1mL/min; Eluent: 40% Acetonitrile/Aqueous; Monitoring wave: 254 nm

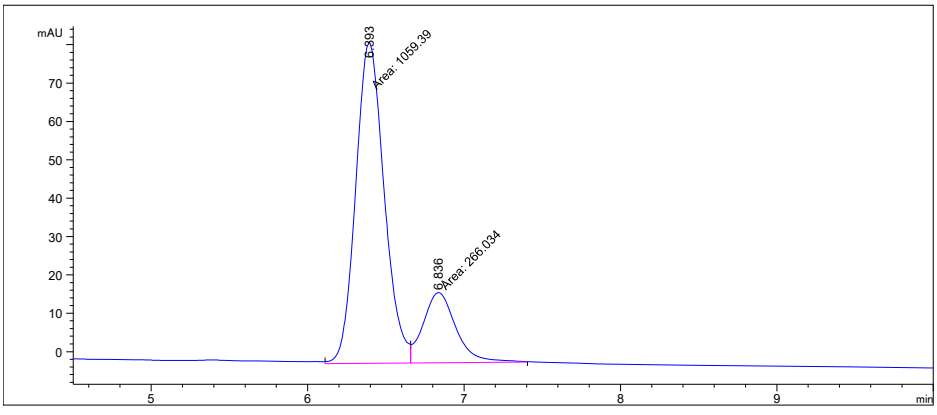

Peak #	RetTime [min]	Sig	Type	Area [mAU*s]	Height [mAU]	Area %
1	6.393	1	MF	1059.39099	83.70535	79.9284
2	6.836	1	FM	266.03412	18.34127	20.0716

Compound *38*- Enantioenriched (after recrystallization)

HPLC Conditions: Column: HPLC OD-RH; Eluent Rate: 1mL/min; Eluent: 40% Acetonitrile/Aqueous; Monitoring wave: 254 nm

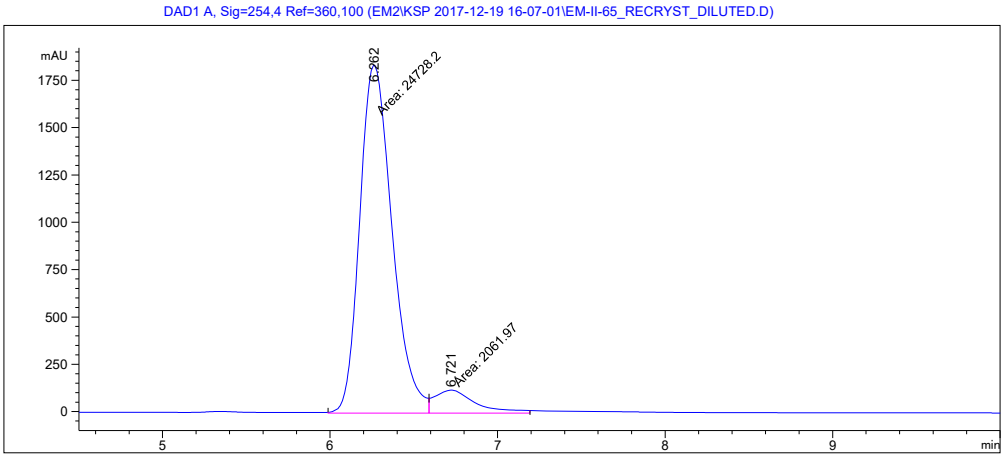

Peak #	RetTime [min]	Sig	Type	Area [mAU*s]	Height [mAU]	Area %
1	6.262	1	MF	2.47282e4	1838.97388	92.3033
2	6.721	1	FM	2061.96826	122.31843	7.6967

Compound *53*- Racemic

HPLC Conditions: Column: HPLC AD-H 4.6 mm x 250 mm x 5 µm; Eluent Rate: 1mL/min; Eluent: 10% IPA/hexane; Monitoring wave: 210 nm

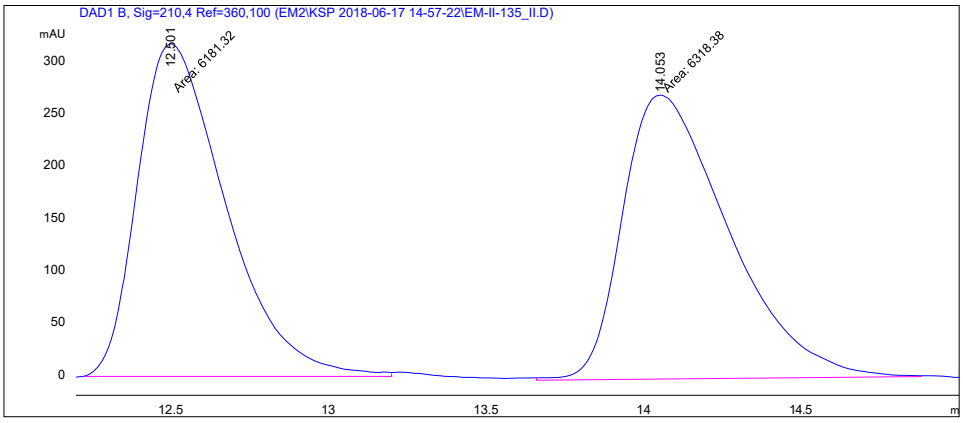

Peak #	Ret [min]	Sig	Type	Area [mAU*s]	Height [mAU]	Area %
1	12.501	1	MM	6181.32471	317.76920	49.4518
2	14.053	1	MM	6318.38184	271.24738	50.5482

Compound *53*- Enantioenriched

HPLC Conditions: Column: HPLC AD-H 4.6 mm x 250 mm x 5 µm; Eluent Rate: 1mL/min; Eluent: 10% IPA/hexane; Monitoring wave: 210 nm

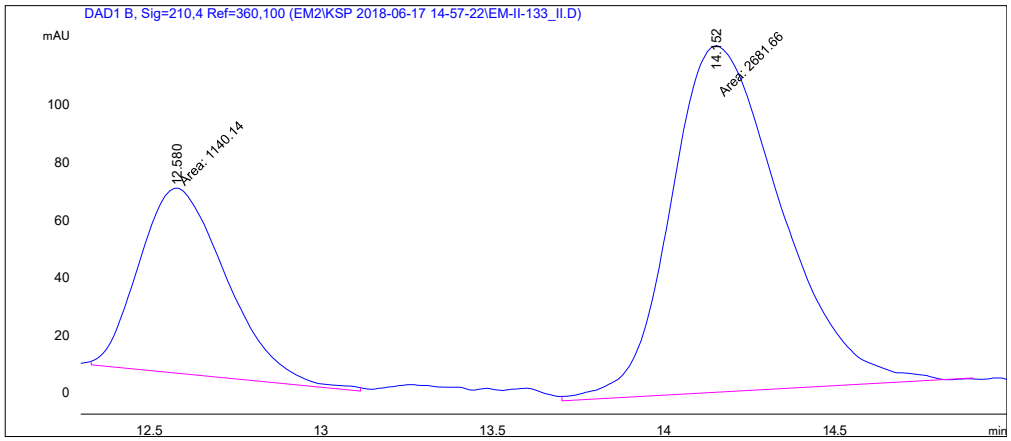

Peak #	RetTime [min]	Sig	Type	Area [mAU*s]	Height [mAU]	Area %
1	12.580	1	MM	1140.13831	64.30721	29.8325
2	14.152	1	MM	2681.65649	120.48559	70.1675

Compound *41*- Racemic

HPLC Conditions: Column: HPLC AD-H 4.6 mm x 250 mm x 5 µm; Eluent Rate: 1mL/min; Eluent: 10% IPA/hexane; Monitoring wave: 254 nm

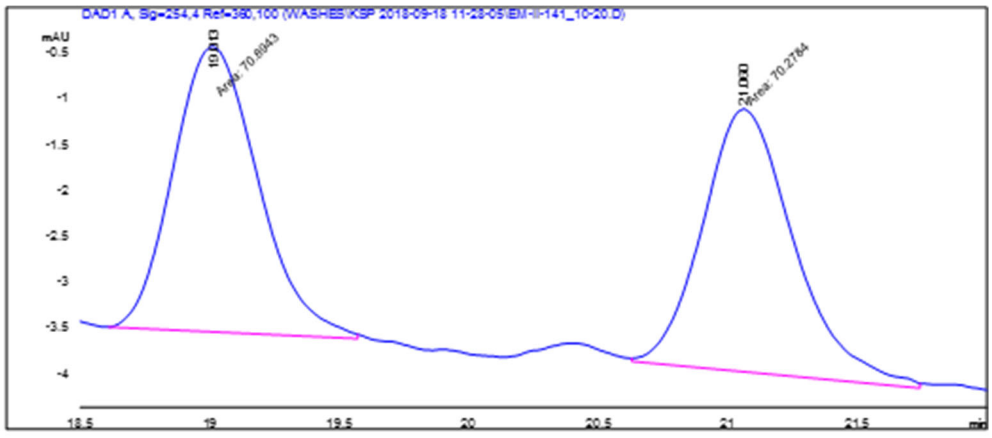

Peak #	RetTime [min]	Sig	Type	Area [mAU*s]	Height [mAU]	Area %
1	19.013	1	MM	70.89430	3.11276	50.2182
2	21.060	1	MM	70.27836	2.86838	49.7818

Compound *41*- Enantioenriched

HPLC Conditions: Column: HPLC AD-H 4.6 mm x 250 mm x 5 µm; Eluent Rate: 1mL/min; Eluent: 10% IPA/hexane; Monitoring wave: 254 nm

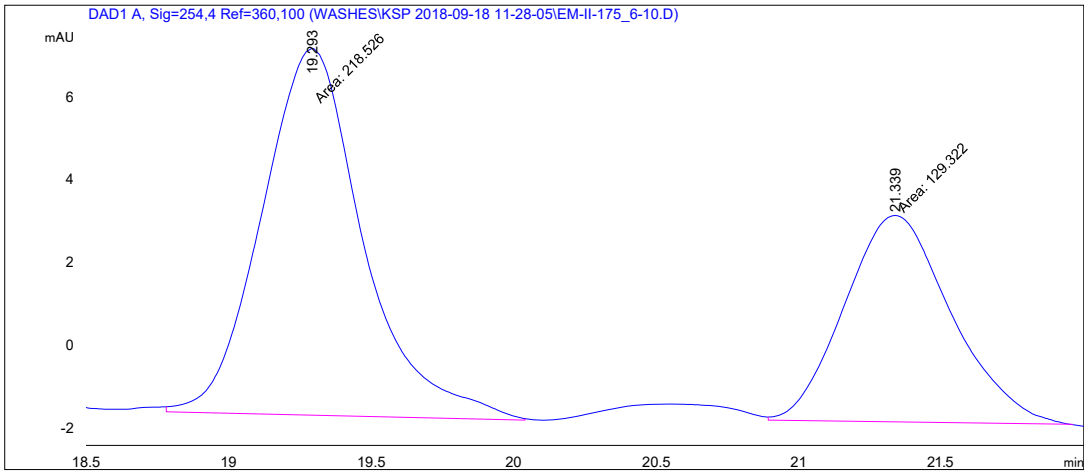

Peak #	RetTime [min]	Sig	Type	Area [mAU*s]	Height [mAU]	Area %
1	19.293	1	MM	218.52594	8.86356	62.8223
2	21.339	1	MM	129.32158	4.98933	37.1777

Compound *70*- Racemic

HPLC Conditions: Column: HPLC AD-H 4.6 mm x 250 mm x 5 µm; Eluent Rate: 1mL/min; Eluent: 5% IPA/hexane; Monitoring wave: 254 nm

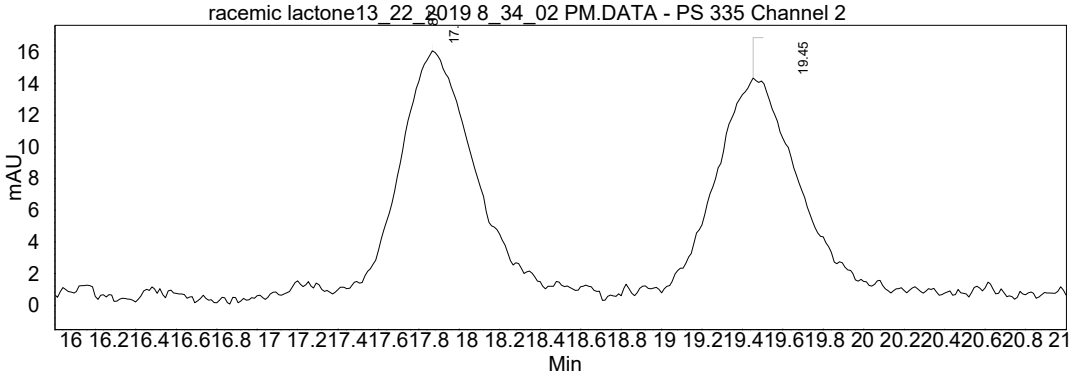

Index	Name	Time [Min]	Quantity [% Area]	Height [mAU]	Area [mAU.Min]	Area % [%]
1	UNKNOWN	17.87	49.91	15.2	6.4	49.913
2	UNKNOWN	19.45	50.09	13.6	6.4	50.087
Total			100.00	28.8	12.7	100.000

Compound *70*- Enantioenriched

HPLC Conditions: Column: HPLC AD-H 4.6 mm x 250 mm x 5 µm; Eluent Rate: 1mL/min; Eluent: 5% IPA/hexane; Monitoring wave: 254 nm

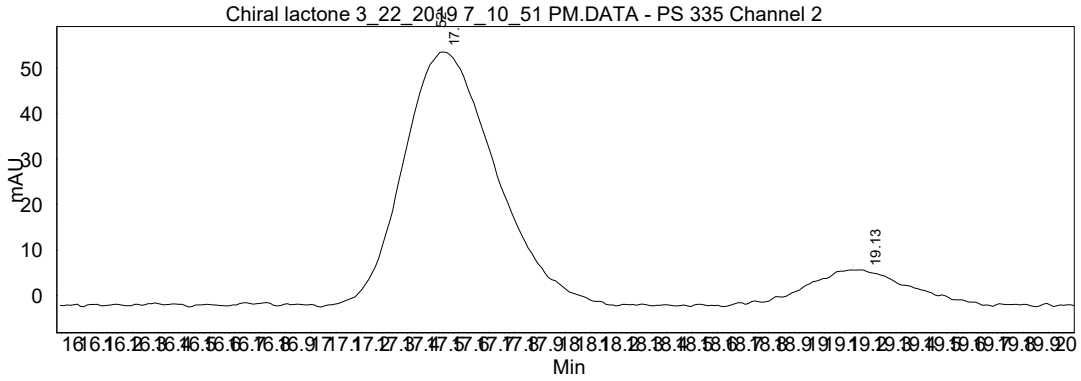

Index	Name	Time [Min]	Quantity [% Area]	Height [mAU]	Area [mAU.Min]	Area % [%]
1	UNKNOWN	17.52	87.77	55.8	23.4	87.771
2	UNKNOWN	19.13	12.23	7.3	3.3	12.229
Total			100.00	63.0	26.6	100.000

Compound *40* - Racemic

HPLC Conditions: Column: HPLC AD-H 4.6 mm x 250 mm x 5 µm; Eluent Rate: 1mL/min; Eluent: 10% IPA/hexane; Monitoring wave: 220 nm

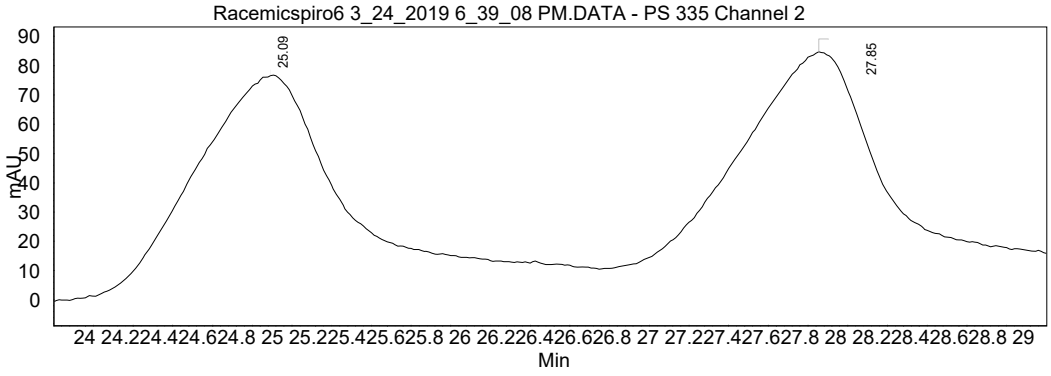

Index	Name	Time [Min]	Quantity [% Area]	Height [mAU]	Area [mAU.Min]	Area % [%]
1	UNKNOWN	25.09	49.83	65.8	46.2	49.831
2	UNKNOWN	27.85	50.17	67.1	46.5	50.169
Total			100.00	132.9	92.6	100.000

Compound *40*- Enantioenriched

HPLC Conditions: Column: HPLC AD-H 4.6 mm x 250 mm x 5 µm; Eluent Rate: 1mL/min; Eluent: 10% IPA/hexane; Monitoring wave: 220 nm

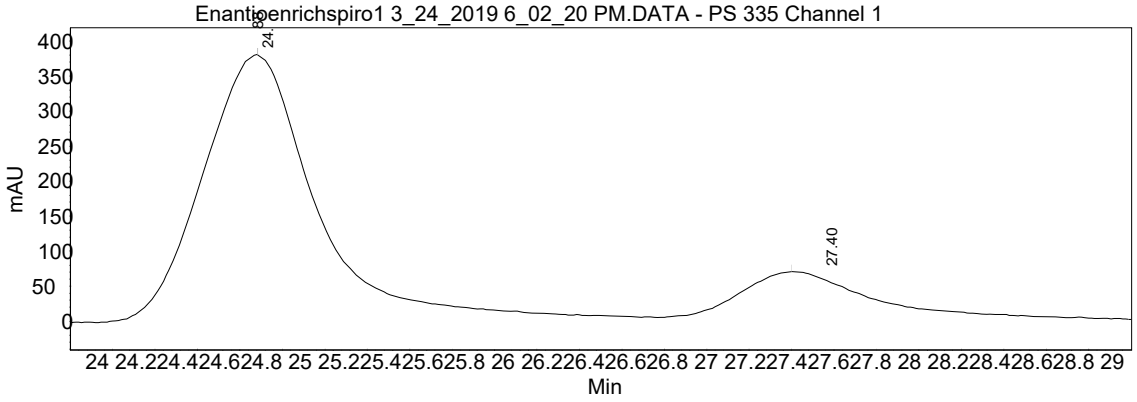

Index	Name	Time [Min]	Quantity [% Area]	Height [mAU]	Area [mAU.Min]	Area % [%]
1	UNKNOWN	24.88	85.99	375.1	214.6	85.993
2	UNKNOWN	27.40	14.01	61.0	35.0	14.007
Total			100.00	436.1	249.6	100.000